MARTIN-LUTHER-UNIVERSITÄT
HALLE-WITTENBERG
Zentrum für Ingenieurwissenschaften

Crystallizing Additives in Protein-Based Biopolymers

DISSERTATION

zur Erlangung des
Doktorgrades der Ingenieurwissenschaften (Dr.-Ing.)

des Zentrums für Ingenieurwissenschaften

der Martin-Luther-Universität Halle-Wittenberg

vorgelegt von

Frau Dipl.-Ing. Isabell Stolte
geboren am 12. Juni 1983 in Aschersleben, Deutschland

Gutachter:
1. Prof. Dr.-Ing. Dr. h.c. Joachim Ulrich
2. Prof. Dr. rer. nat. habil. Markus Pietzsch
3. Prof. Dr.-Ing. Günther Schulte

Datum der Verteidigung: 17.12.2013

Für meine Familie

I believe a leaf of grass is no less than
the journey-work of the stars.

Walt Whitman

Acknowledgment   Danksagung

Table of Contents

1. Introduction

The traditional polymers from petrol origin are still the dominating raw materials for a huge variety of polymeric materials and goods. However, the depletion of the non-renewable feedstock as well as the environmental impact of a product are immensely growing concerns in the whole society and industry. This huge interest in the substitution of the petrol-based feedstock and in overall sustainable solutions has also reflected in a politically given framework that benefits the implementation of the product life cycle analysis approaches and an innovative product design.

Changing the focus towards the production and application of renewable resources from nature is of course not an entirely new idea. Already in the early times of industrialization, these raw materials have also been applied and further modified for the manufacture of durable goods and fabric. The nowadays renewed interest of research as well as industry in the bio-based materials has led to a set of biopolymer generations that can be distinguished either by material shelf life or the origin of the raw material. The origin-based classification of the biopolymers is seen to be most evident and polymers from plant and animal orgin from high-value renewable feedstocks as well as from low-value side-products are considered. Also the production of bio-based monomers for traditional and new polymeric materials is classified here [Hat07, End09, Tab10, Bie12].

The natural-based polymers like proteins are one feedstock pillar in the development of materials and products mainly in market sectors as packaging, agriculture and horticulture as well as in the formulation of pharmaceutics. Their key additional benefits are the biodegradability, compostability and biocompatibility that make the deriving bio-based materials successful in the specific market niches. Depending on the purity requirements of the distinct application, also by-products of the crop and animal industry can be used [Pom05, Bie12, Rie13]. However, the huge market of the petrol-based plastics cannot be served by the natural-based polymers. The reasons are mainly seen in the restriction of the natural resources themselves and the competition with the energy recovery options or the competition with the food supply.

The potential of the protein-based films, sheets and coatings is above all in the products of higher value and a unique product design aside from traditional plastics engineering. Coming from a variety of possibilities of functionality increase, the protein-based materials offer the tailoring of the material properties for the specific application. The tailoring and optimization of the protein-based materials can be achieved by both modifying the protein-based carrier matrices e. g. with biochemical methods as well as the incorporation of functional additives.

Ongoing research is focusing on the crystallization of functional additives within the inner structure of protein films. Those crystallizing additives can be agrochemicals, where the protein-based matrix offers a controlled release during the time of usage and final degradation. The advantages of e. g. crystallizing fertilizer salts are explained in the following by using the product design of protein-based mulching films and seed tapes. The increasing importance particularly of agricultural films is reflected by their consumption of 540,000 t/a in Europe, where mulch films had a share of 25 % of the US$ 2.7 billion market in 2011 [Ami11].

The type of additive, the inner-film crystal growth of the additives in the production process and the crystal growth control have been recognized to define the product quality of the protein-based films with incorporated fertilizer. Therefore, only the linkage to the process optimization leads to a successful product design.

2. State of the art

2.1 Classification and regulations

The definition of the biopolymers (or bioplastics) is in the ongoing discussion within research, industry and politics. Because of the heterogeneous nature of the variety of materials, a clear classification is still challenging and misconceptions of the materials' possible renewable origin and / or the end-of-life characteristics have to be avoided [End09, Pro09, EuB12]. The following grouping of all the polymers by Endres and Siebert-Raths [End09] appears to be most general and widely accepted. It uses the terms 'biobased' as well as biological or physico-chemical 'degradation' and defines the biopolymers to be grouped in the first two categories:

- Biobased or partly bio-based non-biodegradable plastics

- Plastics being both bio-based and biodegradable

- Plastics based on fossil resources, but being biodegradable

- Conventional petrol-based plastics that are non-biodegradable

The certification of the materials' degradability is assessed in Germany by the DIN CERTCO organization that follows the European standard DIN EN 13432 [DIN00]. The standard was formerly designed for packaging materials and rates the material degradation by its disintegration during a composting treatment. This definition implies that a material must not necessarily be compostable in the way of a biodegradation by microorganisms, but the polymer disintegration could also be achieved by pro-oxidant heavy metal salts [Chi07]. Additionally, the DIN CERTCO certification plays a role in the choice of the material additives and fillers as well as the amount of those additives within the final material is limited. E.g. glycerol as a plasticizing agent is limited to a content of 49 % (w/w). For inorganic fillers and dyes, the limit is likewise [End09].

When bringing a biopolymer on the market, several other governmental regulations particularly in Germany have to be considered and discussed for each product made of a polymer or composites. These regulations relate to the desired application of a polymeric material and the desired way of disposal:

- Regulation on the prevention and recycling of packaging waste (Verpackungsverordnung) [VerpackV12]:
  The trading companies and the industry are committed to organize and finance the cycling of packaging waste from the consumers back to the producers. Recyclable materials are aluminum, glass, polymeric materials, composites, paper and cardboard. The collection of that waste labeled with

the "Green Dot" is done in Germany by the DSD GmbH. In other European countries, similar regulations have been established.

- Regulation on the environmentally compatible deposition of municipal waste (Abfallablagerungsverordnung) [AbfAblV09]:
  This regulation classifies the types of municipal waste and defines the treatment of those waste streams. Biopolymers are to be allocated to the refuse derived fuels and are allowed to for incineration.

- Regulation on the recycling of biowaste on land used for agricultural, silvicultural or horticultural purposes (Bioabfallverordnung) [BioAbfV13]:
  The degradation of biopolymers with suitable industrial composting techniques or e.g. the application of biodegradable mulching films is allowed, if the requirements according to DIN EN 13432 [DIN00] are fulfilled. Here, the packaging materials are strictly excluded. Resulting from this novelty, the biodegradable packaging systems have to be collected as residual waste and are typically fed to the conventional waste combustion.

- Regulation on the insertion of fertilizers, soil additives, substrates and plant adjuvants (Düngemittelverordnung) [DümV12]:
  The plant fertilization as end-of-life strategy of biodegradable materials is generally allowed, if the materials have been certified according to DIN EN 13432 [DIN00].

2.2 Biopolymers and their production from proteins

Bio-based polymers can be processed from the naturally occurring polymers like starch, lignin and cellulose derivatives. Otherwise, bio-based monomers are polymerized to traditional or novel polymers. A recent detailed overview on the market can be found elsewhere [Fak07, End09, Ebn13].

Particularly the proteins are naturally occurring polyamides from plant and animal origin that are highly suitable as raw material for the production of biopolymers. In the following, general information on the quite heterogeneous protein structure is given. For a detail view on the fundamentals of the protein synthesis and structural aspects, it is referred to the literature [Wal02, Nel05a, Whi05].

The proteins are typically built up from 20 L-amino acids as the monomers that are polymerized in the sequence according to the genetical information. The monomers are linked with peptide bonds between the amine group of one amino acid with the carboxyl group of the other. This linkage is shown in Fig. 4-1 using casein as an example. The protein molecules may further exhibit a three-dimensional structure that is stabilized mainly by covalent disulfide bridges as well as non-covalent hydrophobic interactions and hydrogen bonding [Ver10]. The properties of the

proteins, e.g. the ability for film formation, are affected by molecular weight, structure and conformation and charge distribution on the protein molecules [Zay97].

Protein-based films, sheets and coatings are produced mainly via two processes to reach the formation of the three-dimensional protein network as it is shown in Fig. 2-1. On the one hand, it is the solvent process and on the other hand the dry process that stands for the methods of thermoplastic manufacture. The solvent process (or solution casting) is based on the dispersion or solubilisation of proteins and additives in large quantities of a solvent medium like water, organic solvents or mixtures thereof. Traditional techniques like film extrusion, compression and injection molding involve only low solvent content and offer economical benefits such as low thermal energy consumption, low cost and high throughput. The applicability of these methods has already been proven for several protein systems, but still remains challenging. The choice of the production process as well as the process parameters decisively influences the final material properties [Gui05, Gue10, Ver10, Bet11, Fro10b, Gäl11]. In particular, the amount of solvent as critical parameter remarkably affects the overall process management and equipment [Gen02, Dan09, Mar11]. Mainly soy protein and wheat gluten have been reported as raw materials in the context with the wet process [Red99, Pom03, Moh05, Her08, Ver10, Che11, Gue12, Nur13].
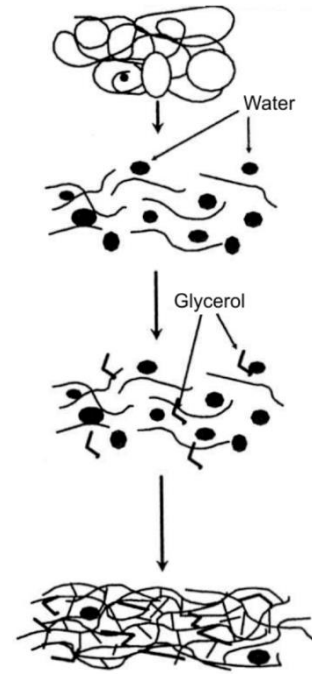
Fig. 2-1: Protein film formation after dissolution in the solvent, plasticization with glycerol and drying [Cui05].

For casein and its processing to materials, an extensive overview can be found elsewhere for a variety of applications [Gen02, Dic06, Mar11, Hu12]. Besides food purposes, casein has been traditionally used as a basis for glue, paint and fibers. Nowadays, this natural polymer and products thereof gain renewed commercial interest because of their functionality and sustainability aspects. The spinning technique was particularly refined to produce casein fibers mainly for the textile manufacture [For67, Fri97, Lam03, Pat05, Ars07, End09, Wan09].

Recently, the casein-based biopolymers have already been successfully processed by the film extrusion technique combined with the reactive extrusion by the application of enzymatic cross-linking. However, the process window was described to be narrow due to the necessity of a relatively long residence time of the material within the system. Furthermore, a considerable built-up of pressure was reported to occur because the viscosity increases during cross-linking. The production of protein-based films by extrusion thus needs a careful temperature and pressure control [Fro10b]. The previous investigations on the extrusion attempt of casein and the

description of the processing issues are mostly related to the food industry or to the production of material blends with other biopolymers [Sze94, Fer04, Lus10].

For the lab scale, the wet process or solution casting is a common method in particular for aqueous protein solutions also due to the rather simple experimental set-up. The formation of the film or coating typically takes place by a controlled evaporation of the excess solvent in a proper mold. The material composition can easily be adapted to new approaches by simply mixing or suspending additional substances into the protein solution. For many protein-based polymer systems, the applicability of the casting method has been proven to be successful. In the up-scale to extrusion-based dry processes, the key factors are mainly the diminishment of the solvent content as well as an accurate temperature and pressure control during the reactive extrusion with the
enzymatic cross-linking [Vir00, Oh04, DiP06, Den09, Pat10a, Fro10, Sto12a, Bai13].

The important factors of the wet process are temperature, pH, viscosity, plasticizers and type and amount of the solvent. Especially, the drying conditions like temperature and air humidity are substantial for the final material properties and qualities. In a harsh drying environment of high temperature and lowest air humidity, the solvent evaporation would go on too fast and inhomogeneous, which results in shrinkage, flaws, tension and breakage. The other extreme is the too slow drying at mild conditions that is usually undesired since it is time consuming and thus uneconomic [Den09, Mar11].

2.3 Modifications in biopolymer functionality and benefit

2.3.1 Plasticization

Plasticizing agents are added to polymeric materials to adjust the mechanical performance and to increase the flexibility of mainly films, sheets and coatings. As a further effect, the plasticized material is shifted from the glassy state to the rubbery state and the glass transition temperature T_g is decreased. Furthermore, the plasticizers may contribute to the overall physicochemical properties of the material. Regarding the naturally derived biopolymers with incorporated plasticizer, usually the water sorption characteristics as well as the water vapor and gas permeability are increased [Cad00, Gen02, Kra05, Sot05, Bou08, Vie11].
The mechanism of action of plasticizers is of huge interest not only for protein-based systems, but for all polymeric materials. The scientific discussion has evolved three major theories that are briefly reflected in the following [Mar04, Kra05, Sot05, Car13]:

- Lubricity theory
  The plasticization results from a substance acting as solvent, as lubricant between polymer molecules or a combination of both interactions. It is

assumed that the plasticizer weakens the polymer-polymer interactions and namely the van-der-Waals forces by shielding the molecules. Additionally, the plasticizer is said to fill the void molecular space in the polymer matrix and thus, building up glide planes between layers of polymer or resin.

- Gel theory

  The plasticized polymer is seen to undergo a solvation-desolvation process, where the plasticizer disaggregates the polymer molecules to a small extend. This gel of polymer and plasticizer was proposed to be more sensitive to mechanical stress because of the loose network held together by weak secondary bonding forces that allow bending and stretching.

- Free volume theory

  The free volume theory was first postulated by Fox and Flory [Fox50] and includes the thermal and the physicochemical behavior of polymers into the description of the plasticization mechanism. The free volume defines the internal space within a polymer. When a plasticizing additive is incorporated into the material, this free volume is expanded and the polymer chain movement is facilitated. The theory explains the lowering of the polymer's glass transition temperature T_g by additives with lower T_g than the polymer. Furthermore, it is proposed that the plasticizer effectiveness is enhanced for substances of relatively low molecular weight and a high degree of branching.

Protein-based materials typically contain a considerable amount of a plasticizing agent. By their nature, proteins tend to form a very brittle dry substance. Otherwise, the water uptake of the usually hydrophilic proteins from a humid environment results in a measurable plasticization [Mat00]. However, the volatility of water results in an instable plasticization. Therefore, a variety of non-volatile substances already have been tested and evaluated in the literature [Gen02, Orl02, Sot05, Her08, Cao09, Kow11, Vie11, Nur13, Wih13].

Useful plasticizers are chosen by miscibility with the protein and the solvent, effectiveness of plasticization and biocompatibility. Here, glycerol, polyethylene glycols, sorbitol and other sugar compounds have been reviewed as the most common additives for hydrophilic protein sources like casein, whey protein and gelatin [Sie99, Cou00, Kim01, Gen02, Khw04, Sot05, Fro10a, Nur13]. They fulfill the definition of external plasticization, which generally means non-volatile substances of low molecular weight that interact non-covalently with the polymer matrix. In case of the protein-based materials, those are mainly hydrophilic substances with relatively low molecular weight compared to the protein molecules. It is known that these plasticizers undergo migration towards the material surface that in the end leads to material aging and increased stiffness and brittleness. Thus, some attempts for internal plasticization methods have been presented. In case of casein, the

plasticizer amino PEG or gum arabic was covalently bound to the protein polymer to avoid migration [Fla06, Pat10b]. However, the linkage of protein and plasticizer so far was reported to be beneficial to the material properties only for a soy protein isolate resin modified with stearic acid [Lod05].

2.3.2 Functional additives

Functional additives in polymeric materials are part of the final product design and contribute to the additional benefit of the product and its unique selling proposition. As a secondary aspect, the functional additives may modify or even enhance the material properties. The possibilities of increasing the functionality of a biopolymer are of course manifold, due to the variety of raw materials, their broad set of properties and the consideration of the final applications. In the following, some major goals of functional additives regarding protein-based biopolymers and other polymers are summarized including examples:

- Release systems
  - Pharmaceutical dosage forms; gelatin capsules [Aug02, New04, Fel13]
  - Wound dressing; hydrocolloidal films containing antibiotics or silver nanoparticles [Suz97, Lo08, Tha09, Els12, Pel12]
  - Medical implants and scaffolds with bioactive agents for *in vivo* tissue regeneration [Gri10, Kha10, Els12]
  - Cosmetic applications, e.g. the release of skin care products from facial masks [Vie09, Fat10, Sta11a]
  - Time-controlled release of fertilizers in agricultural applications [Smi91, Mik94, Mis04, Fro10a]

- Immobilization
  - Waste water treatment against various pollutants with porous biopolymer beads or fibers in which inorganic catalysts / enzymes / cells are immobilized [Vil11, Kho12, Pap12]
  - Soil improvement with alginate beads containing microorganisms for capture of heavy metal ions [Bra07]
  - CO_2 capture by immobilized laccase in a chitosan carrier [Pra09]

- Shelf-life extension of polymer and packaged goods
  - Antimicrobial agents [Gen97, Roj09, Men10, Kuo11]
  - Antioxidants [Gen97, San10, Sal11]
  - Pigments [Cha11, Llo12]

2.3.3 Cross-linking of proteins

In material science, the covalent modification of protein-based films aims for the decrease of the material's water solubility and water vapor solubility. Furthermore, the protein-based biopolymers can be enhanced in their mechanical performance. The proteins allow cross-linking reactions that are accompanied by a viscosity increase during the gelling of the protein solution [Per99, Oh04, Tan05, Fro10a, Pat10a, Zha11, Kua13]. Here, the term 'cross-linking' relates to inter- and intramolecular covalent bond formations and include disulphide bonds as well as isopeptide bonds of any kind [Vin04]. The mechanisms of the covalent bond formation within protein-based materials can be distinguished as follows [Ger12, Kua13, Wih13]:

- Physical treatment with heat or irradiation inducing chemical cross-linking

- Chemical cross-linking

- Enzymatic cross-linking

The heat-induced cross-linking is often a side effect of the processing of proteins, where moderately high temperatures are needed to homogenize the material components or to sterilize edible films and food products [Ver10, Ger12]. The aggregation and denaturation of proteins under severe heat can be easily recognized. Predominantly, these structural changes are due to the increased polymer chain motility, reshuffling of already existing disulphide bonds and the new formation of disulphide bonds [Per01, Rom12, Wih13]. Additionally, the protein molecules' complex reaction system contains the process of the β-elimination of the cystine residues. The resulting free sulfhydryl group and the release of reactive intermediates like lysinoalanine are extensively discussed in the literature [Klo77, Pel99, Rom12, Als13]. Considering the milk proteins, so far, the presence or absence of a reducing sugar component appears to be relevant. Isopeptide linkages resulting from lysinoalanine have been identified, when no sugar was added prior to the heat treatment. Otherwise, the heat-induced cross-linking is connected to the reactivity of advanced Maillard reaction products [Als13].

The γ- or UV radiation processing of proteins is similarly known from the food preservation [Kua13]. To protein molecules, the ionizing radiation affects conformational changes as well as the recombination of the structure and polymerization. Here, the oxidation of amino acids takes place and is accompanied by the breakage of covalent linkages and the formation of free radicals [Gen98, Wih13]. The applicability as a cross-linking method in material science has been confirmed in the literature [Gen98, Rhi00, Sab01, Cie06].

Chemo- and bio-catalytical cross-linking basically follow the same principle. The mechanism is dependent in the reactive cross-linking agent that is usually introduced

into a polymer melt or into a solution. In case of the chemically cross-linking the protein-based materials, glyoxal, glutaraldehyde or formaldehyde are amine-reactive and act as linkers between the polymer molecules [Ave93, Rhi00, Car04, Men10, Wih13]. On the contrary, an enzyme is a biocatalyst and is not involved in the final product. The cross-linking of proteins can be induced by various enzymes like transglutaminase, laccase, tyrosinase or peroxidase. The different reaction pathways and sites as well as the enzyme origins are reported elsewhere for each specific enzyme [Stu94, Hil99, Juv11, Fat12, Hec12, Wih13]. The aspects of the enzyme kinetics are briefly described in section 2.4, whereas detailed information about the transglutaminase reactivity is given in section 4.3.

2.4 Enzyme kinetics

Enzymes are biochemical catalysts and all enzymes are proteins. As the major function of a catalyst, enzymes are able to lower a reaction's activation energy, $\Delta G^{\ddagger}$, but do not influence the equilibrium of a reaction. They induce also thermodynamically unfavorable chemical processes and enhance the reaction rates typically by a factor of 10^5 to 10^7. The enzyme kinetics bases on the concept given in eq. 2-1 and is usually modified to model a specific enzyme reaction. It derives from the assumption of a complex formation of enzyme (E) and substrate (S) until the product (P) is formed and released from the enzyme's active site:

$$E + S \leftrightarrow ES \leftrightarrow EP \leftrightarrow E + P \qquad (2\text{-}1)$$

$$V_0 = \frac{V_{max}[S]}{K_m + [S]} \qquad (2\text{-}2)$$

For this concept, Michaelis and Menten [Mic13, Joh11] have proposed the most successful mathematical model to date for the enzyme kinetics. From their theory, the Michaelis-Menten equation has been derived that is depicted in eq. 2-2. Here, the terms include the substrate concentration [S], initial reaction rate V_0, maximum reaction rate V_{max} and K_m, the Michaelis constant. The fundamentals of the enzyme kinetics and the theoretical background are summarized e.g. in the standard biochemistry literature [Nel05b, Lab08, Voe11, Gar13].

Specifically, the cross-linking reaction of the microbial transglutaminase is assumed to follow a ping-pong bi-bi mechanism that is briefly described by the eq. 2-3 [Fol69, Kas02, Les03]

$$ \text{(2-3)} $$
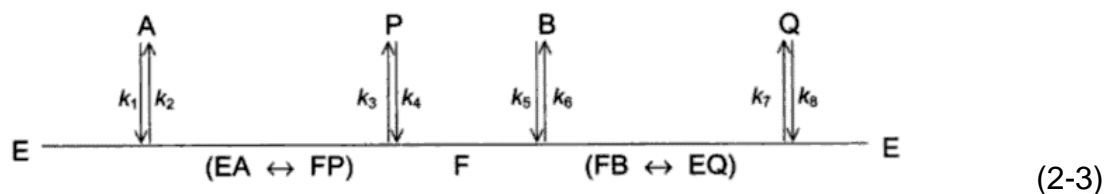
with E…free enzyme, EA… enzyme-substrate complex, FP… amino enzyme-product complex, F… amino enzyme, FB… amino enzyme-substrate complex, EQ… enzyme-product complex, k_i… reaction rates, A, B… substrates and P, Q… reaction products.

The overall reaction kinetics is reduced to eq. 2-4 as is explained in detail by Leskovac [Les03]:

$$ V_0 = \frac{V_{max} \cdot [AB]}{K_B \cdot [A] + K_A \cdot [B] + [AB]} \tag{2-4} $$

The terms of eq. 2-4 involve V_0… initial reaction rate, V_{max}… maximum reaction rate, K_A, K_B… reaction constants, [A], [B]… concentration of the first substrate A and the second substrate B.

The enzyme activity can be influenced positively or negatively by other substances that are present in the same solution. The inhibition of the enzyme reaction appears to be most abundant and the modifications in the kinetic parameters are compared in Tab. 2-1 for the case of reversible inhibition.

Tab. 2-1: Reversible inhibition and the effect on the kinetical parameters with α and α' as factors for the inhibition efficiency [Leh05b].

Inhibitor type	Apparent V_{max}	Apparent K_m
None	V_{max}	K_m
Competitive	V_{max}	αK_m
Non-competitive	V_{max}/α'	K_m/α'
Mixed	V_{max}/α'	$\alpha K_m/\alpha'$

The irreversible inhibition is another process of enzyme inactivation and is specific for each enzyme. It is caused by substances that form a covalent link or a stable non-covalent interaction with the enzyme, resulting in the blockage of the active site and / or conformational changes [Leh05].

2.5 Crystallization – process and tool

Solid substances own an internal structure that can be crystalline or amorphous. The crystallinity relates to a high degree of regularity within the lattice of molecules. Here, the location of atoms or ions is specific for each substance and can be measured e.g. via x-ray analysis. The process parameters during the crystallization are crucial for the crystal nucleation and the formation of the final macroscopic crystals, as e.g.

temperature, pressure, viscosity and pH influence the final crystal lattice and habit. The habit describes the outer shape of a crystal. On the contrary, crystal polymorphs of the same material may occur that are distinguished by their different arrangement of molecules in the internal crystal structure. The chemical nature of the crystal polymorphs remains the same [McC65, Mye02, Ulr04].

The usage of additives is well known in the industrial crystallization to optimize the crystal morphology and habit. Frequently, the increase of the crystal size and uniformity in the crystal dimensions are desired. The typical motivation for the application of additives can be found in processing issues like pressure reduction in filtration or in shaping for a distinct product design. Additives in the crystallization process are distinguished by the mechanism of action as this is summarized in Tab. 2-2. Regarding a detail view on the fundamentals of crystallization and the modifications of the crystal growth, it is referred to the corresponding literature [Mul01, Mye02, Hof04, San07, Ulr11].

Tab. 2-2: Differentiation of additives within the crystallization process [Lee89, Mee02, Ulr04, San07].

Multifunctional additives	Tailor-made additives
Inorganic crystals as target	Organic crystals as target
Polyelectrolytes, surfactants	Specific interaction with selected crystal faces
Simultaneous interaction with many ions on a crystal surface	Adsorption to the crystal surface; similarity of growth inhibitor to solute molecules
High growth inhibition efficiency	Sterical hindrance interrupts further crystal growth at the affected crystal face

The crystallization of substances in a gel medium is known for more than a century and nowadays regains the scientific attention. It is a traditional method for the production of perfect, faceted single crystals, where the gel structure is used as an inert matrix [Hen96]. The crystal growth of the target substance occurs very slowly in an environment of diffusion limitation. Another aspect is the suppression of sedimentation and additional nucleation because of the gel viscosity [Fos10]. Inorganic, organic and protein crystals can be made with improved characteristics and fewer defects. As gel materials, gelatin, agarose, polyacrylamide, silica and low-molecular-weight gelators such as bis(urea) have been described [McC74, Hen96, Lor09, Fos10]. The crystallization in a gel is used not only for proteins, but also for nucleic acid and viruses intending for structure analysis [Lor09, Sch11].

Furthermore, a gelatin matrix is used as a model system for the lactose crystallization in the food processing [Yuc11]. In the pharmaceutical and in the medical field, the crystallization within gels is used as a tool for the pharmaceutical polymorph screening and for the bone tissue engineering [Laf09, Fos10].

2.6 Release of functional additives from polymeric materials

Hydrogels are polymeric matrices of natural or synthetic origin that are water insoluble, but absorb large amounts of water. The hydrogel undergoes swelling without disintegration and is a feasible material for products in biomedicine, bioengineering, pharmaceuticals, food and agriculture [Mis04, Lin06]. In the design of controlled-release systems, the hydrogels play an important role for the time-dependent drug-delivery. Particularly within this framework of API release, the polymer swelling of hydrogels and the release characteristics of incorporated substances have been described in the past literature and are still in the focus of research [Chi76, Lin06, Sin08, Bor10, Lyo12, Pep12].

Protein-based materials with enzymatically induced cross-linking can be applied as hydrogels [McD04]. However, non-cross-linked, water soluble proteins usually tend to polymer dissolution in an aqueous environment. The mechanism of polymer dissolution involves the solvent diffusion into the polymeric material and polymer chain disentanglement as the two main transport processes [Mil03]. In Fig. 2-2, the process of solvent uptake into the polymer is schematically shown for a dissolving polymer. For a hydrogel, the solvent absorption and the surface layer formation are in principal the same, but without the liquid layer.

Pure polymer	Infiltration layer	Solid swollen layer	Gel layer	Liquid layer	Pure solvent
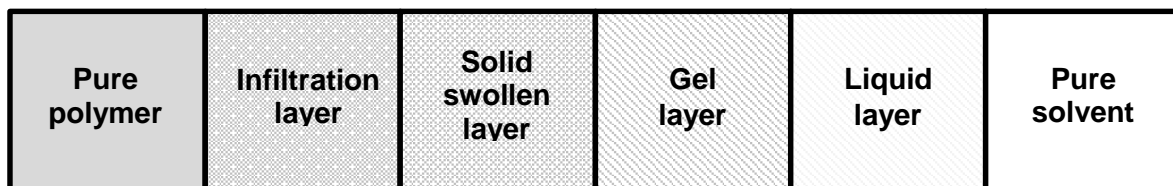
Fig. 2-2: Solvent absorption, polymer swelling and disintegration on the basis of the surface layer formation theory established by Ueberreiter [Ueb68, Mil03].

The release of active ingredients from a polymer therefore is a complex process of solvent absorption, polymer swelling and / or disintegration, dissolution of the target ingredient and its diffusion to the surrounding medium. However, the rather simple power law equation in eq. 2-5 is well capable to give an insight into the operative additive release mechanisms [Kan68, Smi91, Kim92, Mis04, Gan10]:

$$\frac{M_t}{M_\infty} = k \cdot t^n \tag{2-5}$$

The terms M_t [g] and M_∞ [g] refer to the amounts of additive that is released at an incremental time t [s] and in the equilibrium state, respectively. The factor k [s^{-n}] indicates formation of the swelling front. By the factor n [-], the nature of the release mechanism can be determined. In Tab. 2-3 is summarized, how the transport mechanism is distinguished by the diffusional exponent n.

Tab. 2-3: Transport mechanisms and diffusional exponents n in the polymeric network of hydrogels [Kim92, Gan10].

Type of transport	Diffusional exponent n	Time dependence
Fickian diffusion	0.5	$t^{1/2}$
Anomalous transport	0.5 < n < 1	t^{n-1}
Case II transport	1	Time independent

In some cases, the diffusional exponent n is below 0.5 and a classification of the diffusion process might be difficult. Here, Wang [Wan08] mentioned that this mechanism can be still regarded as Fickian behavior. In order to find a differentiation to the real Fickian diffusion, the transport with n < 0.5 is named a less (or pseudo) Fickian behavior.

2.7 Plant nutrition

Besides oxygen and water, plants need 14 essential nutrients that are distinguished in macro- and micronutrients because of the required amounts [Maa13]. These substances are summarized in Tab. 2-4 and are compared to the overall composition of the earth's crust. It is commonly accepted that the bioavailability of the nutrients clearly differs from the element composition of the earth's crust, since a plant requires the nutrients in the form of dissociated ions. E. g. most of the potassium is bound to solid, water insoluble minerals and is therefore not available to the plants.

Tab. 2-4: Comparison of the element composition of the earth's crust by weight [%] and the needs of plant nutrition resulting from the typical relative proportion of minerals found in plant tissue assuming N levels at 100% [Maa13].

Earth's crust composition		Plant tissue levels			
		Macronutrients		Micronutrients	
Oxygen	46.6	Nitrogen	100	Chlorine	0.05
Silicon	27.7	Potassium	50	Iron	0.03
Aluminium	8.1	Calcium	25	Boron	0.03
Iron	5.0	Magnesium	10	Manganese	0.02
Calcium	3.6	Phosphorous	8	Zinc	0.007
Sodium	2.8	Sulfur	5	Copper	0.002
Potassium	2.6			Nickel	0.0004
Magnesium	2.1			Molybdenum	0.0001
All others	1.5				

The plant's complex assimilation processes of nutrients from the soil into the root and the symbiotic associations of fungi and plant roots are described elsewhere [McD01, Mor01, Sch06, Maa13].

The soil composition and the availability of plant nutrients vary to a high extent. Here, the environmental aspects from weather and climate, erosion as well as soil type and pH are important factors [Maa13]. Additionally, the crop rotation and the high nutrition requirements of the recent agricultural used plant varieties may greatly affect the

need for additional fertilization of the soil to balance the nutrient consumption. The various fertilizer types can be classified following Tab. 2-5.

Tab. 2-5: Classification of fertilizers [Sch06].

Organic fertilizers	Synthetic (mineral) fertilizers
Litter and manure from farming	Nitrogen fertilizer (urea, ammonium-, nitrate-based)
Commercially available (peat, guano, horn meal, bone meal)	Phosphate
Secondary feedstock (sewage sludge, compost, digestate)	Potassium and magnesium
	Lime
	Micronutrients

The organic fertilizers have a slow release rate, since the complex organic matter has to be converted first by the soil microorganisms to the inorganic, water soluble matter that is available to a plant. Drawbacks of organic fertilizers are the less precise knowledge on the nutrient composition, the typically low nutrient content and the possibility of nitrogen depletion by a microorganism action. Comparing the synthetic fertilizers with the said issues, it is obvious that the composition of a synthetic fertilizer is always known and the nutrient content can be tailored according to the soil requirements. Limitations of synthetic fertilizers are seen in the fast leaching due to the high water solubility and the risk of overdosage, which leads to desiccation of the plants [Sch06, Hat11].

3. Motivation and aim

The approach of ecological product design aims for the minimization of any environmentally destructive impacts of a product within its whole life cycle [Bra97]. One important feature of innovative, sustainable products is the integration of bio-based materials. In order to achieve completely new product benefits and tailor-made material properties, however, the simultaneous consideration of both product and process design is highly necessary [Ste10].

Protein-based matrices are well known as carriers and release systems for pharmaceutically active substances or as environment for controlled crystal growth. Frohberg [Fro10a] first combined these traditional applications to introduce a new field of research in both material sciences and industrial crystallization. Here, protein-based films, sheets and coating contain homogeneously distributed micro-scale crystals of functional additives. The functionality of those crystallizing additives is reasoned in their controlled release from the material in order to function at the site of purpose and with a specified aim.

As one product example of protein-based films with incorporated crystallized additives, Frohberg [Fro10a] proposed the agricultural films, where additional benefits in the biodegradability of the material and the controlled fertilizer release are expected. The possibilities of functional additives and applications are of course manifold. But considering the agricultural mulching films and seed tapes, the advantages in the product design are the nearness to the final product and the high potential in scaling up the production process. Therefore, the application of the biobased films and inner-film crystallized fertilizing agents is investigated as the model product design approach within this work.

Regarding the process design, special attention is paid to the crystal growth of the fertilizer salts, the crystal size and the crystal morphology and their modification by secondary additives. These factors mainly influence the film's appearance and product quality and are seen to also affect the additive release properties.

Other parameters are in relation with the additive crystallization, but have been analyzed mainly according their effect on the material's mechanical and barrier properties combined with the preservation of the product quality:

- Application of enzymatic cross-linking during the film manufacture
- Regime of drying the protein-based films
- Environmental conditions for storage

The crystal growth control via specific additives is a common technique in the industrial crystallization, but a completely new approach for protein-based matrices. With the analyzed process parameters, it is intended to give recommendations for achieving an optimum product design that is demonstrated in a product test.

4. Materials

4.1 Sodium caseinate

The protein fraction in bovine milk consists of approximately 80 % casein and 20 % whey protein. Casein protein is extracted from skim milk by precipitation at its isoelectric point (pI) at pH 4.6. Casein is further distinguished into the sub-fractions α_{S1}-, α_{S1}-, β- and κ-casein differing in molecular weight and amino acid sequence. Despite that, the pI was analyzed to be roughly the same for all casein fractions.

The backbone of the casein's polymeric structure is the primary sequence of the 20 L-amino acids that is schematically drawn in Fig. 4-1. During manufacture of casein, the colloidal calcium phosphate is removed from the casein micelles. Therefore, casein and its derivatives are able to form films from aqueous solutions due to its random coil structure and its ability to form weak intermolecular interactions [Enn00, Jos07, Mar07, Men10, Pos12].

Casein fraction	MW [g/mol]	Amount [%]
α_{S1}-casein	24,529	39-46
α_{S2}-casein	26,019	8-11
β-casein	25,107	25-35
κ- casein	21,269	8-15
γ-casein	---	(degraded β-casein)
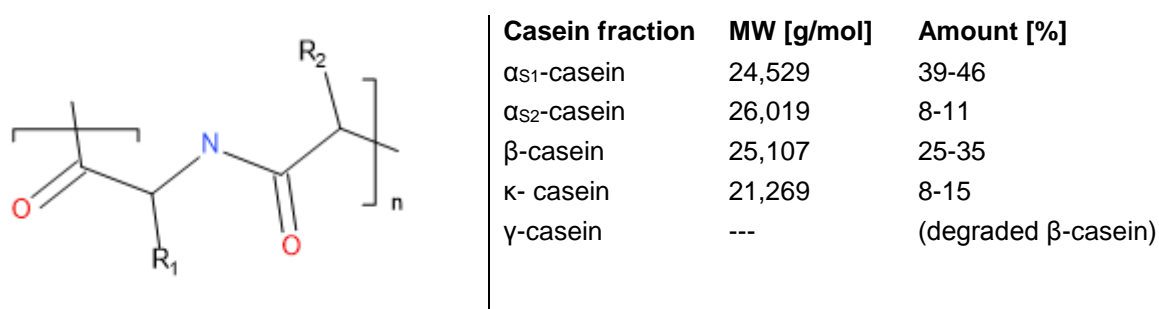
Fig. 4-1: Detail from polymeric structure of caseins (two amino acids linked with peptide bond) and information on bovine casein fractions [uniprot, Kam07].

Sodium caseinate is better water-soluble then the casein precipitate and is produced from fresh, acid casein curd or dried casein curd by reaction with usually 2.5 M NaOH to adjust the final pH to 6.6 – 6.8 [Enn00, Var01].

Technical caseinate as raw material for non-food applications is derived from non marketable milk obtained e.g. from cows with mastitis infection. In Germany, this kind of milk can amount to up to 2 million tons per year. Another source is the so called surplus milk resulting from production exceeding the milk quota given by EU regulations [Bad05, Fis11].

4.2 Glycerol

Glycerol (1,2,3-propanetriol; Fig. 4-2) was supplied by Caldic with purity of 99.5 %. The trivalent alcohol is usually a by-product from biodiesel production and is prepared by the hydrolysis of fats. Also synthesis from petrol-based propylene is possible. It owns a colorless, odorless, viscous and hygroscopic appearance and sweet taste. It is completely miscible in water, aqueous buffer as well as ethanol. As non-toxic, non-irritating and even edible chemical with no negative impact on the

environment, glycerol is being extensively using e. g. in food industry and pharmaceuticals, cosmetics and toiletries to function as humidifier, sweetener, solvent, preservative or filler [Mag98, Cog07, Agl10].

Molecular weight	92.1 g/mol
Density (20 °C)	1.263 g/cm³
Viscosity (20 °C)	1760 mPa·s
Melting point	18 °C
Boiling point	290 °C
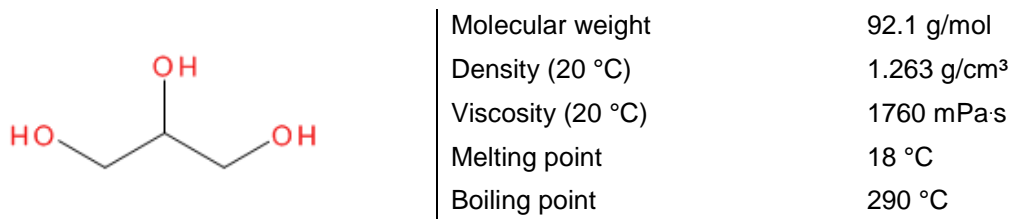
Fig. 4-2: Chemical structure of glycerol and property data [Che95b, Oga00, Cog07].

The ability of glycerol as plasticizing agent in biopolymers is well described in literature and is further described in chapter 2.3.1. Especially, the protein-based materials are known to benefit from the addition of glycerol if high material flexibility is desired. Therefore, glycerol has already been incorporated into a variety of protein systems from animal and plant origin [Her08, Gon10, Kow11, Wit12, Nur13].

4.3 Transglutaminase

Transglutaminases (EC 2.3.2.13, protein-glutamine γ-glutamyltransferase) occur in eukaryota and prokaryota with the general function to induce covalent bonding of proteins and peptides. The enzymatic catalysis is performed by an acyl transfer between the γ-carboxamide group of one protein-bound glutamine and primary amines, e.g. the ε-amine group of a protein-bound lysine. The reaction leads to an ε-(γ-glutamyl)-lysyl isopeptide bond being typical for enzymatic cross-linking of proteins. The reaction mechanism is shown in Fig. 4-3 as well as the 3D enzyme structure.
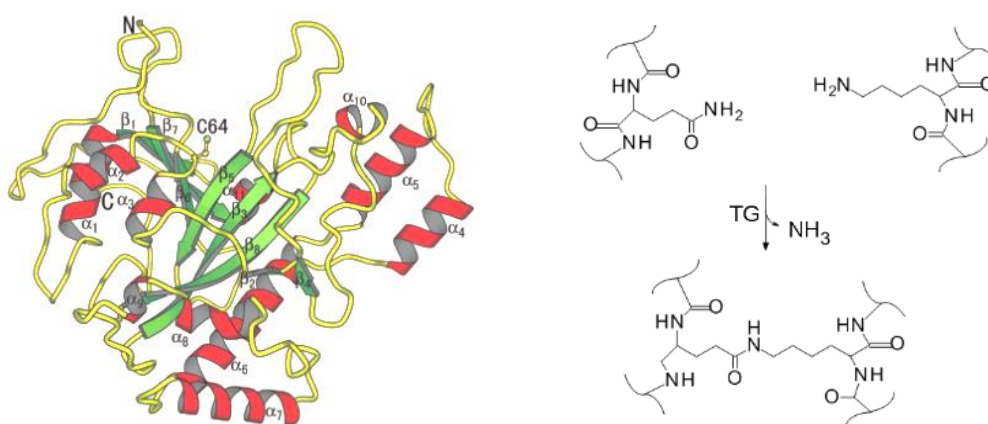
Fig. 4-3: Illustration of the transglutaminase molecule from *Streptomyces mobaraensis* [Kas02] and the enzymatically mediated cross-linking reaction, modified from Büttner [Büt11].

The microbial transglutaminase (MTG) was first observed in *Streptomyces mobaraensis*, is Ca²⁺ independent – despite eukaryotic variants – and owns a molecular weight of approximately 38,000 g/mol and isoelectric point at pH 8.9. The MTG molecule was found to form a single, compact domain and a disk-like shape.

The active site is located in a cleft of the molecule with Cis^{64} as the essential amino acid residue for the catalytic activity [And89, Kas02, Seg02, Zhu08, Büt11, Zha12].

The microbial transglutaminase used in the commercially available formulation Activa® WM (Ajinomoto Foods Deutschand, Hamburg) is extracted and purified from the non-GMO *Streptomyces mobaraensis* [Aji13]. Activa WM exhibits a specific TG activity of approximately 100 U/g and contains 1 % w/w of enzyme and 99 % w/w dextrin as stabilizer and filler. According to the specification given by Ajinomoto, Activa WM is applicable in a relatively wide range of reaction conditions. The enzyme is active in a pH range of pH 4-9 and temperature range 40-60 °C with optima at 50 °C and pH 7. Inactivation of the MTG occurs already at temperatures being higher than 40 °C; very fast denaturation can be observed at temperatures higher than 60 °C [Yok04, Küt05, DiP06, Gra12, Aji13].

Microbial transglutaminase is extensively used in food industry to affect functional properties like solubility, water-binding and emulsifiying capacity, foaming, viscosity, elasticity and gelation [Lic04, Jar06]. Important applications are the reconstruction of meat and fish, gelation of milk products, and the improvement of the dough rheology in bread making [Ful09, Car10, Del10, Mor10, Ony10, Bec11, Sta13]. In medicine and pharmaceutics as well as surgery, especially the mammalian transglutaminases are of high research interest, both in terms of therapy and diagnostics of diseases (e. g. in blood coagulation, celiac disease). Other applications are the assembly of artificial tissue / skin and development of wound sealants as described elsewhere [Die97, Gre91, Jac01, Col09, Mut10, Ala11, And11].

Covalent cross-linking is a general method for improvement of functionality, mechanical performance and binding of a variety of active components in textile and leather production, cosmetics and especially in biopolymer technology. Referring to chapter 2.3.3, enzymatic cross-linking of MTG is the non-toxic and natural alternative for the typical use of bifunctional chemicals lacking social and economical acceptance due to health and safety reasons [Jar06, Ike08, Gho09, Por11].

4.4 Potassium nitrate and secondary additives

Fulfilling the purpose of product design, polymer materials can be equipped with functional additives / active ingredients that are incorporated into the polymer matrix to provide an additional benefit as outlined in chapter 2.3.2. Potassium nitrate is known to act as plant fertilizer in the agriculture and horticulture Its potassium (K) and nitrogen (N) content is rapidly available to the plant metabolism since the salt dissolves easily in water followed by direct absorption of the dissociate ions by the plant roots [Pla08]. Therefore, KNO_3 is a supplementary nitrogen (N) source in the

protein-based material as the N rich protein polymers have to be proteolysed by soil microorganisms prior to absorption into the plant roots [Cre01, Son07].

The KNO₃ was already proven to crystallize within a protein-based material because of solvent evaporation during the drying step of the materials manufacture [Fro10]. Additionally, the usage of KNO₃ shows high potential to affect the material properties and thus, it was chosen as model substance for inner-film crystallizing additives in a protein matrix. The key material data of KNO₃ are to be found in Fig. 4-4 that also provides the chemical structure of this inorganic salt. The high water solubility of KNO₃ can be described as quadratic function based on literature data in mass of solute per mass of solvent [Mer04]:

$$Y[g_{anh}/kg_{H2O}] = 0.1776 \cdot T[°C]^2 + 5.5174 \cdot T[°C] + 139.34 \tag{4-1}$$

Molecular weight	101.11 g/mol
Melting point	334 °C
Density (20 °C)	2.109 g/cm³
Water solubility (20 °C)	320 g/L
pH (50 g/L at 20 °C)	5.0-7.5
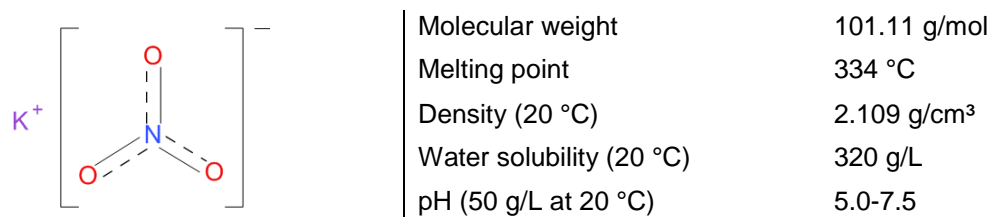
Fig. 4-4: Chemical structure of KNO₃ and material data from MSDS: article no. P021.3, purity ≥ 99 % p.a., Carl Roth GmbH, Karlsruhe.

The polymorphism of KNO₃ was already discovered and investigated in the early years of the 20ᵗʰ century. In the literature, seven crystalline KNO₃ polymorphs are described [Bri16, Kra29, Dav63, Rap65, Hol75, Nim76, Sco87, Rol97]. Their occurrence is dependent on both temperature and pressure. At room temperature normal pressure, the phase-II KNO₃ is the thermodynamically stable polymorph having an orthorhombic crystal structure of which several crystal habits are displayed in Fig. 4-5. Orthorhombic KNO₃ usually grows in elongated, needle-like shape with an aspect ratio L_1/L_2 of about 4:1. Thus in the field of industrial crystallization, the crystal habit of phase-II KNO₃ is desired to be influenced e.g. by specific growth inhibition induced by a variety of additives [Kip97, Her97, Yua07].
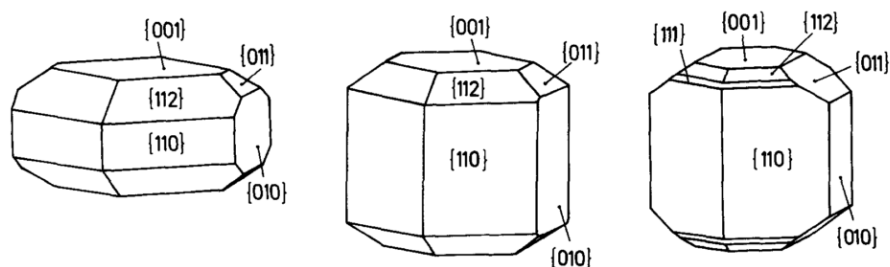
Fig. 4-5: Orthorhombic KNO₃ crystals and nomenclature of crystal faces [Rol97]

KNO₃ is also applied in the formulation of explosives and propellants and is mentioned nowadays as promising material for electronic equipment. Related to the new application, the research interest is driven to production and stabilization of the

phase-III KNO_3 polymorph as it exhibits ferroelectric behavior. Above 128 °C, the phase-II KNO_3 transforms to the phase-I polymorph with trigonal, calcite structure. Out of phase-I, the trigonal phase-III KNO_3 forms when the salt is cooled below 128 °C. Phase-III KNO_3 is metastable at room temperature and can be distinguished from phase-II KNO_3 by crystal habit and XRPD pattern [Ken72, Sch88, Eng02, Kum03, Kum05, Fre09].

From the mixture of KNO_3 and NH_4NO_3 in an aqueous solution, $[K_x(NH_4)_{1-x}]NO_3$ solid solutions are obtained. The ratio of K^+ and NH_4^+ inside the mixed crystal is dependent on the amount of both substances in the aqueous solution. As the system tends to formation of a variety of metastable salts, the information on the crystal lattice and habit is divergent [Whe48, Coa61, Hol75, Cad81, Dej00, Chi05a, Chi05b]. The solubility isotherm of the ternary $KNO_3 - NH_4NO_3 - H_2O$ system was mathematically described by Dejewska [Dej00]:

$$y_1 = 27.62 - 0.3681 \cdot x_1 + 1.102 \cdot 10^{-3} \cdot x_1^2 + 2.693 \cdot 10^{-4} \cdot x_1^3 - 4.447 \cdot 10^{-6} \cdot x_1^4 \qquad (4\text{-}2)$$

with y_1 concentration of KNO_3 in solution [% w/w]

           x_1 concentration of NH_4NO_3 in solution [% w/w]

In Tab. 4-1, other substances are summarized that have been used in the experimental work to affect the inner-film crystallization in protein-based materials. These substances will be named secondary additives in order to avoid confusion with KNO_3 as the main additive studied.

Tab. 4-1: Secondary additives screened for impact on specific crystal growth of potassium nitrate. Information on chemical properties from material safety data sheets given by the supplier.

Substance		Supplier /article no.	Chemical properties
Ammonium nitrate (anhydrous)	NH_4NO_3	Sigma-Aldrich 221244 ≥ 98 % ACS reagent	MW: 80.04 g/mol Melting point: 169 °C Density: 1.72 g/cm³ (20 °C) Water solubility: 2.130 g/L (25 °C) pH: 4.5-6.0 (80.4 g/L at 25 °C)
Calcium dihydrogen phosphate monohydrate	$Ca(H_2PO_4)_2*H_2O$	Sigma-Aldrich 21053 ≥ 85 % p.a.	MW: 252.07 g/mol Melting point: no data Density: no data Solubility in water: soluble pH: no data
Citric acid (anhydrous)	$C_6H_8O_7$	Roth X863.2 ≥ 99.5 % p.a.	MW: 192.13 g/mol Melting point: 153-159 °C Density: 1.67 g/cm³ (20 °C) Solubility in water: 650 g/L (20 °C) pH: 1.7 (100 g/L at 20 °C)
Potassium chloride (anhydrous)	KCl	Roth 6781.1 ≥99.5 % p.a.	MW: 74.56 g/mol Melting point: 770 °C Density: 1.984 g/cm³ (20 °C) Solubility in water: 330 g/L (20 °C) pH: 5.5-8.0 (50 g/L at 20 °C)
Sodium dodecyl sulfonate (anhydrous)	$C_{12}H_{25}NaO_3S$	Roth KK52.1 ≥ 99.0 % for ion pair chromatography	MW: 272.37 g/mol Melting point: no data Density: no data Solubility in water: soluble pH: 5.5-7.5 (100 g/L at 20 °C)
Urea (anhydrous)	CH_4NO_2	Roth 3941.1 ≥ 99.5 % p.a.	MW: 60.06 g/mol Melting point: 132-134 °C Density: 1.34 g/cm³ (20 °C) Solubility in water: 1000 g/L (20 °C) pH: 9.0 (100 g/L at 20 °C)

5. Methods

5.1 Manufacturing of protein-based films

For the lab-scale production of protein-based films, the wet process is seen to have several advantages compared to the extrusion techniques: the casting method can be easily adapted to laboratory equipment as well as the casting procedure is a relatively fast and material-saving method for the testing of new material compositions. Compared to automated techniques, a preceded adjustment of the process parameters is usually not required. The procedure of film casting below described was designed in accordance to Oh et al. [Oh04] and further modified to meet the current objective [Fro10, Pat10a, Gäl11, Sto12].

Experimental

The film forming solution comprised of protein to an amount of 5.0 % wt/wt which was dispersed in an aqueous buffer (20 mM Tris/HCl pH 7) containing glycerol (2.5 % wt/wt) as plasticizing agent. The whole procedure is summarized in Fig. 5-1. In case of gelatin as the raw material for protein-based films, the procedure had to be slightly modified as the dispersed gelatin particles needed to become hydrated in the film forming solution at RT within 30 min prior to further processing. Complete dissolution of the protein was reached after 30 min of magnetically stirring at 90 °C and 300 rpm.
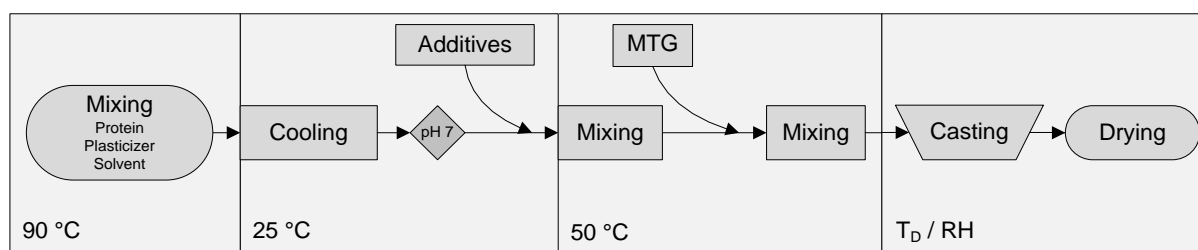
Fig. 5-1: Lab-scale production of protein films by the wet process including the application of enzymatic cross-linking, incorporation of additives as well as varied environmental conditions during film formation and drying.

Inner-film crystallized additives

When drying the film forming solution, a herein dissolved additive would crystallize according to its solubility in the solvent. As additives, inorganic salts and other substances were added to the film forming solution according to Fig. 5-1 and the content within the material is expressed in a protein/additive mass ratio.

Enzymatic cross-linking

For cross-linking of the protein molecules, microbial transglutaminase (MTG, EC 2.3.2.13, Activa™ WM by Ajinomoto Co., Inc.) was added to the film forming solution to an amount of 25 U/g protein. Prior to this step, the temperature of the film forming

solution was set to 50 °C and the pH was adjusted to pH 7 with 1 M NaOH in order to reach optimum reaction conditions for the enzyme. Subsequently, the solution was casted into a 200 x 200 mm PTFE mold in order to evaporate the solvent and to induce film formation.

Monitoring of the drying process

The water evaporation from the film forming solution was accelerated by air ventilation and dried films have been peeled off the PTFE surface after 24 h. Films with approximately 200 µm in thickness were obtained. To reach stable environmental conditions, the molds were placed in a lab room, where constancy of RT could be guaranteed and the air humidity was stabilized to 50 % RH with an additional air humidifying system.

The main process parameters during film drying are the drying temperature T_D and the air humidity. To get an insight into the impact of these environmental conditions on the final products mechanical properties and inner-film crystalline structure, both parameters have been varied according to the experimental design given in Fig. 5-2.

Fig. 5-2: $2^{(3-0)}$ full factorial design for the investigation on the impact of the drying conditions (T_D; RH) on the properties of NaCas films.

The protein films were casted into the PTFE molds being placed into an environmental chamber (Climats EX2221-MA, France) and exposed to the chosen drying conditions for 12 h. The temperature was altered in the range from 25 to 75 °C and for the relative air humidity, a range from 25 to 75 % RH was defined. In the factorial design, (-1) represents the lowest value in the range, (0) was chosen for the interim value and (+1) characterizes the upper limit of the selected range. Following the drying step, the process parameters T and RH were switched to storage conditions that are 25 °C and 50 % RH as mentioned above. For comparison of the influence of both enzymatic cross-linking and the effect of KNO_3 as additive (protein/additive ratio 6:1) in NaCas films, each combination of drying parameters was tested with four film compositions as described in Tab. 5-1.

Tab. 5-1: NaCas films dependent on enzymatic cross-linking and KNO_3 addition.

Film	KNO₃	Activa MTG
A	-	-
B	+	-
C	-	+
D	+	+

The dependency of water evaporation on the drying conditions was gravimetrically determined by weighing the entire films during drying within the casting frames as well as during the time of storage.

5.2 Screening for face specific KNO₃ growth inhibitors by solution crystallization

The solution crystallization in the batch mode is in general a versatile and important unit operation and is commonly applied throughout the chemical industry as well as for research purposes [Wey02, Cho04, Wie13]. Compared to continuous systems, the batch process can be controlled more easily and is therefore a widely used technique for studying crystal nucleation and growth as well as for testing of monitoring equipment. Crystallizers are distinguished into four classes, dependent on their principle of reaching supersaturation: cooling, evaporative, reaction and salting-out crystallizers [Wey02, Fit12]. In case of cooling crystallization, heat exchange from the hot solution / suspension to the coolant is applied in order to reach a certain cooling profile. For KNO₃ as target substance, cooling crystallization from aqueous solvent is beneficial due to a very strong temperature dependence of its water solubility [Wey02, Mer04].

Experimental

The inhibiting effect of various substances on specific crystal faces of KNO₃ was determined by cooling crystallization from an aqueous solvent. An experimental setup of ten temperature-controlled double-walled beakers shown in Fig. 5-3 was used to screen several potential substances and concentrations simultaneously.
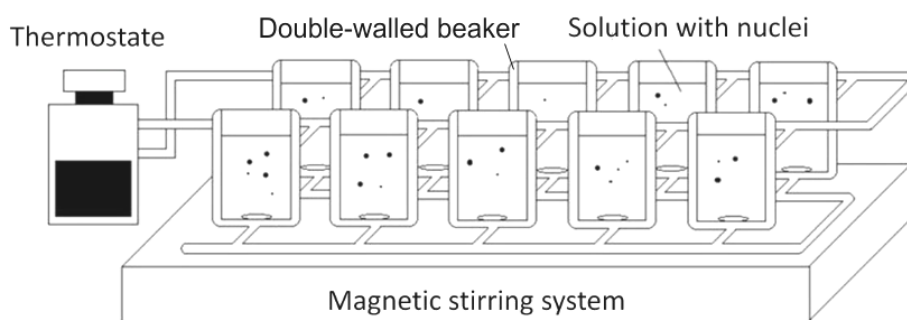
Fig. 5-3: Experimental setup for growth inhibitor screening by batch cooling crystallization [Buc11].

Each beaker contained 20 mL of aqueous solvent (distilled water or buffer) with a KNO₃ concentration of 466 g_{Anh}/kg_{H2O} as well as the amount of substance (see Tab. 5-2) to be screened [Mer04]. The supersaturation of the KNO₃ solution was set by cooling from 50 °C to 25 °C with a constant rate of 5 K/h. Therefore, a relative supersaturation of 1.2 was reached, which was high enough to induce nucleation [Tit03]. After cooling, the temperature of the batches was kept constant at 25 °C for 12 h before the grown crystals were separated from the mother liquor by vacuum

filtration. The crystals have been rinsed first with a pure KNO_3 solution saturated at 25 °C, second with isopropanol and eventually dried at ambient conditions. During the analysis of the crystalline particles, particular attention was paid to the determination of the crystal length and its distribution, which was carried out applying light microscopy (Keyence VHX 500F, Japan) and digital image analysis with the software package analySIS 5.0, Soft Imaging System, Germany.

Tab. 5-2: Substances screened for specific KNO_3 phase inhibition. Given ratios are based on molarity.

Substance	Amount	Reference
Tris	0.86 M Tris/HCl pH 7 buffer	-
Glycerol	Glycerol / KNO_3 3:1, 1:10, 1:100, 1:1000	-
Urea	Urea / KNO_3 1:10, 1:100, 1:1000	-
Dextrine	Dextrine / KNO_3 1:100, 1:1000	-
NH_4NO_3	NH_4NO_3 / KNO_3 1:10, 1:100, 1:1000	[Cad81, Coa61, Wu08]
KCl	KCl / KNO_3 1:10, 1:100, 1:1000	-
$Ca(H_2PO_4)_2$	$Ca(H_2PO_4)_2$ / KNO_3 1:10, 1:100, 1:1000	-
Sodium dodecyl sulfate	20 mg/L	-
Sodium dodecyl sulphonate	20 mg/L	[Yua07]

The investigation on the inhibition of KNO_3 crystal elongation was carried out stepwise in order to determine the effect of an individual substance and impact interferences due to the multi-component biopolymer system. First, KNO_3 crystals were obtained from a two-component batch cooling crystallization only and the crystal morphology was analyzed. In case of promising results, the plasticizing agent and buffer as other components of NaCas films was added to the solution of KNO_3 and its crystal growth inhibitor. Final tests have been performed by producing the NaCas films with incorporated KNO_3 and these secondary additives which had been identified previously to be the most effective inhibiting substances [Sto12b].

5.3 Manufacture of protein-based seed tapes and sheets and plant growth tests

In order to study the effect of protein-based materials on plant germination and growth, radish (*Raphanus sativus var. sativus*) and lettuce (*Lactuca sativa var. capitata*) had been chosen as model plant organisms.

Seeding of radish

For the manufacture of seed tapes with radish seed, protein-based carrier material was produced applying the casting apparatus presented in Fig. 5-4. NaCas was used as raw material and the film forming solution was prepared identically to the production of protein-based films that had been explained in chapter 5.1 regarding the non-cross-linked material (tap water instead of Tris buffer). The composition of the film forming solution had to be adapted to the half of the film surface (0.02 m²)

compared to square film of 0.04 m². Therefore, the aqueous solution contained 2.5 % wt/wt NaCas, 1.25 % wt/wt glycerol and an additive, if indicated.
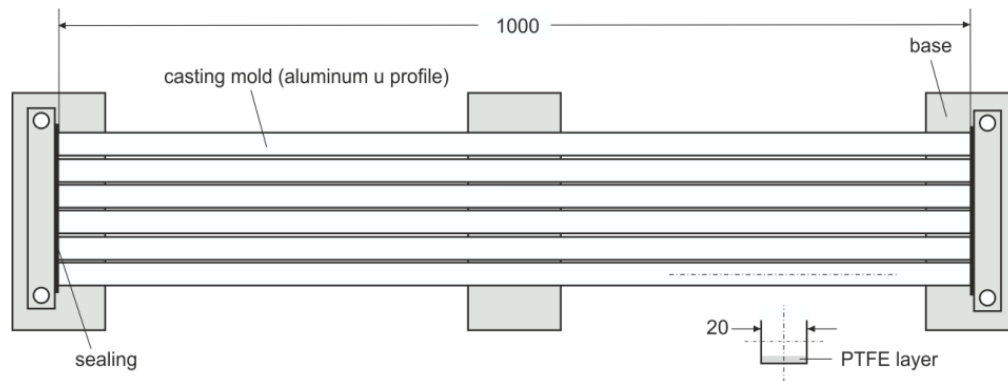
Fig. 5-4: Apparatus (top view) for casting of protein-based carrier material 1000 x 20 x 0.2 mm for seed tapes. With the setup, 6 seed tapes can be produced simultaneously. Plant seeds are to be put into the polymer after 80 % of water evaporation.

Functional additives within the protein-based material were tested for their applicability as fertilizing agents and / or in product design (see Tab. 5-3). The seed tapes with protein film are to be compared with conventional seeding techniques.

As environment, a greenhouse was chosen with conditions 25±5 °C and 40±10 % RH to avoid weather fluctuations during the test. The Potting soil "Floradur B fein" was used, which is a tray substrate with moderate pre-fertilization (0.8 kg/m³, NPK 18/10/20). In each planting pot of dimensions 100 x 18 x 14 cm, 30 radish seeds were placed with seed distance of 3 cm applying the different seeding methods and covered with 1 cm of soil. The latter was then frequently watered (1 x a day) and lighted with natural sun light that had been available for 15 – 16 h per day according to sunset and sundown times for Halle (Saale) in the months May and June.

The seed germination and plant growth was recorded each day and the radish plants have been harvested after 30 days of cultivation and plants have been weighted in total and root only. Each test result refers to analysis of at minimum 20 plants.

Tab. 5-3: Seeding of radish. Experimental planning for investigation and comparison of different seeding techniques.

No.	Seeding technique	Description
R1	Bulk seed	Radish (*Raphanus sativus var. sativus*) Item no. 485 from Kiepenkerl, Germany (as for all the following)
R2	Paper-based seed tape	Item no. 3036 from Kiepenkerl, Germany Seed distance: 3 cm
R3	NaCas-based seed tape	From NaCas film forming solution With radish seed from Kiepenkerl, Germany, item no. 485 Seed distance: 3 cm
R4	NaCas-based seed tape + KNO$_3$	From NaCas film forming solution NaCas / KNO$_3$ = 3 : 0.23 (*) With radish seed from Kiepenkerl, Germany, item no. 485 Seed distance: 3 cm
R5	NaCas-based seed tape + Nutrition dye (red)	From NaCas film forming solution 500 µL of ready-made red nutrition dye (Schwartau, Germany) With radish seed from Kiepenkerl, Germany, item no. 485 Seed distance: 3 cm

(*)   According to average nitrogen requirement of 6 g N/m² for radish [Lan12, Sta11b, Wwe05]

Nitrogen content of casein: 2.93 % w/w [Wol13]

Nitrogen content of KNO$_3$: 13.9 %w/w

Surface area of seed tape: 0.02 m²

→ N in 3 g casein = 0.09 g per 0.02 m²

→ N nutrition gap: 0.03 g per 0.02 m² filled with addition of (R4) 0.23 g KNO$_3$

Seeding of lettuce

The incorporation of the lettuce seed (*Lactuca sativa var. capitata*) into the protein-based carrier material was done by embedding it between two films based on NaCas and seed sheets have been obtained. The arrangement of the seed grains followed the design given in Fig. 5-5. Same as for radish seed tapes, the film forming solution for the material was prepared and casted likewise shown in chapter 5.1 for non-cross-linking films. Tap water was used as solvent and the composition of the film forming solution had to be adapted to the half of the film thickness (100 µm) to reach a final film thickness of 200 µm for the double layer: 2.5 % wt/wt NaCas, 1.25 % wt/wt
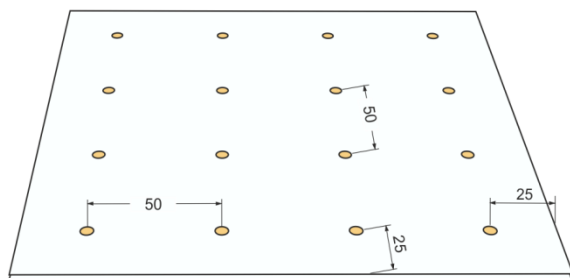
Fig. 5-5: Schematic drawing of a double-layer seed sheet 200 x 200 mm with lettuce seed (*Lactuca sativa var. capitata*).

glycerol and an additive according to the tests summarized in Tab. 5-4. The amount of fertilizing additive was calculated from the nitrogen requirement of lettuce, which exhibits moderate nitrogen consumption of approximately 10 g N/m² [Sta11b]. The seed sheets were produced by first casting and drying two films, followed by pouring 20 g of water on one film, arranging the lettuce seeds, applying of the second layer on top and finally drying the double layer sheet for 24 h with air ventilation.

Tab. 5-4: Seeding of lettuce. Experimental planning for investigation and comparison of different seeding techniques. Double-layer seed sheet assembled of 2 NaCas films 200 x 200 x 0.1 mm.

No.	Seeding technique	Description
L1	Bulk seed	Lettuce (*Lactuca sativa var. capitata*) Item no. 2461 from Kiepenkerl, Germany (as for all the following)
L2	Pilled seed	Item no. 2462 from Kiepenkerl, Germany
L3	Paper-based seed tape	Item no. 2453 from Kiepenkerl, Germany Seed distance: 5 cm
L4	NaCas-based seed sheet (double layer)	From NaCas film forming solution with lettuce seed from Kiepenkerl, Germany, item no. 2461 See Fig. 5-5 for seed alignment
L5	NaCas-based seed sheet (double layer) + KNO_3	From NaCas film forming solution NaCas / KNO_3 = 6 : 1.61 (*) with lettuce seed from Kiepenkerl, Germany, item no. 2461 See Fig. 5-5 for seed alignment
L6	NaCas-based seed sheet (double layer) + urea	From NaCas film forming solution NaCas / urea = 6 : 0.48 (*) with lettuce seed from Kiepenkerl, Germany, item no. 2461 See Fig. 5-5 for seed alignment

(*)   According to average nitrogen requirement of 10 g N/m² for radish [Sta11b]
Nitrogen content of casein: 2.93 % w/w [Wol13]
Nitrogen content of KNO_3 : 13.9 %w/w   Nitrogen content of urea: 46.6 % w/w
Surface area of seed sheet: 0.04 m²
→ N in 6 g casein = 0.18 g per 0.04 m²
→ N nutrition gap: 0.22 g per 0.04 m² filled with addition of (L5) 1.61 g KNO_3 and
   (L6) 0.48 g urea

The seeding tests were carried out in a greenhouse ensuring constant environmental conditions of 25±5 °C and 40±10 % RH. Natural light was provided being available for 15-16 h per day in the months May and June in Halle (Saale). The standard soil ("Einheitserde Classic" with low fertilizer content (80 mg N/L, 80 mg P_2O_5/L, 80 mg K_2O/L), Einheitserde- und Humuswerke, Germany) equipped with additional fertilizer (Blaukorn NPK 14+7+17, Compo, Münster, Germany). Planting pots of size 33 x 20 4 cm have been filled with 13.2 L of soil mixed with 35 g/m² of fertilizer.

The seed germination and plant growth was recorded each day and the lettuce plants have been harvested after 30 days of cultivation. The documentation included the success in seed germination expressed as germination rate as well the gravimetrical determination of the biomass per plant after harvest.

5.4 Analytical methods

5.4.1 Mechanical properties

In many common applications, polymers are exposed to uniaxial stress. Therefore, the uniaxial mechanical response is a key parameter for the material and is usually identified from tension experiments [Bra12, Roy08]. In the field of polymer films, the tensile specimen is usually a rectangular piece from the distinct material with defined gage length and width that is clamped into a testing apparatus and stretched into one direction until rupture. Data collection of the tensile test herein involves the recording of tensile force vs. the increase of the gage length [Dav04, DIN96]. From the materials stress-strain curve, the amounts of elastic and plastic deformations as well as material-specific mechanical parameters are read out as this is demonstrated in Fig. 5-6. As protein-based films exhibited ductility with yield point, this material behavior is specified.
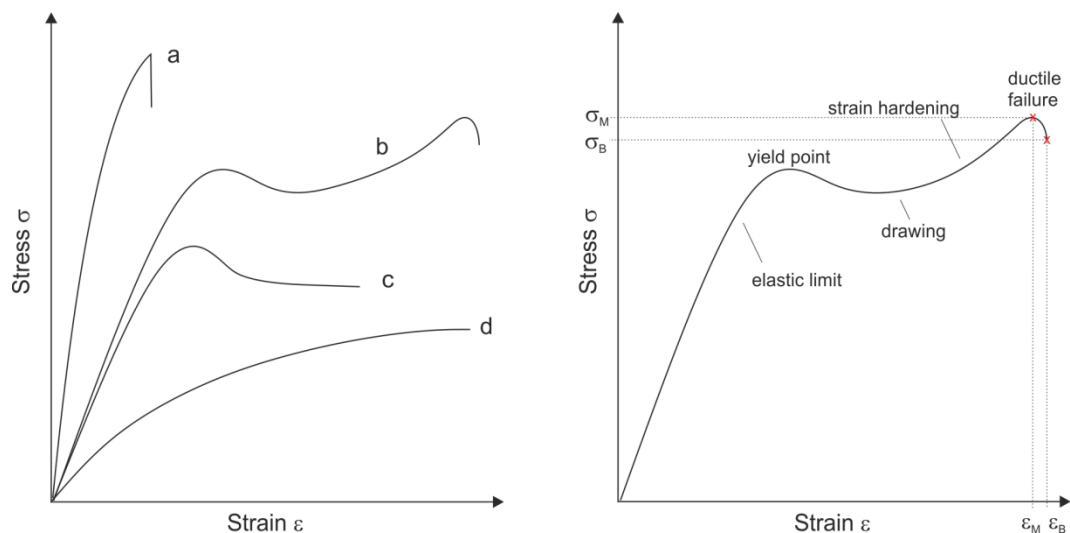
Fig. 5-6: Stress-strain curves showing typical material behavior: (a) brittle; (b, c) ductile with yield point; (d) ductile without yield point [DIN96, Roy08].

In this work, tensile strength σ_M and elongation at break ε_B had been identified as crucial parameters for the mechanical performance of protein-based films. The Young's modulus E as the parameter of the elastic strain region is of minor importance in the technology of polymer films and will therefore not be discussed in detail [Nen06].

Tensile strength and engineering stress

The tensile strength σ_M refers to the highest value of tensile stress [DIN96, Dav04]. Herein, the tensile stress (or engineering stress) is dependent on the uniaxial tensile force measured during the test as well as the effect of the initial cross-sectional area of the specimen [DIN96, Roy08].

$$\sigma_M = \frac{F_M}{A_0} \qquad (5\text{-}1)$$

with σ_M tensile strength   [MPa]

        F_M maximum force   [N]

        A_0 initial cross-sectional area of specimen [mm²]

$$A_0 = w \cdot h \qquad (5\text{-}2)$$

        w   width   [mm]

        h   height   [mm]

Resulting from the film casting as production process, the protein-based films had not been subjected to drawing and thus, the films did not exhibit an axial dependence in their mechanical properties. For this reason, no differentiation in longitudinal and transverse direction was made as this would be generally the case for extruded films [Nen06, Fro10b].

Elongation at break and engineering strain

The engineering strain is defined as the change in gage length related to the initial gage length of a specimen [DIN96]. As visualized in Fig. 5-6, the elongation at break ε_B is then the maximum strain at fracture of the specimen.

$$\varepsilon_B = 100 \cdot \frac{\Delta L}{L_0} = \frac{L - L_0}{L_0} \qquad (5\text{-}3)$$

with ε_B elongation at break   [%]

        L_0 initial gage length   [mm]

        ΔL change in gage length   [mm]

        L   final length   [mm]

Regarding ductile materials, the fracture happens after achieving the yield point. In that case, a distinction in the strain parameters at break is made according to the standard DIN EN ISO 527-1 and it is spoken of the nominal tensile strain ε_{tB} [DIN96].

Experimental

The mechanical performance of polymer films was measured according to the standard DIN EN ISO 527-3 using the test equipment BDO-FB0.5TH (Zwick GmbH & Co. KG, Ulm) combined with the TestXpert II software version 1.42 for data analysis and plotting [DIN03a]. Prior to mechanical testing, the obtained films had to be

equilibrated for 48 h above saturated $Ca(NO_3)_2$ at 25±2 °C and 50±3 % RH as it is defined the standard. Following that, specimens were cut from the films with the help of a twin-blade roller knife [Pat10a]. The parameters for the testing procedure and the chosen specimen dimensions are summarized in Tab. 5-5. Each film specimen was measured in triplicate for its thickness with a micrometer screw and the average value was used for the data processing. Finally, the test specimens were aligned into the pneumatic grips. During the tensile test, the specimens were stretched until fracture.

Tab. 5-5: Parameter setting of the testing machine as well as specimen dimensions for the tensile test according to DIN EN ISO 527-3.

Parameter of testing machine	Value	Unit
Preload	0.1	N/mm²
Testing speed	50	mm/min
Speed tensile modulus	1	mm/min
Gage length (t = 0)	100	mm
Width	15	mm
Length	100	mm

The data collection of the tensile tests involves the measurement of the specimens elongation during the application of tension as well as the recording of the applied tensile force by the load cell. The measurements were carried out automatically by the testing system with an inaccuracy of < 1 % for both parameters according to the accuracy requirements. The obtained mechanical properties of each film are derived from the analysis of at minimum 5 test specimens of that film in order to ensure statistical validation.

5.4.2 Water vapor permeability

The determination of the water vapor transmission rate WVTR is typically performed using the gravimetric dish method which is described e. g. in DIN 53122-1 or ISO 2528 [ISO95, DIN01]. From the data, the WVTR of the steady-state region can be calculated by the numerical value equation eq. 4-4 and describes the amount of water vapor permeating through 1 m² of a polymer film within 24 h and is highly dependent on the chosen environmental conditions [DIN01].

$$WVTR = \frac{\Delta m}{A} \cdot 10^4 \qquad (5\text{-}4)$$

If the time interval between two measurements exceeds 24 h, this is to be encountered applying eq. 5.5.

$$WVTR = \frac{24}{t} \cdot \frac{\Delta m}{A} \cdot 10^4 \qquad (5\text{-}5)$$

WVTR	Water vapor transmission rate	$\left[\frac{g}{m^2 \cdot d}\right]$
Δm	change in mass of the absorbent compared to initial mass	[g]
A	gage area of the specimen	[cm²]
t	measurement interval	[h]

Despite the gravimetrical analysis, alternative methods have been developed to measure the WVTR, e. g. by combination with an infrared detection sensor [ISO03]. However, the wet cup method from the standard DIN 53122-1 is seen to be the favorable method as it does not involve additional sophisticated equipment and delivers precise data with a simple experimental set-up.

Experimental

The DIN 53122-1 method was applied to determine the water vapor permeability of protein-based biopolymer films [DIN01]. The film specimens were initially cut into circular shape with a diameter of 90 mm and equilibrated at 23±2 °C and 50±3 % RH for 3 days using an environmental chamber. Following film preparation, the film specimens have been measured at 3 different positions with a micrometer screw in order to obtain the average film thickness. Additionally, the weight of the specimens was determined with 0.1 mg accuracy. Aluminum test cups have been used as containers of the absorbent and holder for the film specimen. The assembly of the test cups is shown in Fig. 5-7 combined with detailed information about the wax sealing.
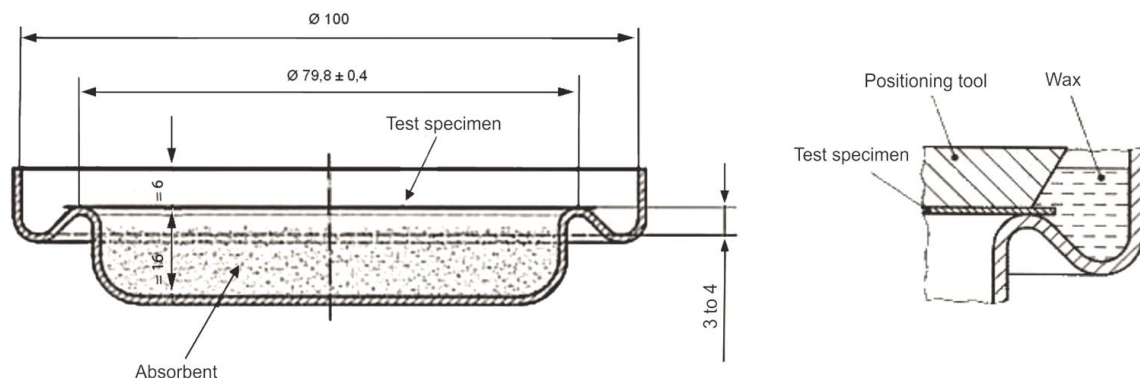
Fig. 5-7: Schematic drawing of an aluminum test cup for determination of the water vapor permeability and the wax sealing [DIN01].

As absorbent, blue silica gel with particle size of 1-3 mm was used in an amount of 30 g and film specimens were placed on the test cup and located in position during the solidification of the sealing with paraffin wax (melting point at 65 °C).

The measurement of the water vapor permeability have been carried out at test conditions of 25±2 °C and 85±5 % RH in an environmental chamber for up to 8 days and the mass increase as the indicator of water vapor absorption in the blue silica gel was monitored.

5.4.3 Water absorption into polymer films

The moisture absorption of polymer films and sheets is characterized by DIN EN ISO 62 that covers the measurement of the moisture absorption within constant environmental conditions as well as the water absorption during immersion of specimens into water [DIN99]. As result from the gravimetrical analysis, the absorption capability is expressed in relative terms and specification of either air temperature and humidity or the water temperature.

$$\alpha = 100 \cdot \frac{m_f - m_0}{m_0}$$

(5-6)

α	relative change in mass	[%]
m_0	initial mass of the specimen	[g]
m_f	final mass of the specimen after immersion	[g]

Experimental

Within the standard DIN EN ISO 62, several methods are described, two were chosen for the evaluation of water and water vapor uptake.

Storage at 50 % RH

Protein-based films have been stored at 23±2 °C and 50±3 % RH in an desiccator for 48 h above saturated $Ca(NO_3)_2$ and subsequently dried at 50 °C in an oven until constant weight was reached. Hence, the uptake of humidity was calculated from the weight decrease during drying.

Immersion in water at 23 °C

From the films, test specimens with dimensions of 2 x 2 cm have been cut and dried at 50 °C in an oven until their weight reached a constant level. Following that, the specimens have been immersed into water and the time-dependent weight increase of the specimens was measured once the free residual water had been removed. For each time interval, 3 specimens have been analyzed. Due to the method, only water insoluble material like cross-linked protein films could be tested.

Water sorption gravimetry

For the gravimetrical analysis of water vapor sorption into protein-based films, the SPS11/23-10μ device from Projekt Messtechnik (Ulm, Germany) was applied. The apparatus consists of a SAG 285 balance (Mettler Toledo) and a hydroclip sensor module from Rotronic (Bassersdorf, Switzerland) for monitorring of both temperature and air humidity. After calibration of the humidity with the salt standards NaCl and

KCl, the experiments have been carried out at temperature set to 25 °C with film specimens of approximately 1 g sample weight. The data was acquired by using the SDS11 3.0.10 software as provided by Projekt Messtechnik.

5.4.4 Dissolution and release behavior

The release kinetics of active components from carrier materials like polymers, hydrogels and gums is an important property in the pharmaceutical field of research concerning drug formulation and delivery with controlled release systems [Ahm07, Wan10, Nun11, Sie12]. Other applications for releasable additives relate e. g. to antioxidants in active packaging or in contrast to prevention of additive (plasticizer) leaching from the material [Jin09, Mas12]. It is understood that studying the release behavior of a component is strongly related to the field of application and experimental conditions have to be adjusted to the parameters of interest. The investigation of the release of fertilizing salts from protein-based films was therefore designed considering the exposure of the films (as seed tape or mulching film) to unsettled weather with rain and alternating temperature.

Experimental

For the analysis of the additive dissolution and release from protein-based films, test specimens of dimensions 4 x 4 cm have been weighed and then exposed for 30 min to 20 mL of distilled water. Prior to the test, the films had been equilibrated at 23±2 °C and 50±3 % RH for 2 days. The experimental setup consisted of Falcon tubes as closed vessels for the release test. The flowing of solvent against the film specimen was provided by a roller mixer system placed into environments with 5, 15 and 25 °C to ensure constant temperature throughout the test. The crystalline additive as well as the protein are water-sensitive and are seen as the most important components of the material. Therefore, the release of both of the substances has been determined from samples that had been withdrawn from the liquid medium in a time-dependent manner.

Nitrate determination

The investigated additives (KNO_3 / NH_4NO_3) in protein-based films dissociate to cation and NO_3^- during dissolution in water. Therefore, a quantitative method of nitrate determination has been used to study the additive release. This spectrophoto-metric test was established by Cataldo *et al.,* involves the nitration of salicylic acid under highly acidic conditions [Cat75]. A tenfold diluted sample (20 µL) from the above described release test was mixed with 80 µL of 5 % w/v salicylic acid in sulfuric acid (SA-H_2SO_4). After 20 min of reaction at 25 °C, 1900 µL of 2 M NaOH was slowly added and the completed preparation was cooled down to 25 °C prior to light absorbance measurement at 410 nm against distilled water as blank. The detection of nitrate is highly sensitive already at low nitrate concentrations. The

calibration of absorbance data vs. aqueous KNO_3 solutions shows linearity up to 15 mM NO_3^-. The data of the calibration is given in Fig. 14-2 that can be found in the appendix.

Determination of protein release

The Bradford assay is a spectrophotometric standard method, which was applied to determine the protein concentration within the aqueous medium [Bra76]. The test was carried as follows. A sample of 25 µL volume was added to 1 mL of Bradford reagent and well mixed to avoid inhomogeneties. The absorbance at 595 nm was measured after a reaction time of 2 min against the blank with distilled water. The assay is accurate up to a protein concentration of 0.5 mg/mL and related calibration data for NaCas as target protein is shown in Fig. 14-2 in the appendix as well.

5.4.5 X-ray powder diffraction

The characterization of solids often requires the X-ray diffraction technique as it delivers precise information about the positions of atoms in molecules and solids leading to the understanding of the degree of structural order [Dan00]. The X-ray diffraction pattern is characteristic for the material it was obtained from and is dependent of a high regularity in the molecular arrangement that is defined as crystallinity of the solid [Jen12]. In contrast to single-crystal experiments, the usage of powdered (polycrystalline) samples in the X-ray powder diffraction (XRPD) measurement has the advantage of more representative data for the substance and easier handling regarding sample quantity and preparation [Dan00, Gup02, Sko07].

$$n \cdot \lambda = 2d \cdot \sin\theta \qquad\qquad (5\text{-}7)$$

n	integer	[-]
λ	wavelength	[m]
d	interplanar spacing	[m]
θ	diffraction angle	[°]

The concept of X-ray diffraction is based on the interaction of X-rays with electrons in matter, thus affecting the scattering of an incident X-ray beam. The X-ray diffraction is decribed by Bragg's law (eq. 5-7) to happen from electrons in defined layers [Bra13, Gup02]. The general set-up of an X-ray measurement device is shown in Fig. 5-8 to consist of the sample stage to be tilted with angle 2θ by a 2-circle goniometer within X-ray tube and detector of the diffracted signal.
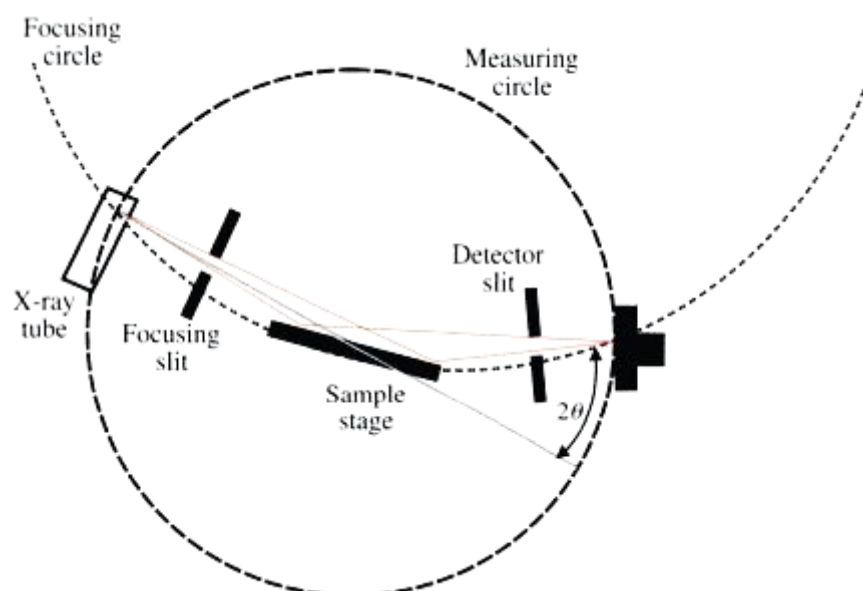
Fig. 5-8: Principle of the X-ray powder diffraction measurement technique [Dan00].

Experimental

The structural differences of NaCas films with and without incorporated crystals were investigated by applying a Bruker D4 Endeavor diffractometer and further data evaluation by means of the DIFFRACplus EVA software. CuKα$_1$ (λ = 1.5406 Å) radiation with intensity of 40 kV and 30 mA was used and patterns were recorded in the range of 2-60 ° 2-theta with a step width of 0.005 ° 2-theta and an acquisition time of 2 s per step. A film specimen of dimensions 15 x 15 mm was placed on a sample holder and covered with a polyimide film to prevent drying of the protein-based film piece during the time of measurement.

5.4.6 Electrophoresis

With SDS polyacrylamide gel electrophoresis (SDS-PAGE) analysis, protein samples can be distinguished in their molecular weight distribution. Therefore, the method was suitable for verification of the enzymatic cross-linking of the protein molecules within the film forming solution. The SDS-PAGE is usually carried out under reducing conditions using an SDS-Tris-glycine discontinuous buffered system described by Laemmli [Lae70, Yil98]. In the first step of the sample preparation, the tertiary and quaternary structure of proteins is destroyed by treatment with 2-mercaptoethanol. Secondly, the surfactant SDS interacts with the surface of the proteins in order to obtain negatively loaded molecules that would migrate in a polyacrylamide gel exposed to an electric field [Ric03].

Tab. 5-6: Composition of resolving gel and stacking gel (thickness 1 mm) in SDS-PAGE [Lae70].

Reagent	2 resolving gels 12.5 % T	2 stacking gels 4.5 % T
Gel buffer	2.5 mL	1.25 mL
Acrylamide / bisacrylamide	4.2 mL	0.75 mL
dH$_2$O	3.3 mL	3.00 mL
TEMED	10 µL	10 µL
APS (saturated solution)	20 µL	8 µL

The preparation of the polyacrylamide gel as the embedding medium was carried out in a two-step process by first composing the resolving gel followed by casting of the stacking gel on top. The amounts of SDS-PAGE reagents used for the gel preparation are given in Tab. 5-6 and in Tab. 5-7, the compositions of the SDS-PAGE reagents themselves are summarized.

Tab. 5-7: Reagents for SDS-PAGE [Lae70].

Reagent	Composition
Resolving gel buffer	181.8 g/L Tris 20 mL of 20 % (w/v) SDS solution 1 mL of 10 % (w/v) NaN$_3$ solution pH 8.8
Stacking gel buffer	60.6 g/L Tris 20 mL of 20 % (w/v) SDS solution 1 mL of 10 % (w/v) NaN$_3$ solution pH 6.8
Acryl/bisacrylamide solution (30 % w/v)	291 g/L acrylamide 9 g/L bisacrylamide in dH$_2$O
APS (saturated solution)	$(NH_4)_2S_2O_8$ dissolved in dH$_2$O until crystallization
Anode/cathode buffer (10 x concentrated)	30.3 g/L Tris 144 g/L glycin 50 mL of 20 % (w/v) SDS solution 1 mL of 10 % (w/v) NaN$_3$ solution
SDS sample buffer	27.2 g/L Tris 30 mL of 3 M HCl 250 mL of 20 % (w/v) SDS solution 500 mg bromphenole blue 500 g glycerol pH 6.8 Addition of 10 µL mercaptoethanol per 1 mL SDS sample buffer prior to usage.

Tab. 5-7 continued

Reagent	Composition
Staining solution	1 g/L Brilliant Blue G-250
	20 % v/v 2-propanol
	10 % v/v glacial acetic acid
Color stripping solution	20 % v/v 2-propanol
	10 % v/v glacial acetic acid
Gel drying solution	20 % v/v ethanol
	10 % v/v glycerol

5.4.7 Transglutaminase activity assay

Enzymes as biological catalysts accelerate the rate of a chemical reaction or first allow it to proceed [Aeh07]. Spectrophotometric assays are probably the most widely used procedures for the analysis of enzymatically catalyzed reactions, if a light absorbance shift can be observed [Eis02].

The activity of the transglutaminase (TG) enzyme (EC 2.3.13.2) is measured by the hydroxamate assay. In this test, the TG-mediated cross-linking of a glutamine substrate and a lysine substrate is transferred to an assay resulting in the formation of a ferrous color complex being photometrically detectable at 525°nm [Fol66].
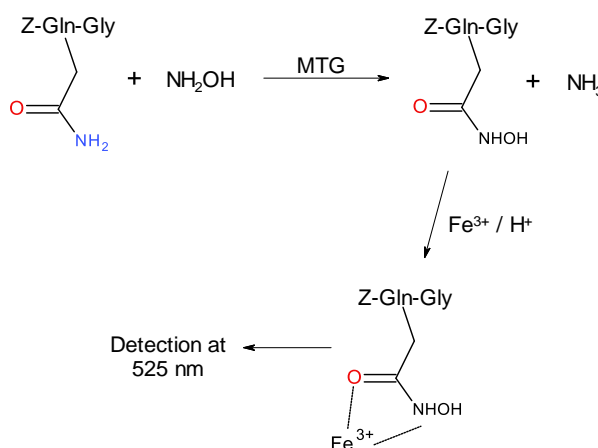
Fig. 5-9: Principle of the hydroxamate assay for determination of the MTG activity [Pat10b].

Hydroxyl amine serves as the lysine substrate of the TG that reacts with the dipeptide Z-Gln-Gly as the glutamine substrate. In Fig. 5-9, the reaction pathway of the assay is summarized and it can be seen that at first Z-γ-glutaminyl hydroxamate glycine is formed. This product then couples with the iron cations added in the second step of the assay. The amount of color complex is directly proportional to the enzymes performance and therefore, it is possible to conclude the transglutaminase activity considering the Lambert-Beer law [Hes05]:

$$E_\lambda = lg\left(\frac{I_0}{I}\right) = \varepsilon_\lambda \cdot c \cdot d \qquad\qquad (5\text{-}8)$$

E_λ	extinction of light at a wavelength λ	[-]
I_0	intensity of the incident light	[-]
I	intensity of the transmitted light	[-]
ε_λ	absorbance coefficient at wavelength λ	$\left[\dfrac{L}{mol \cdot cm}\right]$
c	concentration of the dissolved absorbent	[M]
d	path length of the light beam in the liquid	[cm]

$$\text{Activity}\left[\frac{U}{mL}\right] = \frac{E_\lambda \cdot V_{test}}{\varepsilon_\lambda \cdot t_R \cdot d \cdot V_{MTG}} \qquad\qquad (5\text{-}9)$$

V_{test}	test volume	[mL]
t_R	reaction time	[min]
V_{MTG}	volume of MTG dissolved in buffer	[mL]

Experimental

The aqueous substrate solution consisted of 100 mM Z-Gln-Gly, 200 M Tris-acetate buffer pH 6.0, 10 mM GSH and 100 mM hydroxylamine. For the activity measurement of microbial transglutaminase, no additional calcium source was required as MTG is known to be Ca^{2+} independent [Non89]. The reaction of enzyme and substrates was carried out incubating 650 µL of substrate solution with 100 µL of MTG solution at 37 °C. After 10 min of incubation, the enzyme reaction was stopped by addition of 750 µL of $FeCl_3$-trichloroacetic acid reagent that had been prepared by adding up equal volumetric parts of 3 M HCl, 12 % (w/v) trichloroacetic acid and 5 % (w/v) $FeCl_3*6H_2O$ (dissolved in 0.1 M HCl) prior to the test. The completed test solution was eventually centrifuged for 2 min at 16100 x g until finally the absorbance of the solution was measured at 525 nm.

The calibration shown in Fig. 14-1 was performed by similarly incubating γ-glutamyl hydroxamate solutions, revealing linear dependence up to 5 mM of the reaction product hydroxamate.

6. Results

6.1 Production of protein-based films

With the casting procedure being explained in chapter 5.1, homogeneous protein films have been produced and enzymatic cross-linking with microbial transglutaminase (MTG) was successfully applied. Films made of sodium caseinate (NaCas) had a translucent and slightly yellowish appeal, whereas films with gelatin (280 Bloom) were completely colorless and transparent. As defined by the applied casting molds, different film shapes and sizes were obtained and an average film thickness of 200 µm was achieved. During the film formation in the solvent evaporation step, crystallization of functional additives occurred throughout the film structure. The crystalline phase was found to be uniformly distributed within the protein matrix. The experimental part involved structural aspects, the impact of process parameters, especially regarding the film drying and the enzyme performance. Furthermore, methods for the control of the crystal habit and the release behavior by additives are described. The results are presented in the following.

Other processing, packaging and labelling methods have been additionally successfully tested, but are not further specified here. These include the bag sealing and adhesive bonding of film on film and film on glass made by wetting one side of the protein-based material. Moreover, the protein-based films can be provided with labelling and pictures via conventional inkjet printing as well as by screen printing using natural dyes. Continuous dyeing of the whole material can be reached, e.g. by mixing edible food dyes into the film forming solution prior to casting.

6.1.1 Identification of the crystalline phase within the material

With XRPD analysis, the structure of the NaCas films was determined depending on enzymatic cross-linking as well as on the presence of a crystallizing additive. The XRPD measurement parameters are given in chapter 5.4.5. As shown in Fig. 6-1, the pattern for film A and B (+/- MTG, without crystallized additive) exhibit a large peak at 20 ° 2-theta, clarifying the protein matrix to be completely amorphous irrespectively from MTG addition. In contrast, additional peaks are found in the XRPD pattern from the films C and D (+/- MTG, with KNO_3). Comparing the peaks with a KNO_3 pattern from the database, it can be stated that these are related to inner-film crystallized KNO_3 that was detected within the amorphous NaCas films [Sto12a]. The absence of the peak in 20 ° 2-theta in pattern C may be explained by a shielding of the protein matrix by KNO_3 crystals at the film surface.
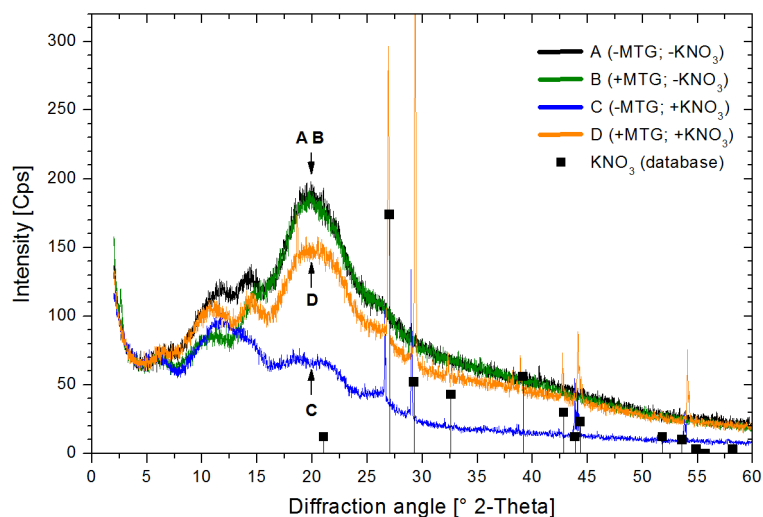
Fig. 6-1: XRPD analysis of NaCas films with and without enzymatic cross-linking (+/- MTG) and detection of KNO_3 as additive salt (in films C & D, + KNO_3) [Sto12a].

6.1.2 Effect of drying parameters

The solvent evaporation is an essential process step in the casting method to produce protein-based films. Therefore, the most important environmental parameters of the drying process, temperature and air humidity have been varied in order to measure their impact on both the mechanical properties of NaCas films and formation of the inner-film crystalline KNO_3 phase as described in chapter 5.1 in detail.

6.1.2.1 Mechanical performance

Cross-linked and non-cross-linked films have been analyzed with a constant NaCas / KNO_3 ratio of 6:1 as well as without any additive. The combined effect of the drying conditions was determined applying a $3^{(2-0)}$ full factorial plan and evaluation by Distance Weighted Least Squares with stiffness factor of 0.25 as provided by Statistica 8.0 [Sta07]. The results for pure NaCas films A and B without crystallizing additive are summarized in Fig. 6-2. For both films A and B, the rise in drying temperature was observed to lead to an increase in tensile strength as a general trend. Such trend was not observed for films A dried at 75 % RH, where no significant increase in tensile strength was determined.
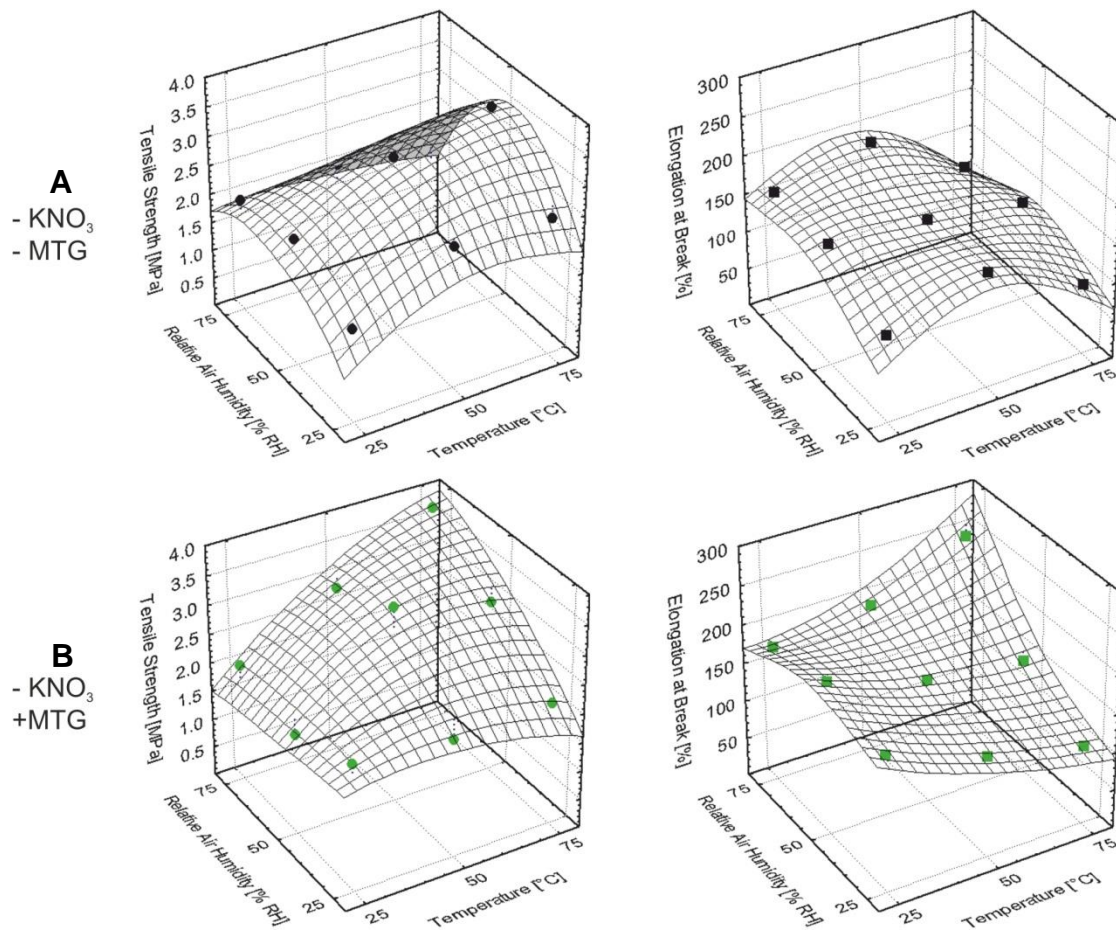
Fig. 6-2: Tensile strength (●) and elongation at break (■) of NaCas films (A, B)) dependent on drying conditions (temperature, relative air humidity) and application of MTG for enzymatic cross-linking. The corresponding data is listed in Tab. 14-2 [Sto12a].

Regarding the effect of drying conditions on elongation with respect to films A, a precise trend was only observed for high temperatures leading to a slightly lower flexibility. The materials A and B behaved differently in their elongation when dried at a higher temperature and humidity. In case of films B, the MTG stabilized the protein matrix in a cross-linked network resulting in enhancement of the polymer's flexibility. The highest values in elongation as well as tensile strength have been obtained for films B dried at 75 °C and 75 % RH. This can be resulted from an altered reactivity of the MTG as well as a thermally induced cross-linking of protein as it is discussed in chapter 7.1.2. Homogeneously distributed macroscopic particles of approximately 500 μm in diameter have been observed in those films (composition B) that are assumed to have an effect on the overall mechanical performance.

The mechanical properties are considerably changed due to the addition of KNO_3 into NaCas films as visualized in Fig. 6-3. For the tensile strength as well as elongation of films with compositions C, no significant effect of the drying conditions has been found. The cross-linked films D with incorporated KNO_3 showed a trend in a tensile strength decrease with higher temperature and a rise of tensile strength with higher air humidity until 50 % RH.
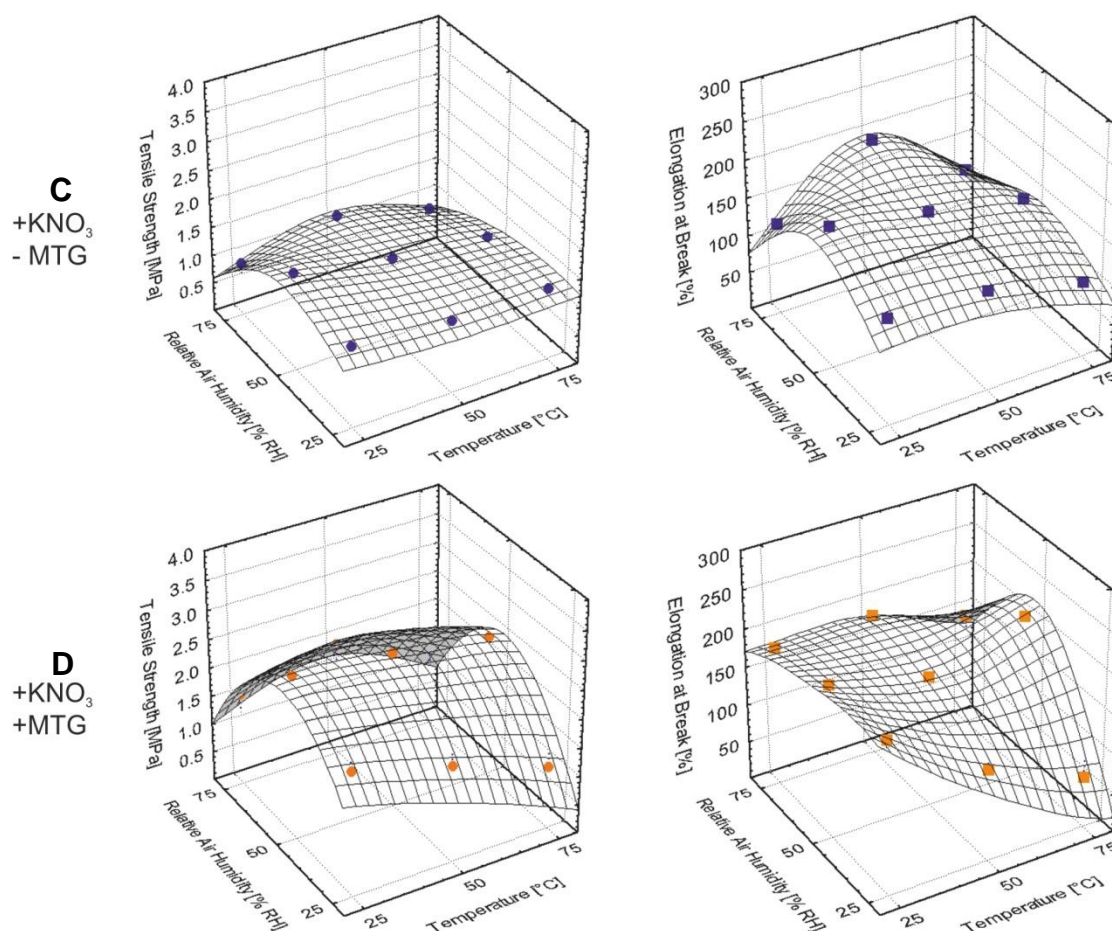
Fig. 6-3: Tensile strength (●) and elongation at break (■) of NaCas films with incorporated KNO₃ as crystalline additive (C, D) dependent on drying conditions (temperature, rel. air humidity) and enzymatic cross-linking (+/- MTG). Data to be found in Tab. 14-3 [Sto12a].

However, the highest investigated value of air humidity generally affected a decrease in the mechanical properties of both film compositions C and D. With respect to the air humidity, a proportional increase in elongation can be considered. However, the loss in the material's quality and mechanical performance regarding both films C and D is to be attributed to a change in the morphology of the inner-film crystallized KNO₃ to acicular structure as shown in Fig. 6-5(II).

6.1.2.2 Film drying and storage

From the mechanical analysis with varied drying parameters, the usage of the standard temperature (25 °C) has been quantified to result in most homogeneous films and high mechanical performance, especially at 50 % RH. The water loss during the film formation process was therefore measured at drying conditions applying 25 °C and rel. air humidity ranging from 25 to 75 % RH. The drying step lasted 12 h, followed by the storage of the films at standard conditions defined in DIN EN ISO 527-3 [DIN03a]. Information on the drying process is provided in Fig. 6-4, where the time-dependent solvent evaporation is shown. Also the residual moisture contents of the films can be extracted from the equilibrium that occurs during storage

conditions. For all investigated film compositions A-D, on the one hand, a strong dependency of the evaporation rate on the air humidity has been verified. Selecting the drying at 50 % RH as a standard and analyzing data of films A-D at 12 h, the process of water evaporation and film formation is on average 63 % faster when a low air humidity was applied. The deceleration of the drying at higher air humidity averages 99 % compared to the standard conditions.
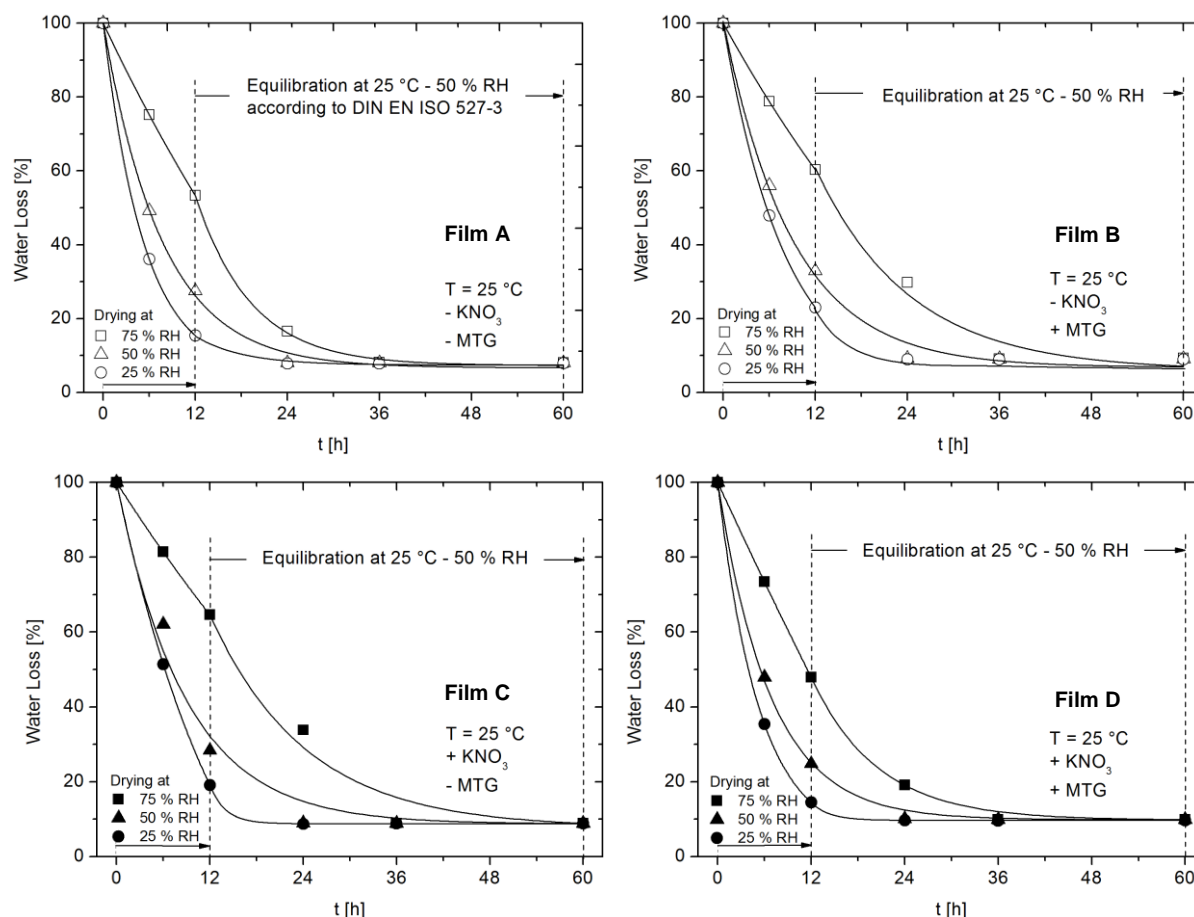
Fig. 6-4: Water evaporation during drying at 25 °C until 12 h and varied air humidity in dependence of MTG-mediated enzymatic cross-linking. Storage conditions were kept constant at 25 °C and 50 % RH in order to equilibrate the films [Sto12a].

The influence of a crystallizing additive or an enzymatic cross-linking appeared not to be relevant. Small dissimilarities in the drying of the different film compositions might be due to measurement error not being determinable with the data acquisition by a single measurement. On the other hand, the difference in the residual water content was successfully equilibrated after 2 days to approximately 10 % w/w at the chosen storage conditions. Thus, the ongoing water loss during storage caused different supersaturation levels for the KNO_3 which is an important factor for the crystallization and the stability of inner-film grown crystals in the films C and D as presented in the following.

6.1.2.3 Crystal morphology

The crystalline structure of KNO_3 within the film has been studied at film specimens taken from films C and D right after film drying and at the day of the tensile tests after 2 days of storage. The results of the light microscopy analysis are assembled in Fig. 6-5 that shows a representative extract of the data. At first, the dried films have a translucent and homogeneous appeal and a smooth touch. The microscopy exposures in Fig. 6-5 (I) show the KNO_3 crystals to be homogeneously distributed in a microscale within the film. Apart from that, the crystal habit and size are strongly affected by the drying conditions. At 25 °C and 25 % RH, KNO_3 crystals with a length of up to 20 µm were obtained and for higher temperatures, a structural change towards dendritic triangles with an average size of 60 µm occurred. Rising humidity as the second important process parameter had an impact on the crystallization towards smaller crystal sizes with up to 35 µm in length and a larger number of crystals.
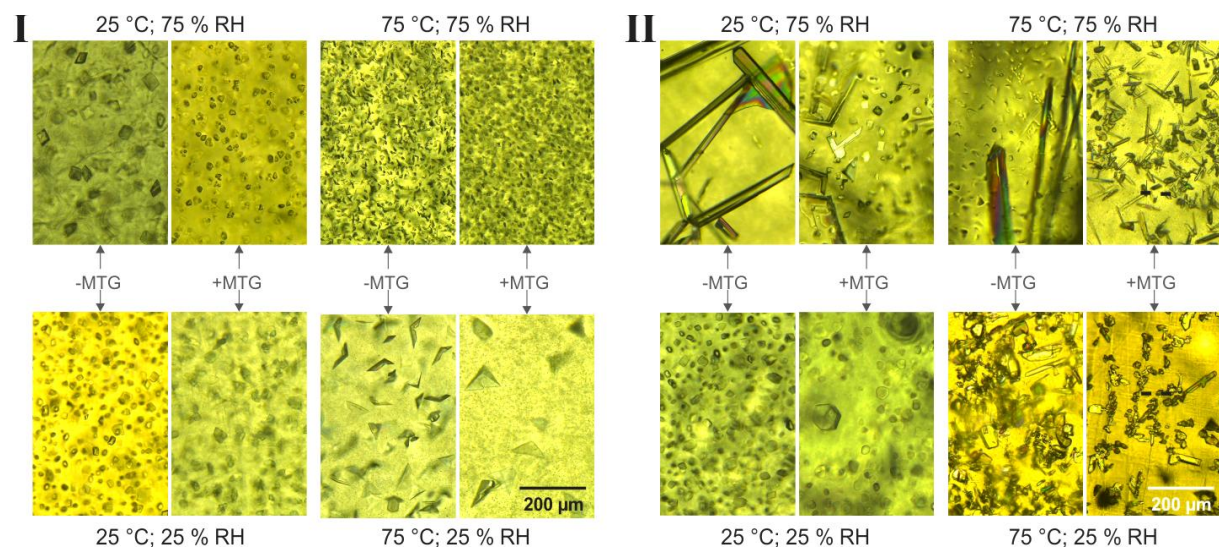
Fig. 6-5: Light microscopy exposures (top view) of NaCas films +/- MTG with the incorporated crystalline additive KNO_3 dried under varied conditions. Films were optically analyzed directly after completion of the drying process (**I**). The same films were examined at the day of mechanical testing after 2 days of storage at 25 °C and 50 % RH according to DIN EN ISO 527-3 (**II**) [Sto12a].

MTG-induced cross-linking had only a minor effect on the crystallizing additive, resulting in more opaque films with slightly larger crystals at low air humidity during drying. In none of the film specimens, the orthorhombic crystal habit was visible. This habit is typical for the phase-II KNO_3 which is the stable KNO_3 polymorph at ambient conditions. Referring to the structure of other KNO_3 polymorphs, the habit of the examined crystals is similar to the trigonal phase-III KNO_3 that is metastable at normal pressure and room temperature [Dav63, Rol96, Fre09, Sto12a].

However, after equilibration of the films as preparation for material testing, the prior observed inner-film crystals had been altered regarding their distribution and habit. The corresponding information is given in Fig. 6-5 (II). Preferentially in those films

dried at high air humidity of 75 % RH, the crystal morphology had undergone a rather obvious transition from the trigonal habit to the orthorhombic shape. Here, a macroscopic acicular crystal network had been formed that even protruded the material surface. Furthermore, it was observed that the prior achieved crystal sizes were more stable in films dried at low air humidity and in a cross-linked protein matrix although these crystalline structures also appeared to be transferred to the orthorhombic phase-II KNO_3. The phenomenon of Ostwald ripening was observed frequently in the specimens of film D (+KNO_3; + MTG) and can be seen best in the exposure of the film D dried at 25 °C and 25 % RH of Fig. 6-5 (II) where crystals of approximately 100 µm had grown to the disadvantage of smaller crystals surrounding the larger particles [Mye02].

6.2 Control of the KNO_3 crystal habit by secondary additives

6.2.1 Additive screening

The specific crystal growth of KNO_3 was intended to be controlled in order to maintain a high material quality and functionality during a long term of storage and preferably in a wide range of environmental conditions. The needle-like morphology of the stable phase-II KNO_3 is generally not desired in protein-based materials, since these elongated crystals exceed the film structure. This effect results in a surface roughness of the film and in the weakening of the mechanical stability. Therefore, it is aimed for a crystal habit with a rather small aspect ratio L_1/L_2 as well as crystal sizes less than the film thickness.

An inhibition of the orthorhombic KNO_3 crystal habit can be reached by a specific blocking of the crystal faces {001}, {011} and {112} by additives as being indicated in Fig. 4-5. The analysis of various substances and screening for crystal growth inhibitors was carried out as described in chapter 5.2. In the following, the crystal size distribution (CSD) regarding length of the KNO_3 crystals, the deriving mean crystal length (D_{L50}) as well as the aspect ratio of crystal length and width L_1/L_2 are compared to evaluate the effectiveness of crystal growth control.

At first, glycerol, the Tris/HCl buffer and urea are considered as components of NaCas films which have been added to the KNO_3 solution in ratios being equivalent to those in the film forming solution. The KNO_3 crystallization from pure aqueous solution was set as reference which was repeated three times in order to evaluate the reproducibility of the experimental data. The pure KNO_3 solution of 466 g_{anh}/kg_{H2O} was measured to have a pH 6.4 at 35 °C. The data of the reference and the crystallization batches with the components of the film forming solution are presented in Fig. 6-6. The crystal size distributions (CSD, based on length) are combined with exemplary microscopy exposures of crystal samples after filtration and drying. The mean aspect ratios from all the screening tests are summarized in Fig. 6-7. As to be seen in Fig. 6-6 and Fig. 6-7, the elongated crystal habit (average aspect ratio of

approximately 4:1) and the mean crystal length of 360 µm could be verified, which is known from literature [Hol75]. The repetition of the experiment revealed a reliable experimental setup with a maximum deviation of ± 8 % regarding CSD.
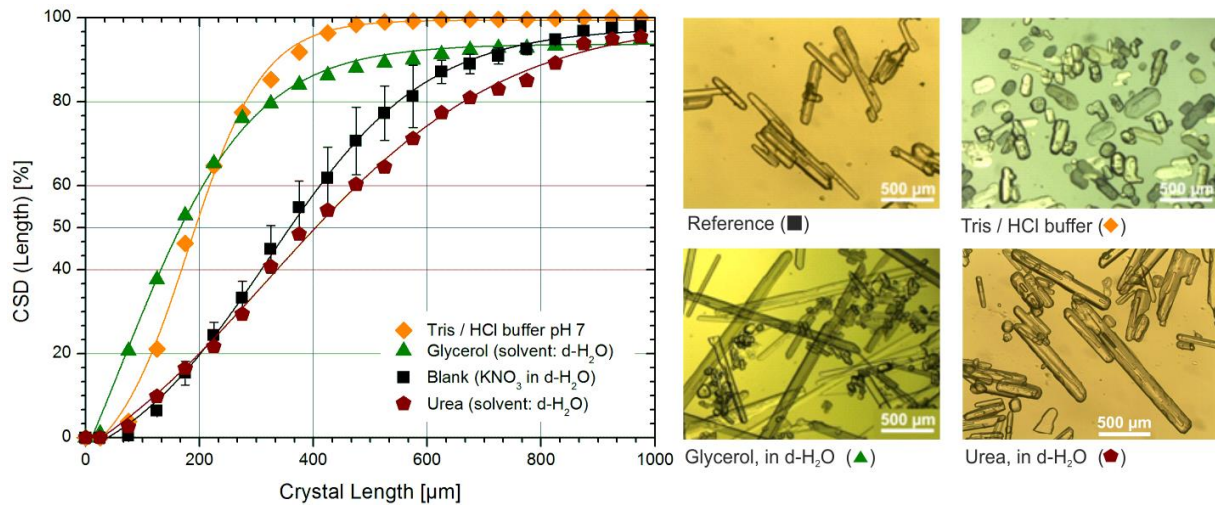
Fig. 6-6: Crystal size distribution (CSD, cumulative) based on length for KNO_3 crystals produced by batch cooling crystallization from a pure aqueous KNO_3 solution (■) and in presence of components from the protein film forming solution, KNO_3/component ratio is same as in film forming solution: 0.86 M Tris/HCl buffer pH 7 (◆); KNO_3/glycerol ratio of 1:3 (▲); KNO_3/urea ratio of 1:2 (⬟). Reference CSD: Three identical experiments, number of particle size measurements n > 100 for each experiment [Sto12b].

When crystallizing KNO_3 in presence of components of the film, the components had been used in the KNO_3 / component ratio referring to the film forming solution (described in chapter 5.1). Both the Tris / HCl buffer pH 7 as well as glycerol appear
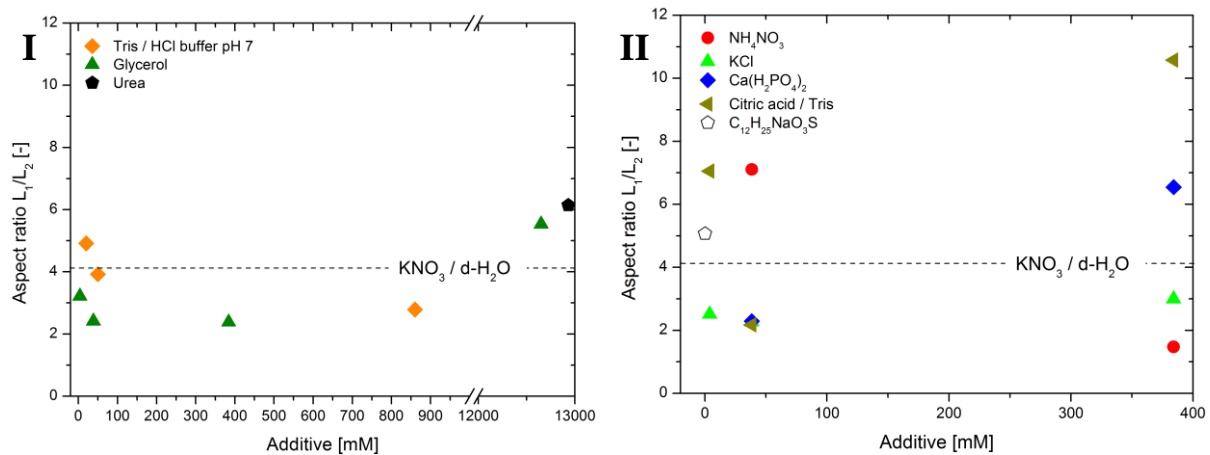
Fig. 6-7: Mean aspect ratio from KNO_3 crystal growth in presence of components of the film forming solution (I) and secondary additives (II). Crystal dimensions L_1 and L_2 (length and width) as determined from D_{50} values in the related cumulative crystal size distribution. Dashed line represents the reference (KNO_3 crystallization in pure water without additives).

to decrease the mean crystal length D_{L50} to about 195 µm and 166 µm, respectively. Despite that, the glycerol affected the growth of needles with length greater than 400 µm amounting to 10 % in the CSD. This is possibly due to the hygroscopic

nature of glycerol leading to locally high supersaturation and could be the case for the effect of urea addition, too. In terms of aspect ratio, the corresponding data to Fig. 6-6 can be found in Fig. 6-7 (I) at highest additive concentrations, giving evidence for the crystal elongation effect of the plasticizing agents and the crystal growth inhibitory effect of the buffer system.
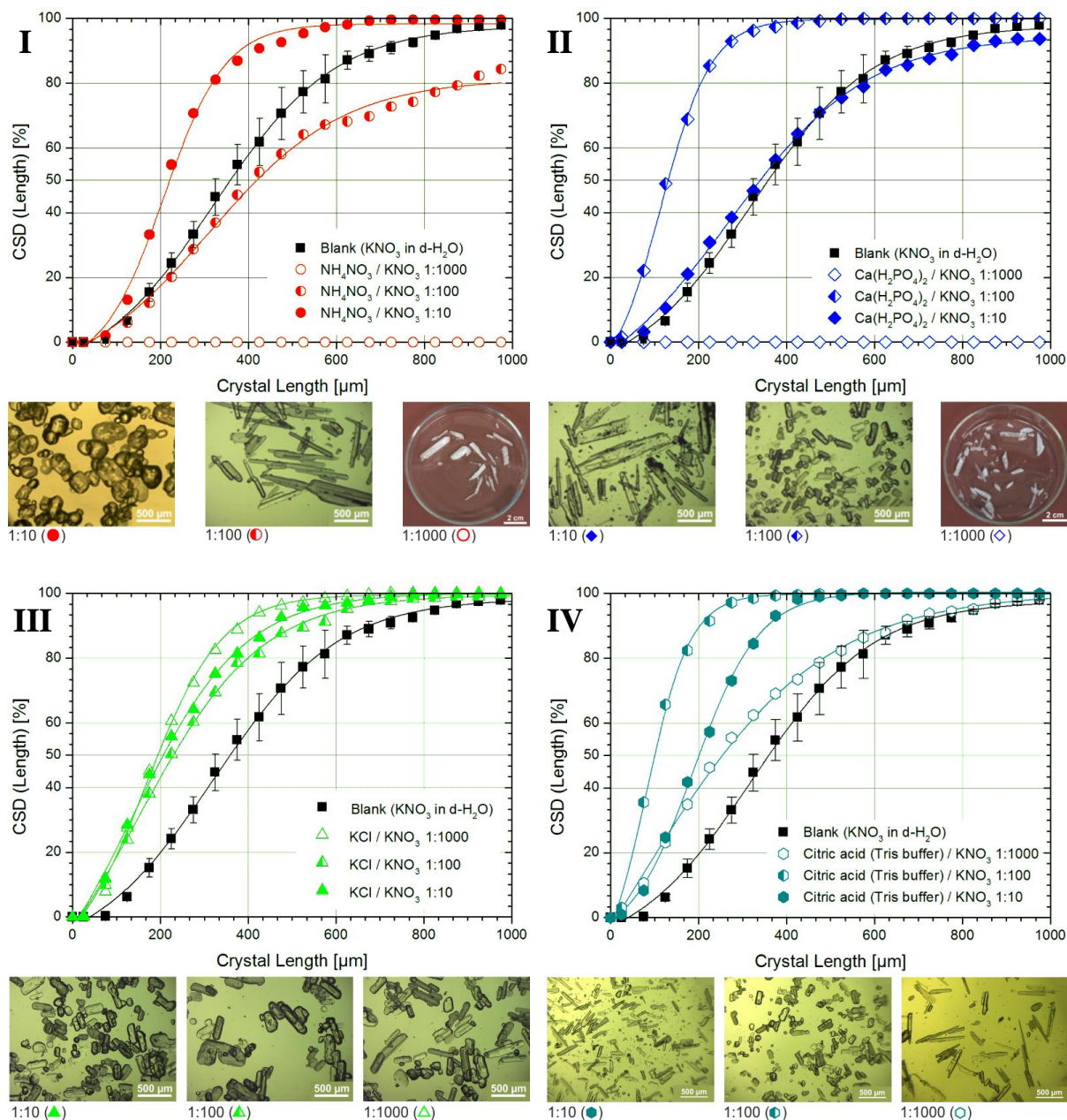
Fig. 6-8: Crystallization of KNO_3 in the presence of various secondary additives. Batch cooling crystallization was carried out and NH_4NO_3 was added in the molar additive/KNO_3 ratios 1:10, 1:100 and 1:1000. CSD based on crystal length was determined and compared to the CSD of KNO_3 crystals obtained from the pure aqueous solution (■). Light microscopy exposures show the different crystal habits [Sto12b].

Among the secondary additives in the screening, the addition of ammonium nitrate has been identified as the most promising substance for the control of the inner-film crystal growth. As known from literature, the two nitrate salts build a NH_4NO_3-KNO_3

co-crystal system [Cad81, Dej00, Chi05a, Chi05b]. As Fig. 6-8 (I) points out, the crystal length decreased proportionally from > 1 mm to 222 µm with increase of the NH_4NO_3 / KNO_3 ratio and a final crystal aspect ratio of 1.5:1 was achieved at highest amount of NH_4NO_3 added in the screening tests (Fig. 6-7). The reason for the formation of very large crystalline aggregates in case of both the NH_4NO_3 / KNO_3 ratio and $Ca(H_2PO_4)_2$ / KNO_3 ratio of 1:1000 remains unknown, but it is suggested to be caused by partly inhomogeneous mixing and therefore an irregular heat transfer into the liquid.

The results for the effect of calcium dihydrogen phosphate are shown in Fig. 6-8 (II), revealing ambiguous information. Since the applied $Ca(H_2PO_4)_2 \cdot H_2O$ is formulated with a purity of > 85 % w/w, the inclosed impurities of the chemical may have an additional impact on the crystal growth of KNO_3 for which no further quantification was carried out.

The crystallization in presence potassium chloride affected the crystal growth of KNO_3 significantly ($p < 0.001$). As seen in Fig. 6-8 (III), the addition of KCl decreased the mean crystal length to an optimum (193 µm) at KCl / KNO_3 ratio of 1:1000 as verified by significance evaluation ($p < 0.001$) as well and corresponding to the smallest aspect ratio of 2.5:1 for lowest KCl concentrations as visualized in Fig. 6-7.
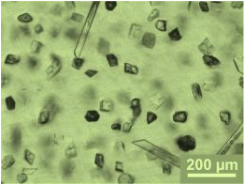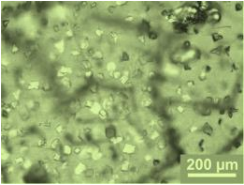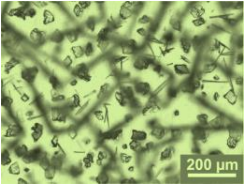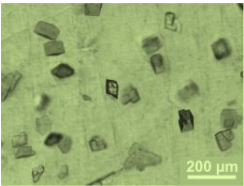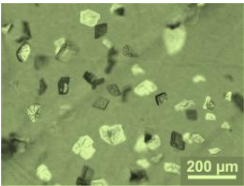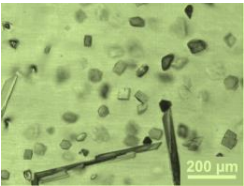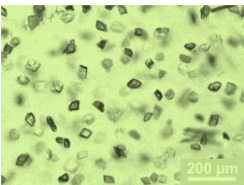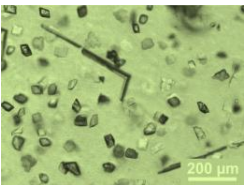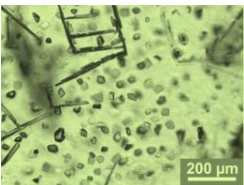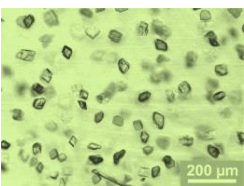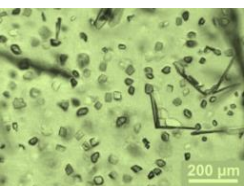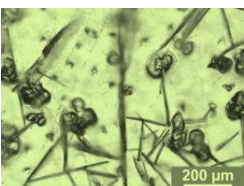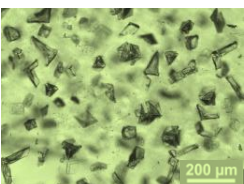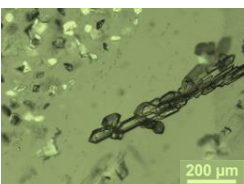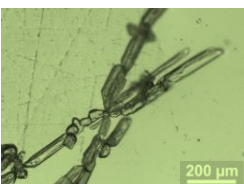
Citric acid as potential face specific crystal growth inhibitor indeed decreased the mean crystal length to 100 µm and the aspect ratio to 2.2:1 when being added to reach an additive / KNO_3 ratio of 1:100 (Fig. 6-8 (IV)). Aqueous Tris / HCl buffer was used as solvent in order to compensate a pH shift by addition of citric acid. A synergistic effect of citric acid and Tris can be considered that may be contributed by their configurational similarity. At highest citric acid content, the pH was decreased to pH < 3.8 (below measurement range of the pH strip), indicating that the buffer capacity had been exceeded. Needle growth resulting from a higher supersaturation level at presence of high amounts of citric acid is due to decrease of water solubility of KNO_3 being slightly pH dependent. If HNO_3 is considered as the acid of the anion, the comparison of the pK_a values is $pK_{a(HNO3)} < pK_{a(citric\ acid)}$ and therefore, it can be assumed that the citric acid as the weaker acid would influence the solubility equilibrium of KNO_3 [Nyl96, Ker08].

The usage of sodium dodecyl sulfonate ($C_{12}H_{25}NaO_3S$) had been recommended in the literature as potential additive in KNO_3 crystal growth inhibition [Yua07]. However, Fig. 6-7 (II) shows that the $C_{12}H_{25}NaO_3S$ with a concentration of 20 mg/L increased the mean aspect ratio from 4:1 (KNO_3 crystallization from pure solution) to 5:1 at the chosen experimental conditions. Any further investigation with this additive was limited by its poor water solubility.

In the further screening procedure, the most promising secondary additives have been used to test their capability in presence of other components of the film forming solution (glycerol, Tris/HCl buffer). The final step of the additive screening was

determined to be the application of the screened additives in manufacturing of NaCas films. To simplify the process, no enzymatic cross-linking was involved here. After film formation, the material was stored at constant environmental conditions as defined by the standard of mechanical testing [DIN03A]. The monitoring of the crystallization and polymorphic phase transition is shown in Tab. 6-1, where representative exposures of the light microscopy analysis are summarized.

Tab. 6-1: Non-cross-linked NaCas films (- MTG) with inner-film crystallized KNO_3 (reference) and incorporation of KNO_3 crystallized in presence of secondary additives. Films have been produced and stored for 7 days at constant environmental conditions (25 °C and 50 % RH) and light microscopy analysis was performed after distinct time intervals. Films contained glycerol in NaCas / glycerol ratio of 2:1 and 20 mM Tris/HCl buffer pH 7 was used as solvent, if not otherwise stated.

Film	After film drying	2 days storage	7 days storage
Reference			
NH_4NO_3 / KNO_3 1:10			
$Ca(H_2PO_4)_2$ / KNO_3 1:100			
KCl / KNO_3 1:1000			
Urea / KNO_3 2:1 Glycerol / KNO_3 1:1			

The analysis of the exposures from the reference film in Tab. 6-1 reveals that prior to time-dependent formation of orthorhombic needles of KNO_3, smaller crystalline particles with the trigonal morphology of the metastable phase-III KNO_3 appeared. This phenomenon corresponds to the observations described in chapter 6.1.2 and is in accordance with the other film compositions including secondary additives (Tab. 6-1). During the time of storage, the stable phase-II KNO_3 was formed in the reference NaCas film, preferentially at the upper side of the material building a layer

of acicular crystals protruding the film surface. The NH_4NO_3 addition with the ratio of 1:10 was recognized to decelerate the transition to the needle-like structure considerably. In a lesser amount, this is the case as well for the secondary additives $Ca(H_2PO_4)_2$ and KCl used in ratios 1:100 and 1:1000, respectively. The KCl additionally affected the formation of agglomerates with a mean diameter of 110 µm as documented after 7 days.

The partial substitution of glycerol by urea resulted in a very flexible, but sticky material. The tendency to the elongated KNO_3 crystal habit was in agreement with the results from the batch crystallization (Fig. 6-7 (I)). Like in Fig. 6-5, the effect of Ostwald ripening was observed here as well [Mye02]. The phase transition and crystal growth were qualitatively analyzed to happen very fast within the first 2 days of storage. However, the appearance of crystalline needles was only observed in the core of the material and unlikely at the material surface. It is assumed that the film attracted considerable amounts of humidity due to the mix of the highly hygroscopic plasticizing agents. Therefore, inhomogenities in the saturation level have been barely present in the material as the water evaporation from the film surface was suppressed.

The final rating of the applied secondary additives was carried out with respect to the inhibition efficiency in the KNO_3 crystallization as well as to compatibility to the overall material composition and processing. Citric acid and $Ca(H_2PO_4)_2$ monohydrate were found to precipitate the protein in the film forming solution when being added as solid. The addition of these chemicals diluted in aqueous solution was successful, but not desired in the process since large amounts of water lead to scale-up challenges and extend the time of film drying. Sodium dodecyl sulfonate ($C_{12}H_{25}NaO_3S$) had no advantageous effect on the KNO_3 crystallization and therefore, the sulfonate was rejected for further analysis also because of its lacking biocompatibility and potential toxicity [Rot12]. The usage of urea brought no minimization of the KNO_3 aspect ratio, but as an advantage to product design, the material was protected from crystal growth upon the film surface. From the substances that had been analyzed via this screening procedure, NH_4NO_3 was determined as most efficient additional component to control the morphology of the inner-film crystallized structure. The aspect ratio of the co-crystals can be diminished proportionally with increase of the NH_4NO_3 content (Fig. 6-8 (I)). When applying NH_4NO_3 in the manufacturing of NaCas films, the presence of crystals with trigonal habit was prolonged and the formation of an acicular crystalline network was prevented to a considerable extent as studied over 7 days of storage. NH_4NO_3 as well as urea, KCl and $Ca(H_2PO_4)_2$ monohydrate served the factor of functionality since these additives are traditionally used as nitrogen, potassium or phosphate sources in plant fertilization.

A change in material composition can affect the physicochemical properties of protein-based films. In the following chapters, the mechanical performance of the modified films and permeability aspects are presented with respect to enzymatic cross-linking as well.

6.2.2 Influence of additives on the film's mechanical properties

6.2.2.1 Potassium / ammonium nitrate mix

The mechanical analysis of NaCas films with an incorporated additive mix of KNO_3 and NH_4NO_3 revealed a combined effect of enzymatic cross-linking and addition of NH_4NO_3 on both materials quality and flexibility. In Fig. 6-9, tensile strength and elongation of NaCas films without any additive (0:0), with incorporated KNO_3 (0:1) and in dependence of increased NH_4NO_3 content (1:10 to 1:1) are displayed. The mix of the two nitrate salts is expressed as molar NH_4NO_3 / KNO_3 ratio. The overall salt content within a film was kept constant at a NaCas / salt mass ratio of 6:1 for better comparison of the differing additive mix. Therefore, the amount of KNO_3 had to be decreased proportionally to NH_4NO_3 addition. Regarding the non-cross-linked films, the elongation property remained constant at approximately 100 % despite of using pure KNO_3 or in the mix with NH_4NO_3 as secondary additive. The tensile strength first diminished from 1.2 MPa for pure NaCas films (0:0, - MTG) to an amount of 20 % when KNO_3 had been incorporated in the NaCas / salt ratio of 6:1. This decrease has been compensated by NH_4NO_3 addition. However, already a small content has led to the slight tensile strength enhancement and no further optimization was reached by more balanced NH_4NO_3 / KNO_3 ratios.
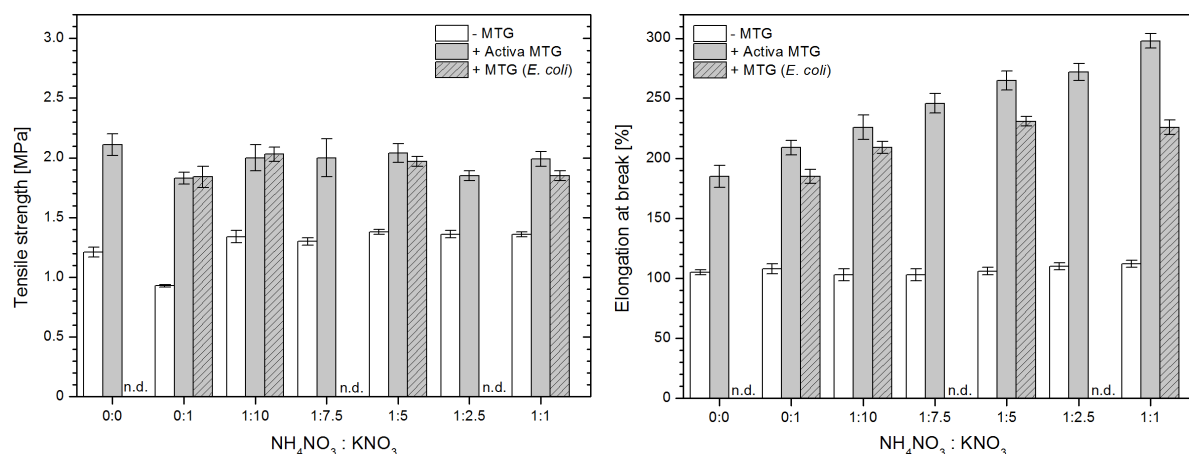
Fig. 6-9: Additive mix of KNO_3 and NH_4NO_3 (given in molar ratios) affecting tensile strength and elongation at break of NaCas films being non-cross-linked or cross-linked applying Activa MTG (containing 99 % w/w maltodextrin) or recombinant MTG from *E. coli* (pure enzyme) supplied by the working group Downstream Processing, Institute of Pharmacy, Martin Luther University Halle-Wittenberg [Sto12c, Mar08].
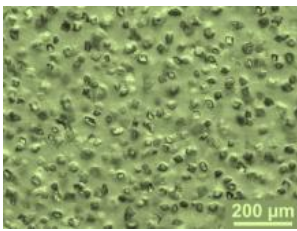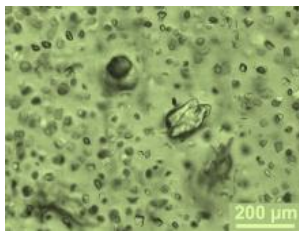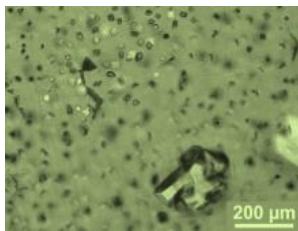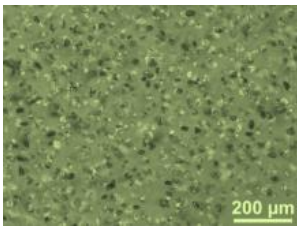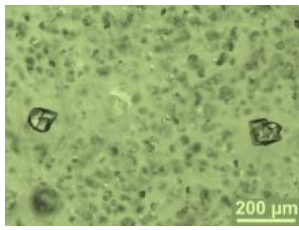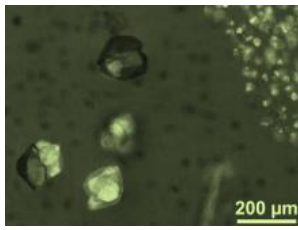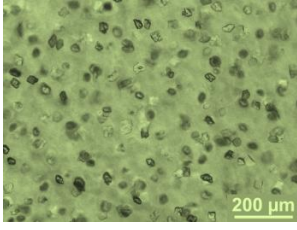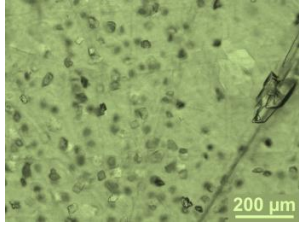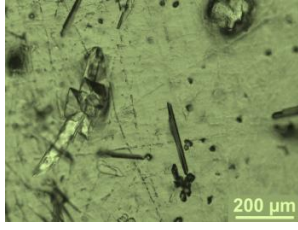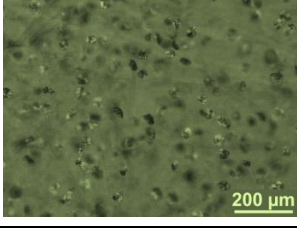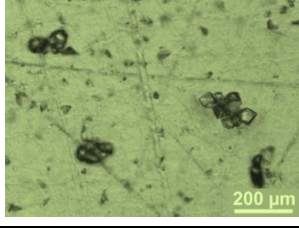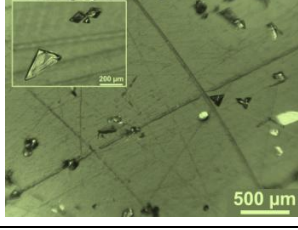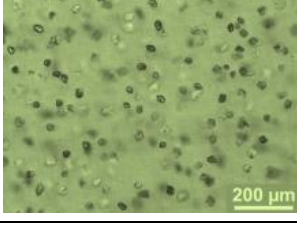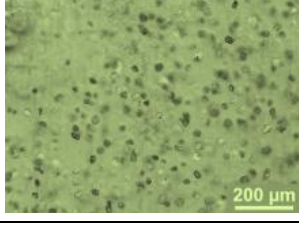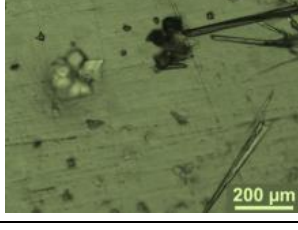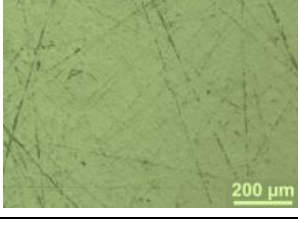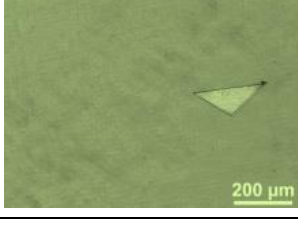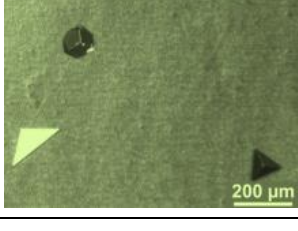
As indicated in Fig. 6-9, the cross-linking of the protein matrix was performed by applying two transglutaminase sources. The Activa MTG is the enzyme preparation that is commonly used in the manufacturing of protein films. As described previously,

it contains 99 % w/w maltodextrin as filler that may affect the material properties. In order to study this influence, pure MTG from a recombinant *E. coli* strain was used which similarly catalyzes the cross-linking of proteins [Mar08]. The results from the enzymatically modified films point out, that cross-linking with Activa MTG is on the one hand generally beneficial to enhancement of the tensile strength (+ 35 %) of NaCas films. On the other hand, the film elongation had been improved up to 300 % which is a relative increase of 100 % compared to initial film compositions without any salt additive or cross-linked films.

NaCas films cross-linked with pure MTG (*E. coli*) exhibited the same trends in mechanical analysis as the films containing Activa MTG, but in contrast with an elongation increase through variation of the NH_4NO_3 / KNO_3 ratio closing at 230 % (Fig. 6-9). This difference is an effect of absent maltodextrin that would be present in the Activa TG formulation. In one NaCas film of the dimensions 20 x 20 cm and 200 µm thickness, 1.5 g of Activa MTG is used in which 99 % (w/w) is maltodextrin. Referring to the protein content in a film, a NaCas/maltodextrin ratio of 4:1 was obtained. Maltodextrin as an oligosaccharide is highly hygroscopic and tends to bind water in the protein matrix. Thus, it acts as additional plasticizer in the material system [Cao09, Ugr07, Chr98].

The crystallization of NH_4NO_3 and KNO_3 from aqueous solution is known to result in $KNO_3 \cdot xNH_4NO_3$ co-crystals as it has been described in chapter 4.4 [Dej00, Cad81, Hol75, Coa61]. Therefore, the study of different mixtures of NH_4NO_3 and KNO_3 in NaCas films also involved the analysis of the crystal morphologies inside the protein matrix of the produced films. Related to the mechanical properties summarized in Fig. 6-9, representative light microscopy exposures of NaCas films with incorporated salt additive mixtures of 1:10, 1:2.5 and 1:1 are given in Tab. 6-2. The exposures of films with the ratios 1:7.5 and 1:5 are not included, because they show a crystal structure that is similar to the films with the mixture 1:10. In comparison to the screening results shown in Tab. 6-1, special attention was paid to the potentials of a further NH_4NO_3 increase and interactions with a cross-linked protein matrix. Regarding the primary nucleation and crystal growth right after film drying, the obtained crystal morphology and distribution in the material are visually the same as already observed in the additive screening. Starting from NH_4NO_3 / KNO_3 ratio of 1:2.5 and being obvious at ratio 1:1, the number of crystals has been qualitatively detected to be decreased until in the cross-linked NaCas film with NH_4NO_3 / KNO_3 ratio of 1:1, no nucleation had occurred any more. This is due to the altered water solubility of the co-crystal structure compared to pure KNO_3 [Dej00]. During the time of storage, crystal growth and polymorphic phase transition from a metastable form to the thermodynamically stable crystal structure occurred. Especially, the crystal habit of NH_4NO_3 / KNO_3 ratios 1:2.5 and 1:1 within the cross-linked films had a different appearance than the orthorhombic shape.

Tab. 6-2: Morphology and distribution changes of inner-film crystallized additive mixtures of KNO_3 and NH_4NO_3 (molar ratio) during storage for 7 days at constant environmental conditions (25 °C and 50 % RH). Light microscopy exposures from NaCas films (+/- MTG) are shown. The films have been produced using Activa MTG (cross-linked films), 20 mM Tris/HCl buffer pH 7 as solvent and a NaCas / glycerol ratio of 2:1. For results of the mechanical analysis see Fig. 6-9.

Film		After film drying	2 days storage	7 days storage
NH_4NO_3 / KNO_3 1:10	- MTG			
	+ MTG			
NH_4NO_3 / KNO_3 1:2.5	- MTG			
	+ MTG			
NH_4NO_3 / KNO_3 1:1	- MTG			
	+ MTG			

The morphologies are divers and plate-like triangles, agglomerates, tetrahedrons, cubes and needles were found. For the case of the $NH_4NO_3 \cdot x KNO_3$ binary system, Chien *et al.* [Chi05] described mixtures of two non-stoichiometric solid phases. Regarding the applied NH_4NO_3 / KNO_3 ratios 1:2.5 and 1:1 would fit to the proposed

(ANK+ANZ) and (ANZ) solid solutions, if anhydrous conditions are assumed. Possibly, these polymorphic forms are present in the structure of NaCas films with NH_4NO_3 / KNO_3 ratios 1:2.5 and 1:1 as well.

For all films it can be stated that larger crystals were formed during the storage. This is described by Ostwald ripening and diffusion processes within the material [Mye02].

6.2.2.2 Effect of ammonium nitrate on the films mechanical performance

In a further investigation, NH_4NO_3 was used as single functional additive in NaCas films and the effect on the material quality and mechanical performance was studied. As to be seen in Fig. 6-10, films with various NH_4NO_3 / NaCas mass ratios have been produced and analyzed. For none of the material compositions, inner-film crystallization of the salt additive was observed and films had a homogeneous, translucent and shiny appearance. Due to its high water solubility of 2146 g_{anh}/kg_{H2O} (25 °C), the NH_4NO_3 was expected to stay in solution as the films residual humidity is sufficient to guarantee the complete dissolution of NH_4NO_3 at the chosen environmental conditions (25 °C and 50 % RH) [Mer04].
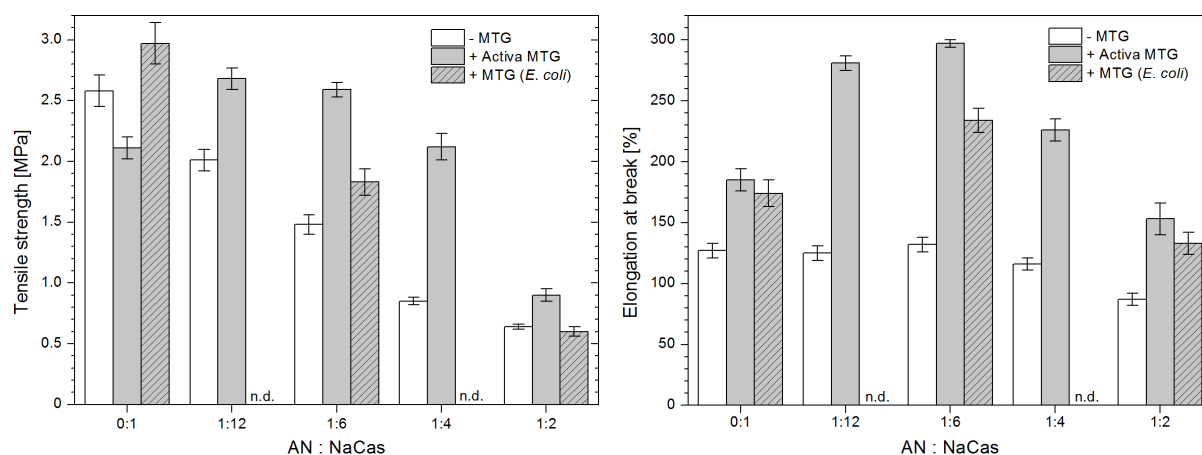
Fig. 6-10: Ammonium nitrate as primary additive in NaCas films affecting tensile strength and elongation at break of the material. The additive content is given in NH_4NO_3 / NaCas mass ratio and enzymatic cross-linking was induced by Activa TG and recombinant MTG (*E. coli*), respectively. Films are dried 24 h at 25 °C and 50 % RH and stored at same conditions.

In the mechanical properties obtained from the various film compositions, the NH_4NO_3 / NaCas ratios of 1:12 as well as 1:6 was found to be most beneficial in the enhancement of tensile strength and elongation when Activa MTG was additionally applied to cross-link the protein network. Furthermore, the tensile strength of NaCas films modified with MTG (*E. coli*) and non-cross-linked films was proven to be highly dependent on NH_4NO_3 addition. Their initial values decreased to about 25 % comparing the films with ratio 1:2 and the film composition without any additive. In case of the films cross-linked with Activa TG, the tensile strength was at first raised to 2.7 MPa (ratio 1:12) and preserved at higher NH_4NO_3 content. At the NH_4NO_3 / NaCas ratio of 1:4, the tensile strength of the Activa TG cross-linked films then

dropped down to reach the same level at ratio 1:2 as the other analyzed film compositions.

Regarding the elongation at break shown in Fig. 6-10, the performance of the non-cross-linked films remained constant at 128 % in average. At the NH_4NO_3 / NaCas ratio of 1:4, the elongation was measured to start to decrease. In contrast, the films with cross-linking by Activa MTG / MTG (*E. coli*) reached their optima in elongation at the NH_4NO_3 / NaCas ratio of 1:6 and relative increases of 37 % and 26 % have been obtained, respectively. However, the elongation performance of the cross-linked materials has been shown to be adversely affected by higher NH_4NO_3 content as well.

6.2.2.3 Potassium nitrate and urea additive mix

Also the combination of KNO_3 as primary additive and urea as secondary additive has been analyzed. Especially, the dependence of the mechanical properties of NaCas films on the urea content increase in presence of KNO_3 was studied. In Fig. 6-11, the data from the mechanical testing are presented, showing that urea acts as plasticizing agent since the tensile strength was proven to decrease continuously with higher urea content while the elongation of the material was enhanced.
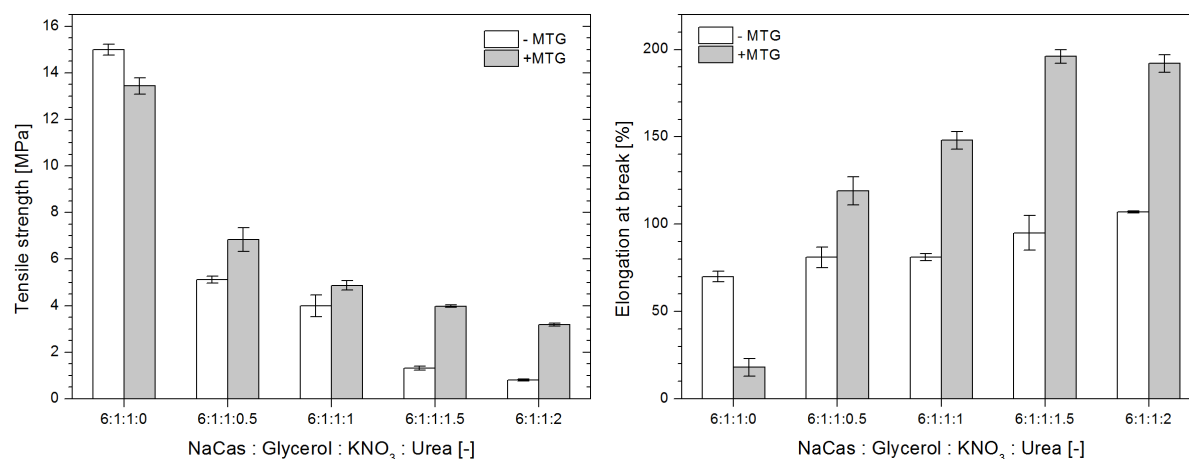
Fig. 6-11: Mechanical properties of NaCas films dependent on plasticizer and additive content and enzymatic cross-linking with Activa MTG (+/- MTG). The glycerol amount was diminished to the NaCas / glycerol ratio of 6:1 as urea was added in varied NaCas / urea ratios. The crystallizing additive KNO_3 was incorporated in the NaCas / KNO_3 ratio of 6:1 [Sto11].

Therefore, the amount of glycerol had to be reduced to the NaCas / glycerol ratio of 6:1 in order to reach film formation [Fro10b]. The mix of functional additives was chosen to include a constant amount of KNO_3 (NaCas / KNO_3 mass ratio of 6:1) and variable urea content (NaCas / urea ratio from 6:0 to 6:2). The KNO_3 crystal morphology and distribution was confirmed to be needle-like after 2 days of storage at 25 °C and 50 % RH independently of the urea amount added. This observation corresponds to the results of the additive screening tests with NaCas films shown in Tab. 6-1. The cross-linking the protein matrix by Activa MTG is advantageous

particularly with regard to the films mechanical performance. On the one hand, the tensile strength can be preserved to some extent. On the other hand, the flexibility of the films has been considerably enlarged, because an elongation increase was reached that is up to 90 % compared to the cross-linked NaCas film without urea.

6.3 Mass transfer

6.3.1 Water uptake and water vapor permeability

The water absorption of particularly NaCas films was analyzed by means of the water uptake of the material being immersed into water as well as the water vapor absorption from a humid environment. The description of the experimental procedures is included in the chapters 5.4.2 and 5.4.3, respectively.

Films with NaCas or gelatin as protein basis have been used for the analysis of the uptake of liquid water. All the film specimens had been cross-linked applying Activa MTG and differed in their additive content. The results for the water uptake of NaCas films presented in Fig. 6-12 (I) indicate a strong influence of the film composition. Additionally, the comparison to the data from the gelatin films in Fig. 6-12 (II) reveals a huge dependency on the choice of protein.
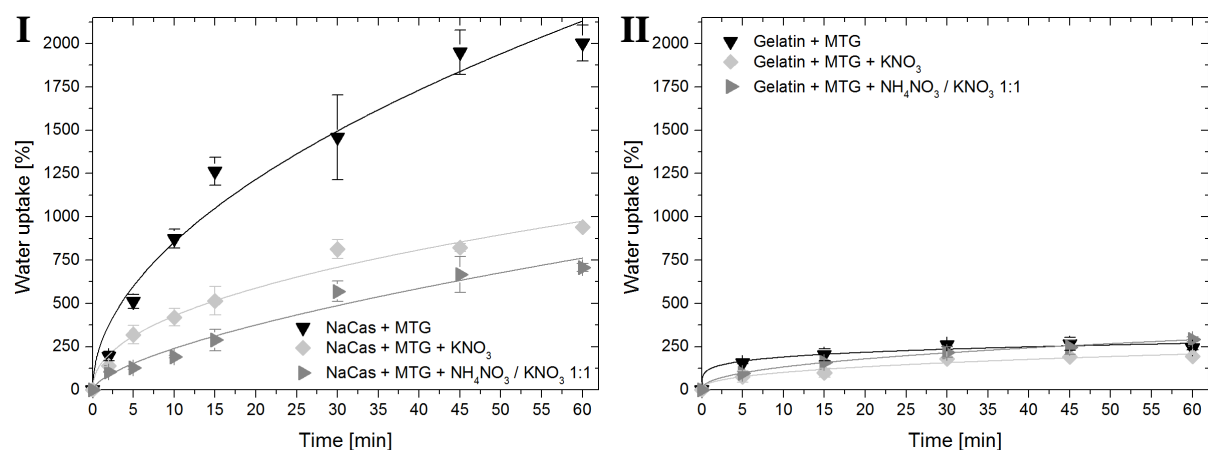
Composition	NaCas		Gelatin	
	k	n	k	n
+ MTG	264 ± 54	0.51 ± 0.06	121 ± 22	0.19 ± 0.05
+ MTG + KNO$_3$	148 ± 23	0.46 ± 0.04	40 ± 11	0.40 ± 0.08
+ MTG + NH$_4$NO$_3$ / KNO$_3$ 1:1	54 ± 14	0.65 ± 0.07	48 ± 3	0.44 ± 0.02

Fig. 6-12: Water uptake of enzymatically cross-linked protein films according to DIN EN ISO 62. Gelatin (280 Bloom) was supplied by Gelita, Eberbach (Germany). The ratio of NaCas / salt additive was kept constant at 6:1. The data are fitted by applying the power law equation $M_t / M_\infty = k \cdot t^n$ and the calculated factors k and n are summarized in the corresponding table below the diagrams [Pep01, Gan10].

Whereas the studied gelatin films show a comparable water uptake with a maximum of approximately 250 % reached after 45 min of immersion, the cross-linked NaCas films exhibit a water uptake of up to 2000 % of their initial mass. The absorption of

water was determined to be decreased to 940 % or 700 %, when KNO_3 or the additive mix of NH_4NO_3 / KNO_3 of 1:1 had been incorporated into the films.

The mechanism of diffusion in the protein network can be judged according to an empirical power law equation (eq. 2-1). The value of the diffusional exponent n is correlated to the type of transport by means of the classification that is given in Tab. 2-3. For the cross-linked NaCas films as well as the gelatin films, still a Fickian diffusion was determined [Wan08]. The NaCas film with incorporated NH_4NO_3 / KNO_3 mix exhibited more an anomalous diffusion behavior. It is assumed that the amount of accessible hydrophilic peptides in the protein matrix effect the water absorption strongly. Salt additives in this case would have an effect on the protein structure and folding, leading to a 'salting out' and protein aggregation. The differing transport mechanisms are considered to affect the additive release from the NaCas materials. This is further discussed in chapter 7.5.

The water vapor absorption ability of protein-based films was quantified dynamically by the DVWSG analysis with the sorption isotherm as the result shown in Fig. 6-13 (I). The measurement data in Fig. 6-13 (II) are obtained by using constant environmental conditions. The protein-based material was detected to be sensitive to higher humidity without any dependency on the additive composition. As to be seen in Fig. 6-13 (I), the data fit was carried by the Guggenheim-Anderson-De Boer (GAB) model that provides generally the most accepted water sorption isotherm for foods [Van84, Gen94, Kim01, Sah06, Kri07, Fab10].

In the comparison of the sorption / desorption processes, a hysteresis can be observed. The Fig. 6-13 (I) shows only the water sorption in order to keep clarity, but the complete data set is given in Tab. 14-12. The storage of NaCas and gelatin films at constant conditions (25 °C; 50 % RH) resulted in an average residual material humidity of 15 % w/w. Herein, no significant difference was found that would derive from the protein raw material and choice of incorporated salts. Despite that, a trend to higher humidity content was visible for films containing the NH_4NO_3 / KNO_3 salt mixture.
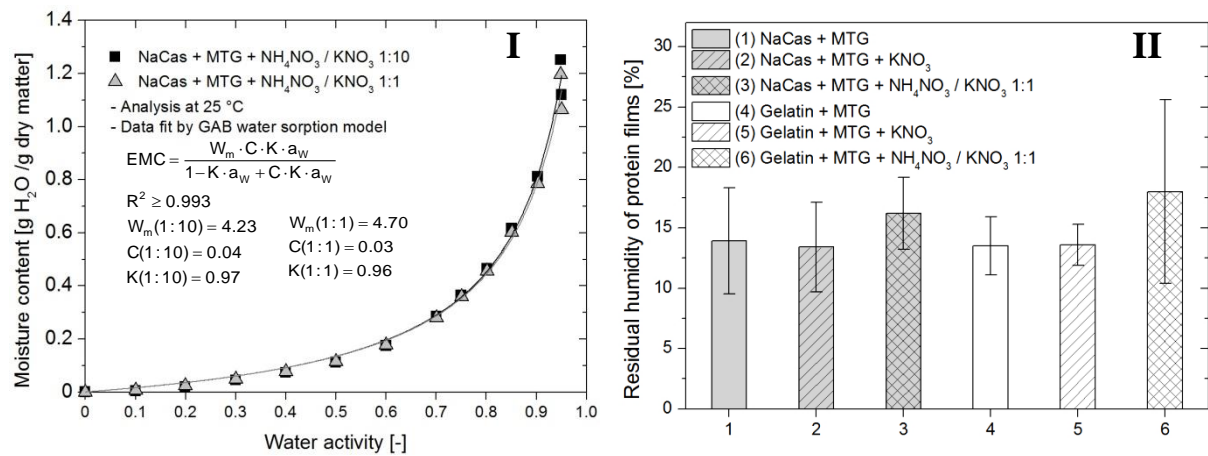
Fig. 6-13: Water sorption isotherm of two NaCas film compositions measured at 25 °C by DVWSG (I) and the residual humidity of protein films (II) stored at 25 °C and 50 % RH prior to drying at 50 °C for 24 h. The water content in the films is quantified by mass loss during drying, n ≥ 15. The ratio of NaCas / salt additive was kept constant at 6:1. The water sorption data have been fitted by the Guggenheim-Anderson-De Boer (GAB) model, where EMC… equilibrium moisture content (dry basis); W_m… monolayer moisture content [g H_2O / 100 g film]; C and K… adsorption constants [-]; a_W… water activity [-] [Van84, Kim01, Sah06].

The hydrophilic nature of the protein-based polymers typically results in good water vapor permeability values. Considering that, the water vapor transmission rate of the produced NaCas films was tested with the gravimetric dish method explained in chapter 5.4.2. According to the data listed in Tab. 6-3, both non-cross-linked and cross-linked NaCas films are well permeable to water vapor, if no coating was applied.

Tab. 6-3: Water vapor transmission rate (WVTR) of NaCas films +/- MTG and +/- beeswax coating, conditions: 25 °C, driving force 50 % RH (outside the cup) to 0 % RH (inside the cup); n = 3.

Film composition	WVTR [g/m²d]	SD [g/m²d]
NaCas film - MTG	1986	± 349
NaCas film + Activa MTG	1390	± 150
NaCas film – MTG + beeswax coating	29	± 4
NaCas film + Activa MTG + beeswax coating	43	± 13

Furthermore, the comparison of the WVTR data shows the ability of the cross-linked protein matrix to retain the water vapor to a higher extent than the non-cross-linked films (high significance, $p < 0.001$). However, the measurement with both the film compositions had to be interrupted after 36 h since the adsorption capacity of the desiccant was reached. With a beeswax coating on the top surface of the NaCas films, the high sensitivity of these protein-based materials can be controlled. By the coating method, the WVTR was decreased by 45 times. The thickness of the coating amounted to about 100 µm. Variations in the WVTR of the coated films are seen to be related rather to inhomogenities in the coating than to a material property of the protein films.

6.3.2 Dissolution and release

The protein-based materials have been analyzed according to the release of the incorporated functional additives. In chapter 5.4.4, the experimental set-up is described. Summarizing the method, film specimens have been put into tubes filled with water. The tubes have been placed in an environment of controlled temperature and have been rotated. Over time, samples have been withdrawn from the solvent and analyzed for the nitrate content and protein amount. The nitrate analysis is representative for the total dissolution and release of the functional additives. Protein dissolution into the aqueous medium has been expected to happen, when non-cross-linked NaCas films were studied. The results then have been normalized taking the estimated amounts of the measured components into account.

The test films were chosen to be non-cross-linked and Activa MTG cross-linked NaCas films, without any additive or with a salt additive content in NaCas / salt ratio of 6:1. KNO_3 or the mixture of KNO_3 and NH_4NO_3 in molar ratio of 1:1 was added in the film manufacture. In Fig. 6-14, the nitrate release from these films is shown. First of all, the films without additive (NaCas +/- MTG) have been determined to contain no nitrate that could have been brought in by impurities of the films raw materials. Therefore, the detection of the additive release was proven not be disturbed by entrapments by the matrix material. Comparing the time-dependent release of the functional additives, it is clear that the protein-based carrier played a minor role in the retention of the mass transfer. However, a slight temperature dependency of the release kinetics is pointed out by Fig. 6-14 (IV), where the estimated linear release rates are plotted. When the protein matrix had been cross-linked, the temperature dependent release rates show a polynomial trend that remains unsolved on the part of the physical background. However, the faster release of the salt additive mix compared to pure KNO_3 is attributed to the lower degree of the additives crystallinity within the films as described in chapter 6.2.2.1.

Higher measurement deviations and equilibrium data deviating from 100 % are likely to result from inhomogenities in the additives inner-film distribution. Furthermore, the measurement error from the photometric data acquisition is known to count up to 20 % in average. Considering the possible occurrence of random errors, the triple measurement of the data was necessary and revealed an adequate reproducibility of the results.
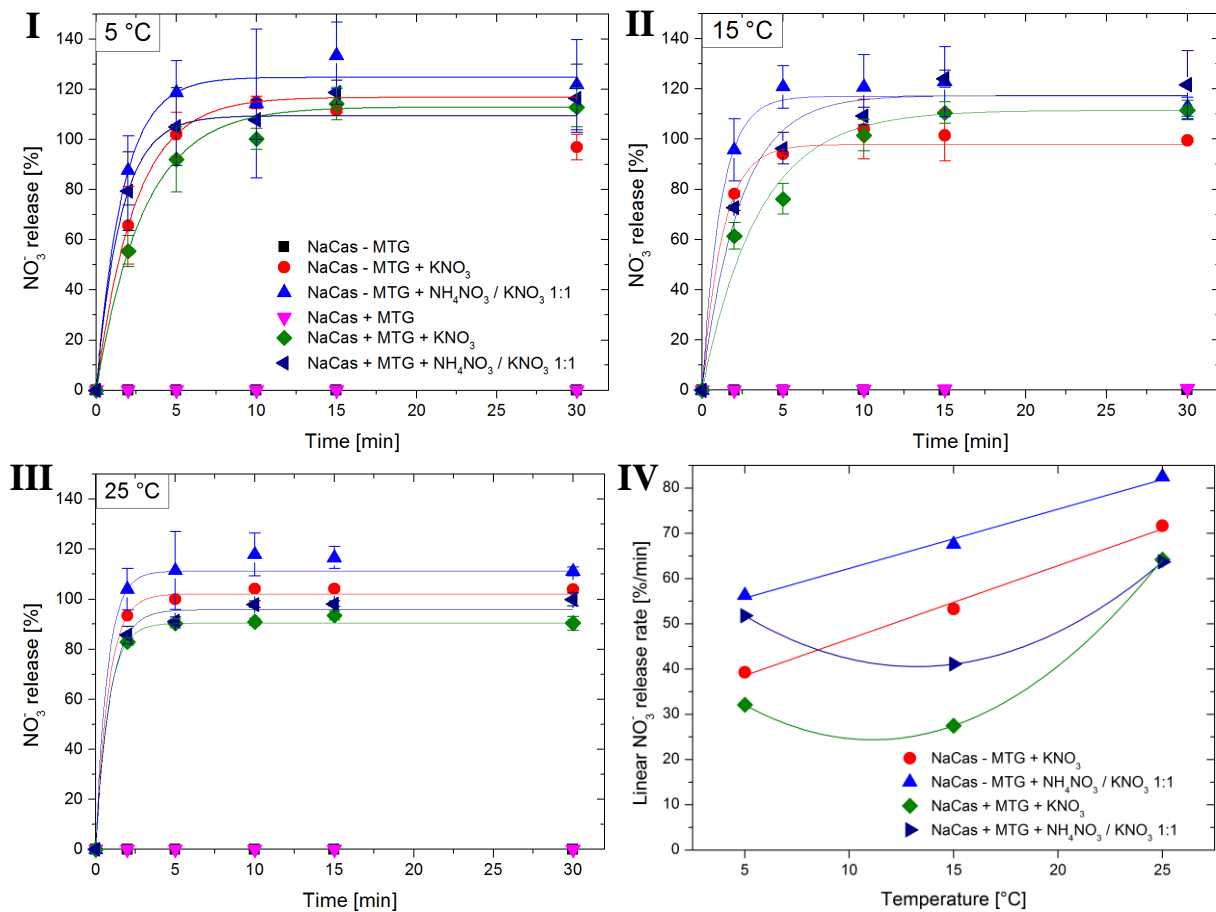
Fig. 6-14: Active ingredient release (KNO_3 / NH_4NO_3) from NaCas films determined from the nitrate concentration in the solvent; measurement in triplicate. The linear nitrate release rate (IV) is determined from the asymptotic data fits (I-III) and estimates the nitrate release after 1 min of the tests.

During the additive release tests, the protein-based carrier typically undergoes a water uptake, swelling and (partial) dissolution as it was pointed out in the previous chapter 6.3.1. Therefore, the protein concentration in the liquid medium was monitored. The results of the protein release analysis can be gathered from Fig. 6-15.
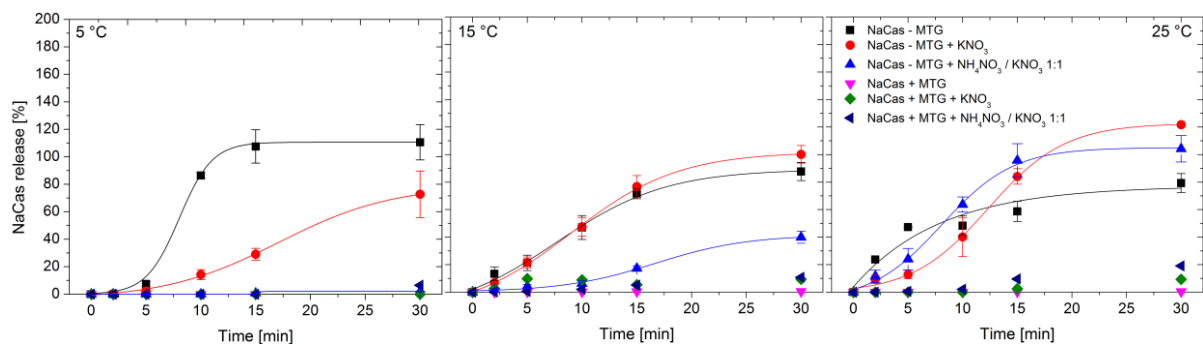
Fig. 6-15: Protein loss from the polymer matrix during active ingredient release tests; measurement in triplicate.

The cross-linking of the inner-film protein matrix was indeed observed to counteract the water solubility of the NaCas (+ MTG), leading to total insolubility. The cross-

linked protein behaved differently in films containing incorporated KNO_3 and NH_4NO_3, respectively. At room temperature and after 30 min of the test, approximately 10 % of the NaCas was released from the material when KNO_3 was present in the matrix. For films with incorporated KNO_3 and NH_4NO_3 mix, even 20 % of the total protein was determined to be dissolved in the medium. Herein, a decrease in the temperature decelerated the protein dissolution and release.

Regarding the non-cross-linked NaCas films, the protein content was completely dissolved after the end of the test at 25 °C. A sigmoidal curve progression was assumed in the data fit (Fig. 6-15), since the polymer tends to swell by water absorption. Finally, the protein molecules dissolve and are released from the network [Sie12]. With decreased temperature, the NaCas release characteristics have been measured to specify according to the material composition of the film specimens. The reference NaCas film (- MTG) dissolved completely at all temperatures applied. In the contrary, the films with KNO_3 still dissolved at 15 °C, but appeared to reach a solubility equilibrium at approximately 80 %, when the test was carried out at 5 °C. A similar trend was observed for those non-cross-linked films with incorporated NH_4NO_3 / KNO_3 mixture: an equilibrium of 40 % of the total protein was detected at 15 °C. At 5 °C, the share of dissolved protein was again diminished towards less than 5 % of the total amount. These tendencies correspond to the results achieved in the analysis of the water uptake provided in Fig. 6-12.

6.4 Effect of additives on the reaction kinetics of microbial transglutaminase

The solubility of the materials protein-based network was found to be dependent on the presence and type of a functional (salt) additive as seen in chapter 6.3.2. Therefore, the applied additives have been assumed to influence the enzyme activity of the Activa MTG. Also the reactivity of the protein molecules in the cross-linking reaction can undergo changes. Here, the additives interfere with the interactions in the protein folding and lead to conformational changes. The study on the MTG reaction kinetics was carried out using the photometric hydroxamate assay as well as the SDS-PAGE method. Information on the methods is given in the chapters 5.4.7 and 5.4.6. The studied additives have been chosen by means of their application as inner-film crystallizing component or as potential face specific crystal growth inhibitor.
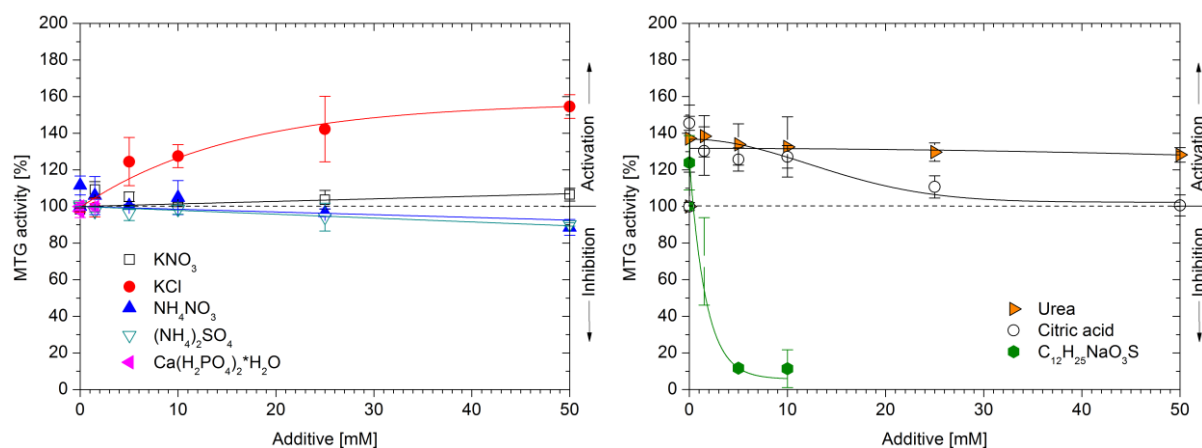
Fig. 6-16: Dependency of Activa MTG reaction kinetics on additives (inorganic / organic) and additive concentrations. The transglutaminase activity was measured by hydroxamate assay described in chapter 5.4.7. The MTG activity (100 %) without influence of additives is represented by the dashed line and grey field marking the measurement error of the reference. $C_{12}H_{25}NaO_3S$ is sodium dodecyl sulfonate.

The obtained data and trends are visualized in Fig. 6-16 and clearly reveal the specific influence of the chosen inorganic and organic substances. The specific additives have been found to act as either activators or inhibitors of the transglutaminase catalysis function. In a film forming solution with NaCas / salt ratio of 6:1, the molar ratio of enzyme and inorganic additive (MTG / salt) is typically 1:21.250 (in case of KNO_3) and differs depending on the molecular weight of the salt to be used. Within the hydroxamate assay, an enzyme concentration of 1.5 µM was used throughout the tests. Thus, an additive concentration of approximately 30 mM (in case of KNO_3) is suitable to reach the MTG / salt ratio being comparable to the film forming solution. The results from the hydroxamate assay can be therefore transferred to the assessment of the additive effect in the protein film manufacturing.

Among the activating agents, KCl, urea and citric acid have been identified. Herein, the enzyme activity is highly dependent on the additive concentration. For KCl, the MTG activity was detected to reach a maximum (+ 55 %) at about 50 µM. Regarding the usage of citric acid, the MTG activity was observed to have an optimum (+ 46 %) at lowest citric acid content with subsequent decrease of the enzyme activity at higher citric acid concentrations. To a small extent, also KNO_3 can positively influence the MTG activity, if applied at higher concentration. The $Ca(H_2PO_4)_2 \cdot H_2O$ was only applicable at low concentrations in the activity assay, as this additive is poorly soluble in aqueous solutions.

The Fig. 6-16 also provides information on enzyme inhibitors that have been determined to be both the ammonium salts NH_4NO_3 and $(NH_4)_2SO_4$ that lead to 10 % activity loss at 50 mM. Furthermore, the sodium dodecyl sulfonate ($C_{12}H_{25}NaO_3S$) strongly inhibits the MTG activity. In the test, the sulfonate was applicable until

10 mM, because of its poor water solubility. However, the MTG was inactivated to an extent of 90 % at the highest sulfonate concentration used.

The presented study on the MTG reaction kinetics gives quantitative information on the sensitivity of the enzymatic cross-linking on several potential additives in protein-based material. The substrates and reaction conditions of the hydroxamate assay are not identical to the real process, but still the data is highly valuable for a first evaluation of an additive's influence on the MTG.
Since KNO_3 and NH_4NO_3 are seen as the most important additives in this work regarding functionality, product design and inner-film crystalline structure control, the effect of these salts on the MTG reaction kinetics have been further examined. The NaCas film forming solution was used as batch reaction. From the solution, samples have been taken and subsequently analyzed by SDS PAGE (Fig. 6-17). The determination of the cross-linking reaction progress inside the film forming solution summarizes all eventual influencing factors. These can be interactions within the whole material composition including the protein and plasticizer, all steps of making the solution as well as the dilution of substrates, enzyme and additive in the solvent.

In the SDS PAGE gels in Fig. 6-17, the ongoing cross-linking reaction is visually detectable by the time-dependent disappearance of the NaCas substrate. The NaCas fractions are originally visible as bands with high color intensity like in lane 2 representing the reaction batch right before MTG addition. The three distinct NaCas bands are derived from the individual NaCas fractions α_S-, β- and κ-casein (from top to bottom). The highly diluted MTG is hardly to be seen in the gel. Additionally to the intensity loss of the substrate bands, the most prominent evidence for cross-linking is the formation of high molecular weight protein aggregates that exceed the gels pore size. These aggregates stick to the boundary of the resolving gel or stay within the stacking gel. In order to quantify the SDS PAGE differences of film forming solutions without additive, with KNO_3 and with NH_4NO_3, a densitometric gel analysis was carried out. The data have been added to the diagram in Fig. 6-17. The SDS PAGE result points out that the MTG reacted with the 'monomeric' NaCas substrate as well as with the already cross-linking aggregates as long as reactive sites in the protein structure are available to the MTG.
Therefore, the consideration of the NaCas bands intensity loss supplies an incomplete result, but still serves well for the comparison of the MTG activity in presence of the chosen salts. Corresponding to the photometric measurements in Fig. 6-16, the NH_4NO_3 was proven to act as inhibitor to the MTG activity since the reaction with NaCas substrate was considerably slowed down and a competitive enzyme inhibition is assumed. After 120 min of reaction time, 55 % of the initial NaCas content had been cross-linked by the MTG and according to the asymptotic curve progression.
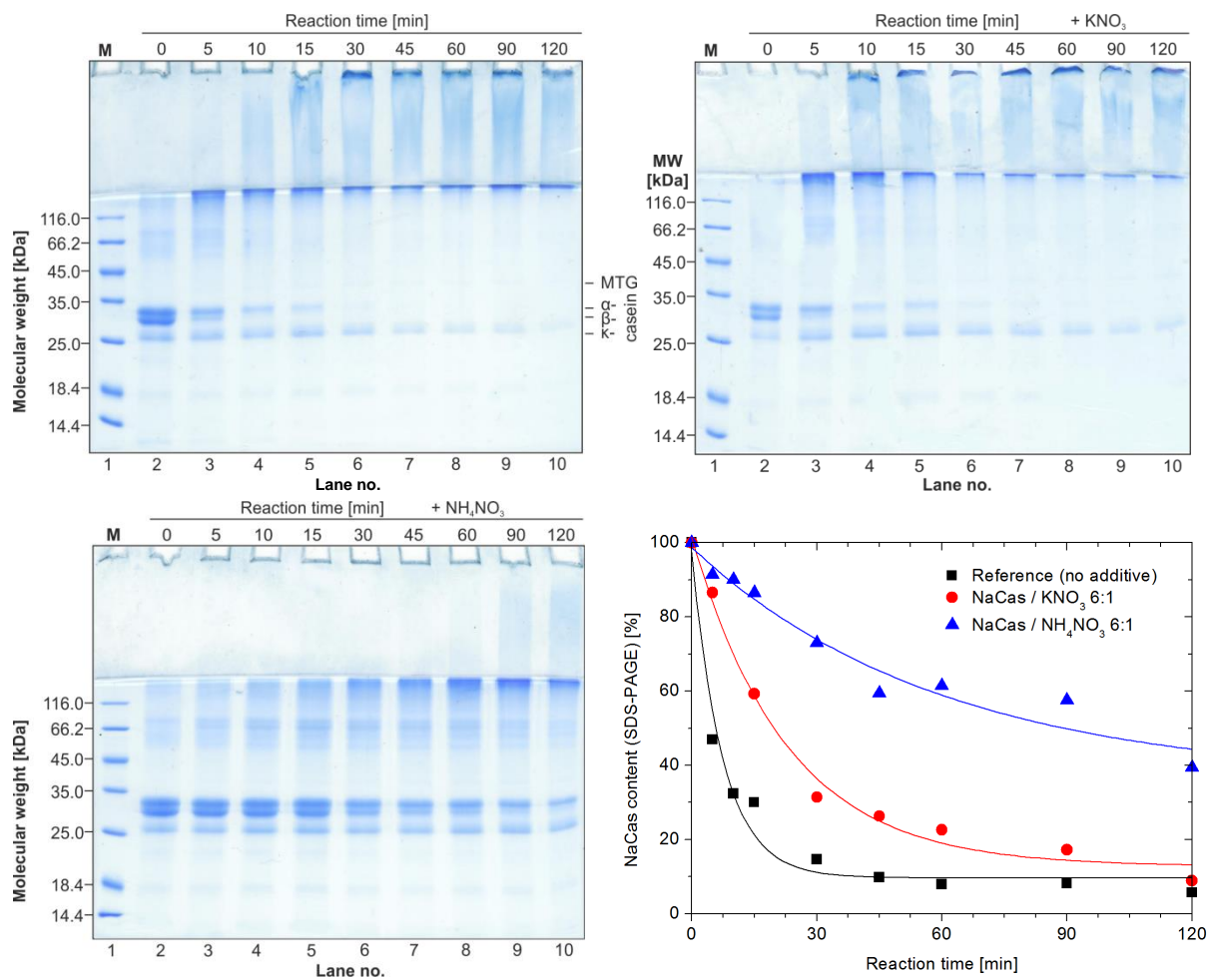
Fig. 6-17: Investigation of cross-linking kinetics affected by salt additives as visualized by SDS PAGE and densitometry analysis of the NaCas bands intensity (bands within range of 25 – 35 kDa) showing the decrease in the original NaCas content by enzymatic cross-linking. Samples were withdrawn from film forming solutions containing NaCas and Activa MTG. The NaCas / salt mass ratio amounted to 6:1 for both salts KNO_3 and NH_4NO_3.

It is estimated that the reaction should have been finished at a consumption of about 60 % of the NaCas protein. This might be due to an additional effect of heat inactivation of the enzyme. The Activa MTG exhibits a relatively high instability at the reaction temperature of 50 °C (see chapter 4.3). Furthermore, the folding of the NaCas protein might have changed and the reactive amino acid residues of the protein substrate could have been sterically blocked to the MTG.

Also the results of the KNO_3 containing film forming solutions showed good agreement with the previous activity tests (Fig. 6-16). The NaCas content was determined to be consumed until a residual amount of approximately 10 % after 120 min of reaction. The progress is similarly to the reference data from the film forming solution without functional additive. Visible differences in the reaction progression have been possibly caused by inhomogenities in the solutions while sample drawing, random errors in the preparation of the SDS PAGE gel and inaccuracies regarding the densitometry.

6.5 Application of protein-based seed carriers

In this study, the well-known radish (*Raphanus sativus var. sativus*) and lettuce (*Lactuca sativa var. capitata*) have been seeded with different techniques as described in chapter 5.3. Regarding both model plants, the protein-based seed tapes and sheets resulted in best performance considering plant growth and biomass production.
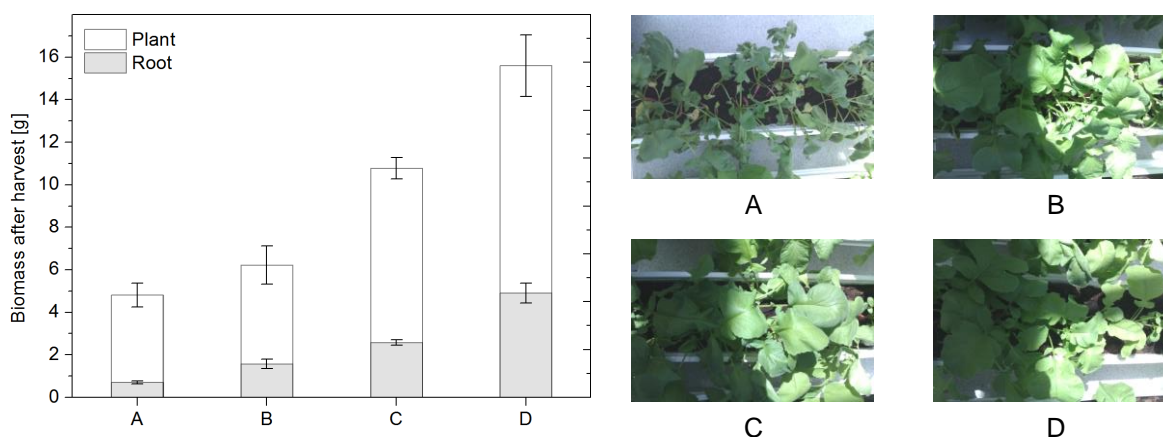
Fig. 6-18: Plant growth of *Raphanus sativus var. sativus* determined as final biomass (wet matter) dependent on various seeding techniques: (A) bulk seed, (B) paper seed tape, (C) protein-based seed-tape, (D) protein-based seed tape + KNO_3. The photographs show the radish plants after 30 days of cultivation right before harvesting.

The plant growth of radish from protein-based seed tapes has been compared to the yield in biomass obtained from bulk seed and commercially available paper-based seed tape. The biomass of the harvested radish plants was taken as the final measurement data. From Fig. 6-18, the effects of the distinct seeding technique can be extracted. The biomass of the whole plant and the root mass are distinguished.

In the case of the radish plants, the protein-based seed tape with the incorporated additional fertilizer (D) led to the highest biomass of in average 16.6 g in total and 4.9 g of the root. The root is the relevant part of the radish plant. Considering that, the application of protein biopolymer and KNO_3 resulted in a 3.2 times higher mass of the root compared to bulk seed (A). Furthermore, a 50 % higher mass was achieved than with the protein-based seed tape without any additional fertilizer (C). NaCas itself and generally all proteins serve as nitrogen sources when biologically degraded in the soil [Wid60]. Therefore, the protein-based seed tape (C) itself positively affects the conditions for seed germination and plant growth as it benefits fertilization and humidifying of the soil. Thus, the protein material helped to strengthen the plants against dehydration in the rather inconvenient environmental conditions in the green house.

In contrast to the seed tapes with radish, the protein-based sheets for the seeding of lettuce have been prepared as two-layer material with the seeds fixed in between the films. The advantage of this prototype is based on the improved product handling.

The radish seed tapes had been found to lose the attached seed easily. In Fig. 6-19, the seed germination data and biomass of the lettuce as well as pictures from the last cultivation day are summarized.
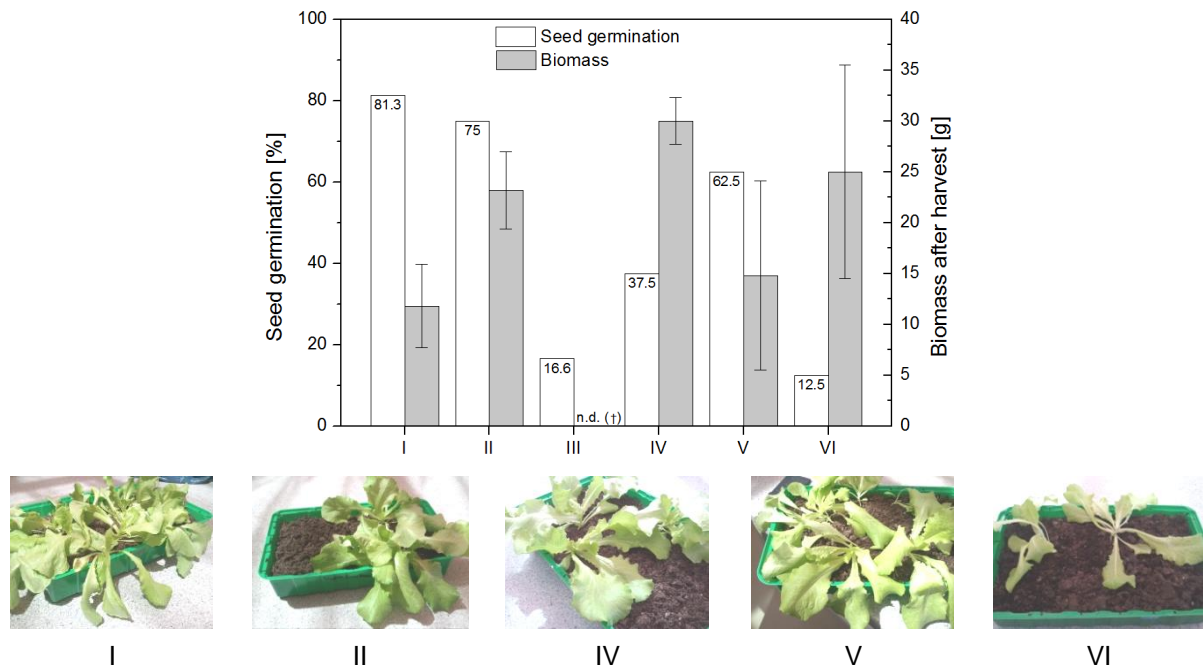
Fig. 6-19: Dependence of seed germination of *Lactuca sativa var. capitata* on different seed techniques and average biomass (wet matter, per plant) after cultivation time of 30 days. (I) loose seed – germination: 13 of 16 seeds; (II) pilled seed – 3 of 4 seeds; (III) paper-based seed-tape – 2 of 12 seeds (stunted growth of seedlings, dead during cultivation time); (IV) protein-based seed-tape – 6 of 16 seeds; (V) protein-based seed-tape + KNO_3 – 10 of 16 seeds; (VI) protein-based seed-tape + urea – 2 of 16 seeds. Pictures below present the appearance of the salad plants right before harvest.

The plant growth test pointed out, that the seeding with bulk seed (I) and pilled seed (II) has been most successful regarding the germination level. At minimum 75 % of the seeds has been observed to germinate and to form seedlings.

However, the protein-based seed sheets showed a trend to an optimum ability in biomass production, in particular considering the sheets (IV) without any extra fertilizer with which in average 30 g of wet biomass have been produced. The incorporation of KNO_3 (V) or urea (VI) was determined to accelerate the plant growth leading to a final biomass being 20 % and accordingly 53 % increased compared to bulk seed (I), whereas the protein-based sheet without additive (IV) resulted in a biomass increase amounting to 61 %. The higher germination level of (V) compared to (IV) is possibly due to the formation of micro-pores resulting from the dissolution of the KNO_3 crystals in the seed sheet (V). It is known that protein-based materials typically exhibit efficient gas barrier properties. The pores are considered to accelerate the air transfer to the seed [Che95a, Car04, Jim12]. Therefore, the germination from the protein-based seed sheets is assumed to be limited by the two-layer protein carrier leading to poor air supply to the germinating seeds.

7. Discussion

7.1 Production process

The manufacturing of protein-based materials by the wet process was proven to be a simple and stable lab-scale method that can be easily adapted to changes in the material composition and modifications within the process parameters. As described in the chapters 6.1 and 6.5, respectively, homogeneous films and products have been produced with different shapes and application of functional additives aiming for novel product design purposes. As briefly described in chapter 6.1, the protein-based films have been further processed to ensure their capability in packaging applications and carrier for a labeling and / or an advertisement to attract the consumer's interest.

7.1.1 Material structure

The XRPD analysis of the freshly produced protein-based films was successfully applied for the identification of the proteins degree of structural order as well as for the verification of crystallinity regarding the KNO_3 particles incorporated into the material. The data are presented in chapter 6.1.1 with additional attention to the effect of cross-linking. The pattern of the NaCas films without additives (Fig. 6-1) revealed a completely amorphous structure of the protein network irrespective of enzymatic cross-linking. Caseinates are known to contain mostly random coil chain segments [Sie99, Kri07]. The formation of a non-ordered NaCas structure in the material therefore was expected. Furthermore, the peaks of the inner-film KNO_3 are in good accordance with the KNO_3 pattern from the database. The specification of KNO_3 polymorphs is possible by comparing literature data from the pure polymorphs phase-II and phase-III KNO_3 in the region of 20 – 40 °2θ.
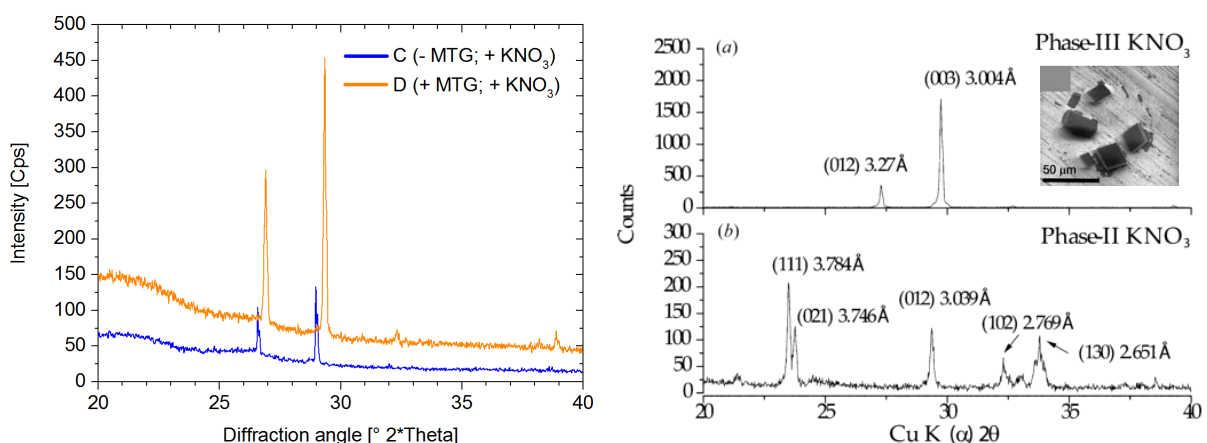
Fig. 7-1: Detail view on XRPD pattern of NaCas films (+/- MTG) with incorporated crystallized KNO_3 (original graphs in Fig. 6-1) and comparison of phase-III KNO_3 and phase-II KNO_3 in their XRPD signal, obtained from literature. SEM image shows rhomboid-shaped phase-III KNO_3 [Fre09].

The Fig. 7-1 underlines that mainly the peaks of phase-III KNO_3 had been detected [Fre09]. Since smaller peaks in the range of 30 – 40 °2θ had been found as well as a

peak shift in the C pattern, it can be stated that phase-II as well as phase-III KNO_3 have been detected inside the samples. Therefore, it is assumed that the phase transition to the thermodynamically stable form was ongoing and it is likely that the XRPD would not give evidence for the crystals lattice periodicity of the orthorhombic phase-II KNO_3, because of the formation of macroscopic acicular crystal network that has been observed e.g. in the additive screening, chapter 6.2.

7.1.2 Drying as a crucial step

The solvent removal by drying is an important step in the manufacturing of protein-based materials both in the solvent process as to be seen in chapter 6.1.2 and in the scale-up to the industrial process involving extrusion techniques. In the traditional polymer industry working with thermoforming of a polymer melt, the cooling of the prior extruded or injection molded products is the equivalent process step and major issues are expected to occur in the processing of proteins as well. Besides thermal and orientation shrinkage effects, the material properties can undergo a change in the mechanical performance and barrier function as well as quality reduction in the organoleptic characteristics. Only few data concerning the modification of the drying conditions can be found in literature. In case of peanut protein, the increase of the drying temperature was shown in the literature to lead to a decrease in film solubility, water vapor and oxygen permeability. At the same time, the tensile strength as well as the elongation of the films have been enhanced significantly. It behaved differently for soy protein films and protein-containing amaranth flour films. The soy protein films have been determined to exhibit differing dependencies of the mechanical parameters on the drying conditions, with the method of protein extraction as the most important factor. For amaranth flour films, the tensile strength was evaluated to be highest at low air humidity and room temperature and the elongation values have been shown to decrease proportionally to the drying temperature increase. The divergent information gives rise to the assumption that the optimization of the drying process is indeed first a matter of the protein system [Ebe00, Jan99, Tap05, Nen06, Thr08, Den09, Fro10b].

For NaCas based materials, no specific characterization of the drying process had been published before. Therefore, a first study on the mechanical properties of NaCas films was carried out in order to provide information on the tendencies in effects of the drying conditions variation for further process design [Sto12a]. As shown in Fig. 6-2 regarding the non-cross-linked NaCas films without crystallized additive (A), the materials tensile strength was enhanced at increased temperature if low or medium air humidity was applied. The elongation of the films A was measured to be stable at varied drying conditions, but generally decreased at the highest drying temperature applied.

In Fig. 6-3, tensile strength and elongation values of KNO_3 containing NaCas films C and D (+/- MTG) are provided. Considering the cross-linked NaCas film B and the KNO_3 containing films C and D (+/- MTG) as well, partly the same trend of stiffness increase at high drying temperature was observed. This trend can be related to heat-induced cross-linking within the protein during film formation. Thermal treatment is known as a cross-linking method and thus, it promotes the covalent association of protein molecules independently of a cross-linking catalyst as mentioned in chapter 2.3.3. The specific reaction mechanism of a physical cross-linking is dependent on the treated protein. In case of caseinate, a self-aggregation property is characterized to form isopeptide bonds under heat influence [Gen96, Ali97, Mil97, Rhi00, Sab01, Gho09, Als12, Ger12].

The heat-induced stiffness increase is higher in particular regarding the enzymatically cross-linked films B and D (when dried at 25 / 50 % RH). A synergistic effect of the Activa MTG (containing 99 % w/w maltodextrin) and heat treatment can be assumed. This consideration is based on the described polymerization mechanism of casein that has been reported to occur on heating and being due to molecules deriving from β-elimination reactions. However, in presence of a sugar compound these molecules are mainly Maillard reaction products that react rather unspecific with a variety of amino acid residues of the protein sequence [Klo77, Kle80, Pel99, Als12, Ger12].

The heat treatment is a traditional post-processing method in polymer technology as well as in metallurgy to modify the materials properties, e. g. for hardening and to affect relaxation of internal stresses (tempering) [Ala06, Zha10]. This heat curing can be an advantageous method in the manufacture of protein-based materials as well and was already applied as final production step for cast films aiming for increased stress, decreased strain as well as decreased water solubility and water vapor permeability [Ali97, Zha10, Pop11, Pel12]. Concluding from the own results from the manufacturing of NaCas films, the curing happens simultaneously to film drying and the combination of the two time-consuming processes can be therefore advantageous to make the overall production process more efficient.

The mechanical performance of the NaCas films A-D has to be discussed separately in case of drying at 75 % RH, since the time for formation of the protein network and structure re-arrangement had been considerably increased by the high air humidity and therefore longer drying time and in case of the MTG addition (films B, D), the cross-linking reaction might have continued . Indeed, the films reached a minimum residual material humidity of 10 % not until the storage conditions of 25 °C and 50 % RH were adjusted. This effect was confirmed by the analysis on water loss of the film forming solution during the drying at different air humidity (see Fig. 6-4). On the one hand, this process modification has led to a higher data scattering and an

overall decline of the mechanical performance regarding the non-cross-linked films A, C and D.

Herein, the films C and D with incorporated KNO_3 have been most affected by the transition of the inner-film crystalline structure to the needle-like orthorhombic morphology as demonstrated by the light microscopy exposures shown in Fig. 6-5. The elongated crystals exceeded the film thickness, protruded the film surface and weakened the protein film mechanically. This phenomenon is possibly due to both an incomplete crystallization after the drying process as well as the transition of the trigonal to the orthorhombic form, preferentially for films dried at high air humidity (75 % RH). Therefore, the macroscopic acicular network weakened the non-cross-linked films, leading to inferior mechanical performance. As briefly described in chapter 4.4, KNO_3 crystals can occur as different polymorphs that can be distinguished by their crystal lattice and habit. By microscopical analysis of the inner-film crystals over time, it was found that first the metastable phase-III KNO_3 crystallized with a trigonal structure. This phenomenon is explained by the Ostwald's rule of stages and the determination of the distinct polymorph is supported by the XRPD result discussed the section before [Thr03]. The phase transition to the thermodynamically stable phase-II KNO_3 is assumed to be solvent-mediated, because the acicular network has been observed to appear faster with increased drying time (and thus higher residual moisture in the material due to increased air humidity).

Hence, the control of the inner-film crystalline structure is possible by monitoring of the drying parameters, but seems to be restricted to low air humidity during film drying in order to avoid the time-dependent formation of acicularity. The metastable phase-III form was demonstrated previously to be stabilized by atomization at RT and low air humidity [Fre09]. In fact, inner-film crystallized KNO_3 was observed to affect the mechanical properties positively when films were dried at 25 °C and 50 % RH. For NaCas films, the application of pressure during production can be embedded into the production process, if extrusion techniques are considered. The kinetics of transition is also seen to be inhibited by fast drying and storage at air humidities below 50 % RH, because of a diffusion effect. Nevertheless, the solvent-mediated polymorphic phase transition is a thermodynamic process and can be retarded, but not completely suppressed.

NaCas films derived from film forming solutions containing Activa MTG dried at 50 / 75 °C and 75 % RH deserve special attention since the mechanical analysis revealed an exceptional increase of both tensile strength and elongation up to 3.8 MPa and 245 %, respectively (Fig. 6-2/B). At first sight, this result appears to be contradictory since heat treatment combined with a cross-linker should act both towards a higher stiffness of the material [Pel12]. Although the precise mechanism of the own investigation remains unclear, it can be stated that the relatively longer

drying time at high air humidity supported most probably the diffusion of the MTG to the reactive amino acids of the protein molecules. Therefore, a higher cross-linking degree is assumed and could be verified in the future, e. g. by firstly a visual SDS-PAGe analysis and by quantifying the cross-links. As another factor, the thermal treatment is assumed to affect partial un-folding of the protein molecules, exposing the reactive sites of the protein. This effect may have led to a higher cross-linking level compared to films dried at 50 / 75 °C and lower air humidity. Heat-induced cross-linking could have played a role resulting from the built-up of lysinoalanine (LAL) as one reactive component being involved in the formation of isopeptide bonds. Pellegrino *et al.* [Pel99] found that the LAL would have mediated the covalent linkage more on the intramolecular level of β-casein in presence of glucose during a thermal treatment at 110 °C for 6 h. A corresponding effect of sodium caseinate, maltodextrin and heat treatment may be assumed, which is a motivation for an investigation in the future. Additionally, heat-affected intermolecular cross-links have been possibly inhibited by the slower water evaporation resulting in molecule disintegration of the dissolved or humidified protein. Therefore, the cross-linked protein matrix within the material is suggested to have mesh characteristics with flexible protein stabilized in the secondary structure by non-covalent interactions and intermolecular isopeptide bonds induced by enzymatic cross-linking. Considering the macroscopic particles seen in the films B dried at higher temperature and high air humidity, protein aggregates are assumed to be junction points of the mesh that had been possibly formed by cross-linkage within the molecules during the heat treatment.

7.2 Inner-film crystallization

The crystallization of additive salts within the structure of polymer materials is a relatively new field of research, if the purpose with respect to material science is considered. The overall principle is similar to the crystal growth of a substance in a (hydro-) gel which is typically a lab-scale method rarely applied in research as briefly summarized in chapter 2.5. Up to now, the most important goal of the diffusion-limited crystallization in a gel is to obtain high quality crystals with a desired particle size for structure analysis of the crystallizing target.

The idea to provide controlled release of plant fertilizers from polymer carriers is not entirely new, but without a special attention to the crystallization of additives [Kan68, Smi91, Mis04]. Frohberg *et al.* [Fro10a, Fro10b] first showed the beneficial synergy of protein-based materials and inner-film crystallizing additives as a key factor for modification and optimization purposes regarding product functionality as well as material performance.

Here, the methods for crystal growth control are discussed to identify ways for mainly the material quality maintenance by assuring a defined mean crystal size and a

specific crystal shape. The challenges in the KNO₃ crystallization have already been touched in the previous chapter on the effects of variations in the drying process. The stable phase-II KNO₃ generally exhibits an elongated, needle-like morphology and the phase transition from the more compact shaped phase-III KNO₃ was proven to be solvent-mediated. Thus, no long-term stabilization of the phase-III KNO₃ and no influence on the morphology of the orthorhombic phase-II KNO₃ is possible by adjusting different supersaturation levels during the drying of the material.

In particular, the field of industrial crystallization provides knowledge on the face specific crystal growth inhibition of a target substance by the use of additives (as the inhibitors) in the crystallization process [Kip97, Mee02, Ulr04]. The aim of inhibition is usually the controlled modification of a plate-like or elongated crystal habit to a shape that should ideally be cubic or spherical. This fits the need in optimization of the inner-film crystallized KNO₃ in NaCas films in order to avoid quality and performance loss due to orthorhombic needle growth. As presented in chapter 6.2, various secondary additives have been screened for their ability to influence the final crystal habit of the stable phase-II KNO₃ during storage of the protein-based material at environmental conditions of 25 °C and 50 % RH. An inhibition of the elongated crystal habit of KNO₃ can be reached by the specific blocking of e.g. the crystal faces {001}, {011} and {112} being indicated in Fig. 4-5. Furthermore, the crystal growth can be substantially affected by those chemicals that enhance or diminish the KNO₃ water solubility and thus change the supersaturation.

7.2.1 Influence of film components on KNO₃ crystal growth

Considering the batch crystallizations and Fig. 6-6, it has been shown that mainly glycerol, but also urea as potential film components strongly promote the growth of orthorhombic KNO₃ needles. These plasticizing agents of protein-based films own high hygroscopic property and it is assumed that glycerol as well as urea had bound large amounts of free water via non-covalent hydrogen bonding [Chr98, Fel06]. Considering this effect, it is supposed that the local supersaturation in the solution resulted in the formation of crystals with a length greater than 400 µm amounting to 10 % and 50 % of the CSD for glycerol and urea addition, respectively. The high content of fines in the batch crystallization of KNO₃ in presence of glycerol might be due to attrition in the magnetically stirred system and during separation of the crystals from the mother liquor, leading to breakage of the thin crystal needles.
On the contrary, the application of Tris buffer as solvent in the batch crystallization instead of distilled water resulted in the desired decrease of the KNO₃ crystals mean aspect ratio possibly due to stabilization of the pH in the suspension, thus shifting the Colulomb interactions being dominant in the crystallization of ionic salts [All02, San07]. However, the positive effect of the buffer system is interfering with the

necessary glycerol content in a NaCas film. Thus, other secondary additives as face specific crystal growth inhibitor had to be screened.

7.2.2 Potential secondary additives

The calcium dihydrogen phosphate $Ca(H_2PO_4)_2 \cdot H_2O$ is a superphosphate serving as both calcium and phosphate source in the plant fertilization purpose. The hydrogenated derivate of the phosphate rock $Ca_3(PO_4)_2$ is soluble in water [Fai02]. The monohydrate form was chosen, because of further increased water solubility. Still, the applicability of the chemical is limited in the manufacturing of protein-based films as only traces of $Ca(H_2PO_4)_2 \cdot H_2O$ can be incorporated, not only as a consequence of the poor water solubility, but also restricted by the salting out of NaCas and protein precipitation already at molar $Ca(H_2PO_4)_2$ / KNO_3 ratio of 1:100, being here a NaCas / $Ca(H_2PO_4)_2$ mass ratio of approximately 256:1 in the material. The salting out is driven by ionic cross-linking of the caseins phosphoseryl residues with calcium ions [Sou85, Men10]. Due to named facts, highly inhomogeneous films have been obtained since the film forming solution could not casted evenly into the mold. Therefore, a $Ca(H_2PO_4)_2$ solution would have to be prepared prior to addition of the salt into that would further dilute the film forming solution. As to be seen in Fig. 6-7 and Fig. 6-8 (II), on the one hand the mean aspect ratio L_1/L_2 of the KNO_3 crystals has been diminished to 2.3:1 with an average crystal length of 131 μm by addition of the calcium salt in the $Ca(H_2PO_4)_2$ / KNO_3 ratio of 1:100. On the other hand, the usage of lower and higher ratios of 1:1000 and 1:10 resulted in an opposite effect on the crystal size distribution. The reason for this fluctuation remains unclear, but it is assumed that the $Ca(H_2PO_4)_2$ and its impurities (sulphate ≤ 1000 mg/kg, chloride ≤ 50 mg/kg) may exhibit a contradictory interrelation on the crystal growth of KNO_3. Summarizing the benefits and drawbacks of $Ca(H_2PO_4)_2$ as secondary additive and inhibitor, it can be stated that the fertilizer functionality of protein-based films could be considerably enhanced by mixing KNO_3 and the phosphate source. The phase-II KNO_3 shape in a NaCas film has been controlled to a certain extent, but the processing revealed challenges. These could be overcome by usage of the high-pressure film extrusion instead of the casting method, because protein precipitation after calcium addition can be beneficial for the material stabilization against water solubility and sensitivity. Furthermore, calcium phosphate crystals have been reported to occur in a protein precipitate showing high potential in bone tissue engineering in the medical field [Guo03, Gu11, Pos12, Str12].

Potassium chloride has great importance as fertilizing agent as well, being typically the main component in potash fertilizer mixtures [Uni98, Pru06, Che08]. Regarding the batch crystallization of the target salt KNO_3, the KCl was found to act as face specific crystal growth inhibitor already in traces since the mean aspect ratio L_1/L_2 was diminished from 4:1 (reference) to 2.5:1 in case of KCl usage in KCl / KNO_3 of

1:1000. Detailed information can be extracted from Fig. 6-6 (III) and Fig. 6-7 (I), respectively. The growth inhibition of specific crystal faces with the inhibitor substance in low concentration suggests the KCl to be a multi-functional impurity within the KNO_3 crystallization, interfering the ionic interactions [Mye02, Ulr04, San07]. In the NaCas film with incorporated KCl and KNO_3 in ratio 1:1000, however, the inhibitor effectiveness of KCl resulted in the formation of crystalline agglomerates, but is insufficient to prevent needle growth in the complex multi-component system of the material (Tab. 6-2).

A study from Yuan *et al.* [Yua07] dealt with the batch crystallization of KNO_3 from solution and among the applied potential face specific crystal growth inhibitors, citric acid as well as sodium dodecyl sulfonate, $C_{12}H_{25}NaO_3S$ have been tested. Surfactants like the anionic sulfonates are well known to act in the crystal habit modification mainly by adsorption of monomeric species on crystalline faces. Therefore surprisingly, the beneficial effect of $C_{12}H_{25}NaO_3S$ on the KNO_3 crystal habit shown by Yuan *et al.* [Yua07] was not confirmed in the own work, although comparable conditions in the batch crystallization had been chosen [Teo73, Can93, Cha03]. On the contrary, the addition of 20 mg/L $C_{12}H_{25}NaO_3S$ resulted in a further increase of the mean aspect ratio of the KNO_3 crystals as presented in Fig. 6-7 (II). Additionally, the usage of polymeric surfactants is not desired in the product design for the agri-/ horticultural purpose, because of environmental and health concerns [Rot12]. Thus, the further research with $C_{12}H_{25}NaO_3S$ as additive in the KNO_3 crystallization was stopped.

The results for the batch crystallization with addition of citric acid instead are quite in accordance with the data from Yuan *et al.* [Yua07]. As described in the literature, the KNO_3 crystal growth in presence of a high amount of citric acid results in very thin needles with a high aspect ratio.

7.2.3 Potassium / ammonium nitrate solid solution

The addition of NH_4NO_3 and KNO_3 into the film forming solution was shown to be most efficient regarding the control of the crystallizing additive within a NaCas film. In the literature, the binary system of KNO_3 and NH_4NO_3 is well described to crystallize as a solid solution of an $NH_4NO_3 \cdot x KNO_3$ structure [Whe48, Coa61, Hol75, Cad81, Dej00, Chi05a, Chi05b]. A solid solution is a crystal structure of at minimum two solid-state compounds being mixed in one homogeneous phase [Mul01]. The stoichiometric composition of the solid solution and the occurrence of a variety of different phases are dependent on both the temperature and the mass fractions of the single compounds. A recent phase diagram of the $NH_4NO_3 \cdot x KNO_3$ solid solution was supplied by Chien *et al.* [Chi05a]. It is reproduced in Fig. 7-3. Here, the region of interest is defined by the preference of 25 °C for the film drying and the ratios of the NH_4NO_3 and KNO_3 salt additive used in the manufacturing of NaCas films.

Furthermore, the solubility isotherm of the ternary $KNO_3 - NH_4NO_3 - H_2O$ system is provided in Fig. 7-2. The effect of water on the solid solution has to encountered, since the NaCas films contain residual moisture at the chosen environmental conditions of 25 °C and 50 % RH.

In the following, the application of the NH_4NO_3 / KNO_3 mix in non-cross-linked and cross-linked NaCas films is discussed. The $NH_4NO_3 \cdot x KNO_3$ solid solution is supposed to crystallize within the protein-based material structure during the drying process. Thus, special attention is paid to a potential interrelation of solid solution, specific crystal growth and the material performance. The corresponding results from the screening procedure can be obtained from Fig. 6-8 (I) and Fig. 6-7 as well as from Tab. 6-1. Regarding the further investigation of the additive mix in the NaCas films, Tab. 6-2 summarizes the observed changes in the crystal morphology. An insight in the mechanical parameters is provided in chapter 7.3.1.

In the batch cooling crystallization, the needle growth of KNO_3 was successfully prevented when NH_4NO_3 was applied in the molar NH_4NO_3 / KNO_3 ratio of 1:10. Within the screening, ratios of 1:1000, 1:100 and 1:10 have been applied and with increasing an NH_4NO_3 amount, the trend to minimization of the crystal length and aspect ratio has been recognized to be highly significant ($p < 0.001$). When the NH_4NO_3 was added in the ratios 1:100 and 1:1000, very large crystals with a mean length of more than 420 µm have been grown. The formation of macroscopic crystal aggregates in the batch with the NH_4NO_3 / KNO_3 ratio of 1:1000 might be attributed additionally to an inhomogeneous heat transfer during the cooling or secondary nucleation. However, an elongated KNO_3 crystal shape was determined for the batches that included NH_4NO_3 in the ratios 1:100 and 1:1000. The shape was similar to the orthorhombic crystal habit of phase-II KNO_3 that had been observed previously in the reference batches with the pure KNO_3 solution. In these batches with NH_4NO_3 / KNO_3 ratio of 1:100 and 1:1000, the salt composition amounted to more than 95 % w/w KNO_3 and less than 5 % w/w NH_4NO_3, if anhydrous conditions are assumed. For this composition range, the binary phase diagram in Fig. 7-3 supports the assumption that the pure phase-II KNO_3 (or KN-II) has been crystallized in the presence of NH_4NO_3 traces.
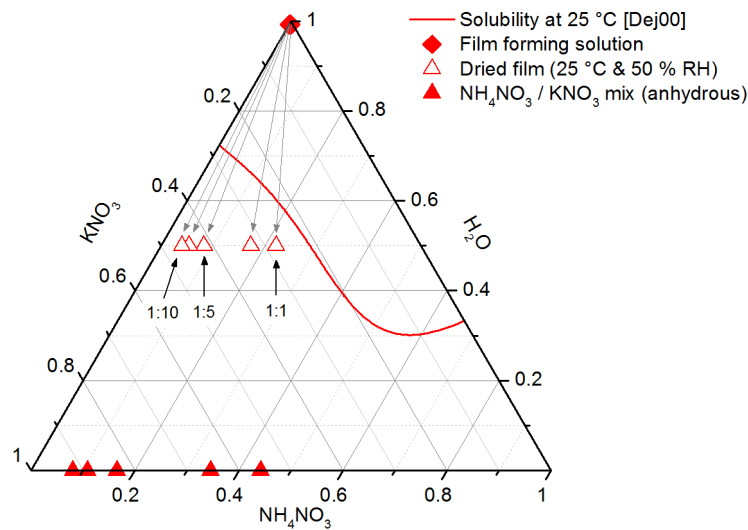
Fig. 7-2: The solubility isotherm of the KNO_3 – NH_4NO_3 – H_2O system at 25 °C and comparison to the said system in a film forming solution and within a dried NaCas film. The phase diagram is based on mass fractions, representing the molar NH_4NO_3 / KNO_3 ratios varied from 1:10 to 1:1 in NaCas films +/- MTG (see Fig. 6-9). The solubility data is given by Dejewska *et al.* [Dej00].

On the contrary, the NH_4NO_3 / KNO_3 ratio of 1:10 in the salt additive compound corresponds to a binary composition of 92 % w/w KNO_3 and 8 % w/w NH_4NO_3 for which a solid solution of the two nitrate salts is expected. Chien *et al.* [Chi05b] characterized the related solid phase as ANZ+KN II. The mixed crystals were determined to consist primarily of the phase-II KNO_3 crystal lattice and of a not further specified non-stoichiometric NH_4NO_3 solid phase ANZ. The entrapment of NH_4NO_3 in the KNO_3 crystal may have led to a hindrance in the crystal growth of the faces {001}, {011} and {112}, respectively. Since otherwise these crystal faces would favor the length growth of KNO_3, now a small crystal aspect ratio of 1.5:1 was achieved. The mean crystal length was analyzed to be 222 µm that is in the range of the NaCas film thickness. Therefore, the probability of a surface roughness by protruding crystals is less likely than with the original non-controlled elongated habit. According to that, the screening aim was fulfilled and the positive screening results have been confirmed finally by the analysis of NaCas films with the incorporated additive mixture.
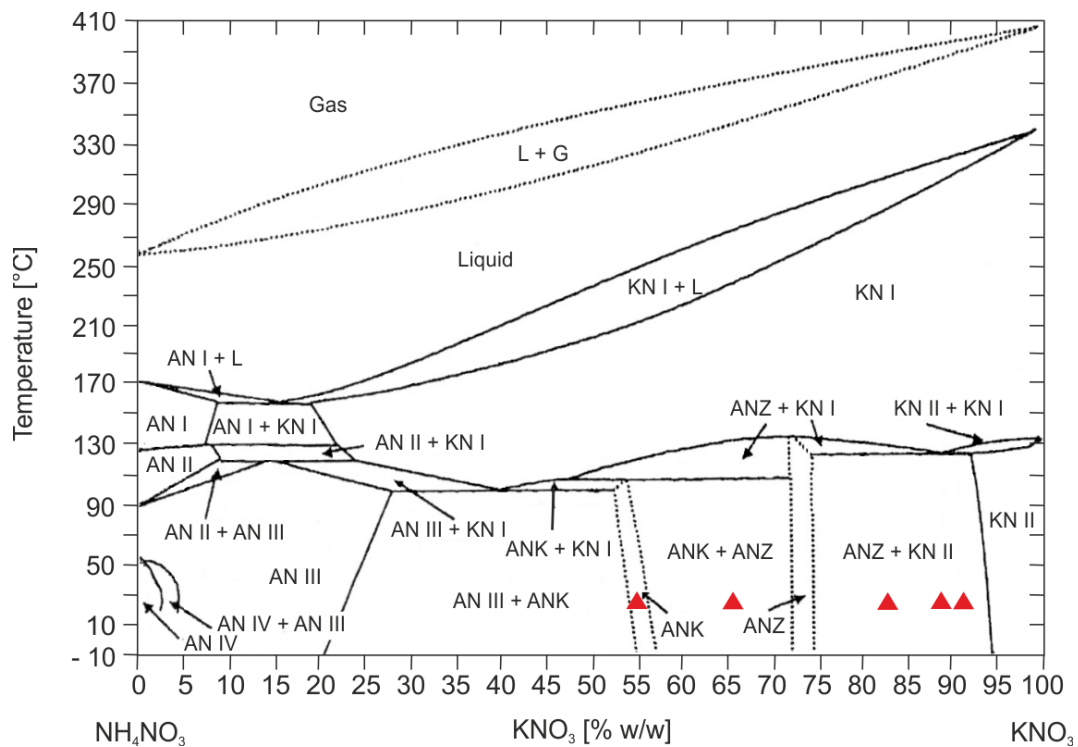
Fig. 7-3: The binary phase diagram of NH_4NO_3 / KNO_3 solid solutions and their polymorphic forms modified from Chien *et al.* [Chi05b]. The filled triangles (▲) correspond to the NH_4NO_3 / KNO_3 solid solutions 1:1, 1:2.5, 1:5, 1:7.5, 1:10 (from left to right, see Fig. 7-2) that have been added to NaCas films (anhydrous). Within this work, the following polymorphs are in the focus: KN II… phase-II KNO_3; ANZ and ANK… proposed non-stoichiometric solid phases (no detailed structural information available).

The NH_4NO_3 content in NaCas films has been further increased from the molar NH_4NO_3 / KNO_3 ratio 1:10 up to 1:1 in order to analyze the impact on the crystal habit and crystal size distribution within the films. With respect to the overall salt content in the material, the mass ratio of NaCas and salt additive was always kept constant at 6:1. Furthermore, the additional influence of enzymatic cross-linking and the time-dependent stability of the crystals have been studied. In Tab. 6-2, the light microscopy exposures of the NaCas films (+/- MTG) with the NH_4NO_3 / KNO_3 mix in the ratios 1:10, 1:2.5 and 1:1 are assembled. Also the ratios 1:7.5 and 1:5 have been examined, but the crystal morphology within the films exhibit a similar appearance like the NH_4NO_3 / KNO_3 mix of 1:1. The similarity in the crystal structure is proposed to be due to the formation of the same NH_4NO_3-KNO_3 solid solution. This is the ANZ+KN II phase as indicated in the binary phase diagram in Fig. 7-3.

The effect of the protein matrix itself on the additive crystallization is seen to be negligible since the molecular weight of the protein molecules and the dissociated salt ions differ strongly. The protein mostly acts a filler material of the crystallizing salt and only effects the deceleration of the crystal growth by diffusion limitation. Additionally, protein and glycerol are hygroscopic film components that bind water to the material. Within the monitoring of the drying process shown in Fig. 6-3, the

residual moisture content in a NaCas film was determined to be approximately 10 % w/w at the chosen storage conditions of 25 °C and 50 % RH.

Thus, the crystallization of the functional additives can be discussed independently of the carrier material and is simplified to the ternary $KNO_3 - NH_4NO_3 - H_2O$ system. The water content derives from the material moisture that has to be considered in the system. In a film of the dimensions 200 x 200 mm, 10 % w/w material moisture corresponds to an absolute water content of 1 g. The amount of salt in a film is the same and therefore, salt additive and water are assumed to be present in equal proportions.

This is depicted in Fig. 7-2, where the different NH_4NO_3-KNO_3 mixtures ($\triangle$) are compared with the solubility isotherm of the ternary system. Obviously, all prepared NH_4NO_3-KNO_3 compositions tend to crystallization, but starting from differing levels in driving force. Here, the supersaturation is 20 % higher in case of the NH_4NO_3 / KNO_3 mix of 1:10 than the supersaturation of the salt mix with ratio 1:1.

The theoretical view on the solid solution solubility is validated by the results from the optical analysis of the NaCas films with the incorporated NH_4NO_3-KNO_3 compositions (Tab. 6-2). The crystals had grown immediately during the film drying within the films with the NH_4NO_3 / KNO_3 content of ratio 1:10. Irrespectively of the enzymatic cross-linking, homogeneously distributed crystals with an average crystal size of 50 μm and large number have been visible. During the time of storage, a phase transition possibly occurred and large crystals or crystalline aggregates of up to 200 μm have formed that appear to exhibit the orthorhombic crystal habit. Additionally, the growth of larger crystals and disappearance of the smaller crystals is favored by the phenomenon of Ostwald ripening [Mye02]. Comparing these observations with the exposures of the NaCas films with the NH_4NO_3 / KNO_3 mix of 1:1, a completely different result is found. Right after the film drying, the number of crystals was lower within the non-cross-linked films than in the films with the additive mix of 1:10. In the cross-linked films with the salt mix 1:1, no crystalline particles had been present at that time. The further diminished crystal growth rate in the cross-linked film is possibly due to the maltodextrin content in the Activa TG formulation. In the contrary, a similar composed film formed crystals of large crystal number already after the film drying, when pure MTG without maltodextrin was applied instead of Activa MTG. The maltodextrin in the NaCas film is proposed to fill the pores in the protein matrix. Therefore, the diffusion might be further limited in the cross-linked films. Here, the first few crystals had been observed after 2 days of storage and were found to have continued growth after 7 days. The crystals had grown with a low particle density in the protein material and a variety of crystal habits had been found. In the non-cross-linked as well as in the cross-linked specimens, a triangle shape, cubes, tetrahedrons and needles have been visible that differ considerably from the orthorhombic morphology.

The changes in the crystal morphology from the NH_4NO_3 / KNO_3 composition of ratio of 1:10 to the ratio of 1:1 can be explained by the formation of differently structured NH_4NO_3-KNO_3 solid solutions within the NaCas films. To clarify the distinct phases of the solid solutions, anhydrous conditions have to be assumed. The filled triangles in both phase diagrams in Fig. 7-2 correspond to the theoretical case of completely dry material (▲). With the assumption of the binary $NH_4NO_3 \cdot x KNO_3$ solid solution; it is revealed that salt mixture of 1:2.5 results in the 'ANK+ANZ' phase. In the same context, the salt mixture of 1:1 grows as the 'ANK' phase of the mixed crystal. Both phases do not follow stoichiometric considerations and are not further specified in the literature [Chi05b].

7.3 Impact of the additive mix on the mechanical performance

In agriculture, mulching is the most commonly used technique in protected cultivation and is a particularly promising application for biodegradable polymers [Pla06, Kap08, Mar11, Kas12, Ber13]. The material parameters of mulching films have been standardized according to their type and main application in the European standard DIN EN 13655. Among the mechanical properties, the flexibility of the polymers is generally crucial for every kind of mulching film. The reason is the automated laying of the mulching films on the ground which allows only polymer films resisting more than 250 % of elongation [DIN03b]. The Fig. 7-4 summarizes typically applied polymer films for the mulching purpose and compares their mechanical performances with the data for protein-based materials. Furthermore, the standard values of a 'normal use' mulching film are added into Fig. 7-4 for an evaluation of the corresponding parameters.
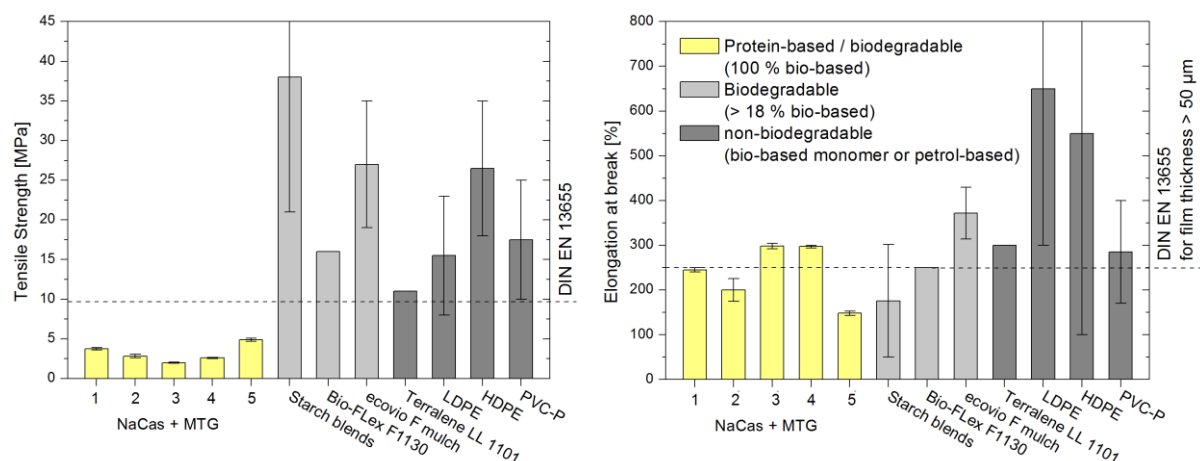
Fig. 7-4: Tensile strength and elongation at break of protein-based materials and commercial polymers compared to the minimum requirements for the application as mulching films (normal use) according to DIN EN 13655. Films based on enzymatically cross-linked NaCas (200 µm thickness): 1… no additive, drying at 75 °C and 75 % RH (Fig. 6-2); 2… NaCas / KNO_3 6:1, drying 25 °C and 50 % RH (Fig. 6-3); 3… NH_4NO_3 / KNO_3 1:1 (Fig. 6-9); NaCas / NH_4NO_3 6:1 (Fig. 6-10); NaCas / glycerol / KNO_3 / urea 6:1:1:1 (Fig. 6-11) [DIN03b, Bau07, End09, Fku12a, Fku12b, Bas13a, Bas13b, Bas13c].

From the protein-based films, the compositions with enzymatic cross-linking have been chosen for the discussion related to the mulching technique. The cross-linking of the material's protein basis results in insolubility in water, a decelerated biodegradation and enhanced mechanical performance. Thus, the method is highly beneficial for the optimization of the mechanical stability, but even more beneficial for the prolongation of the materials lifetime on the soil. The Fig. 7-4 clearly reveals that the protein-based films fulfill the requirements in the elongation property, with the additional benefit of the incorporated fertilizer within the films. Functional additives and enzymatic cross-linking have been found to have a synergistic effect on the materials mechanical stability. The following subchapters 7.3.1 to 7.3.3 highlight this phenomenon. Still, the drawback of low tensile strength values limits the application of the 100 % bio-based NaCas-based material. This can be overcome by blends with other protein systems or the use of the extrusion technology that is described to contribute to the stiffness of protein films as well as it is recommended for the large scale production [Dan09, Fro10b].

Seed tapes and sheets are designed as final goods that the consumers are expected to use manually in the gardening. Therefore, a long shelf life and a low water uptake are more important factors of the protein-based carrier material than optimized mechanical properties.

7.3.1 Application of KNO_3 doped with NH_4NO_3

The effect of the additive mix NH_4NO_3 / KNO_3 on the crystalline structure within the NaCas films has already been discussed in chapter 7.2.3. It was described that different phases of the NH_4NO_3-KNO_3 solid solution occur, when the amount of NH_4NO_3 was increased within the molar ratio to KNO_3 from 1:10 up to 1:1. The variations in the crystal morphology and crystal number play an important role for the mechanical performance of the NaCas films as shown in Fig. 6-9.

The second key factor is the enzymatic cross-linking of the protein molecules in the material structure. Compared to non-cross-linked films, an increase in the tensile strength of approx. 20 % was observed in all cases, whereas film elongation was enhanced to up to 300 % by a synergistic effect of both the MTG activity and the concentration increase of NH_4NO_3. In an assumption, the structure formation of the NaCas molecules was modulated by the dissociated ammonium within the film forming solution [Gra12]. The MTG-induced cross-linking may have preserved the conformational changes that resulted in the higher film flexibility proportionally to the NH_4NO_3 increase in the salt composition.

An inhibition of the MTG activity by the ammonium salt was expected, as with the NH_4NO_3 / KNO_3 mixtures of ratios 1:2.5 and 1:1, the critical NH_4NO_3 concentration of 25 mM in the film forming solution was exceeded. The Fig. 6-16 shows the

corresponding study on the MTG reaction kinetics in presence of different additives measured by the hydroxamate assay. However, no particular evidence for an MTG inhibition had been found in the mechanical parameters of the films with the NH_4NO_3 / KNO_3 mix. Therefore, the results from the MTG activity assay have to be interpreted carefully. The assay is performed with an idealized reaction solution in which the substrates and conditions are not entirely similar to the film forming solution. Thus, the film manufacturing process has to be comprised into the discussion. It is most likely that within the film forming solution, the ammonium was bound to the NaCas proteins by ionic interactions. The MTG enzyme molecules then have been protected from the ammonium. The further examination of NaCas films with NH_4NO_3 as single additive gives rise to the assumption that a higher amount of the salt is necessary to inhibit the Activa MTG. The corresponding trends are presented in Fig. 6-10.

A potential influence of the maltodextrin content in the Activa MTG on the mechanical properties of the films was assessed by the measurement of NaCas films that had been cross-linked with pure MTG S2P. The commercially available Activa WM^{TM} contains maltodextrin in an amount of 99 % w/w as a filler and stabilizer for the enzyme. A pure MTG with comparable parameter profile was obtained from the recombinant expression in *E. coli* [Mar08]. Shown in Fig. 6-9, the mechanical analysis revealed that the maltodextrin content has no effect on the tensile strength values of the NaCas films treated with Activa MTG and MTG S2P, respectively. The maltodextrin is proposed to have caused an increase of the flexibility of the protein-based material. This is visible in terms of deviations in the elongation at break that are possibly due to the water uptake by the hydroscopic maltodextrin [Chr98].

Regarding the non-cross-linked NaCas films, the tensile strength was at first decreased by about 20 % when KNO_3 has been added to the material. This effect was described previously to happen due to volume increase by the KNO_3 and its crystals inside the protein arrangement of the material structure. Therefore, the crystallizing additive acts as a plasticizer and the mechanism relates to the free volume theory [Mar04, Fro10]. However, the addition of NH_4NO_3 compensates the plasticizing effect of KNO_3 possibly by further modification of the three-dimensional protein folding.

7.3.2 Ammonium nitrate as single functional additive

The potential benefit of NH_4NO_3 as the primary functional additive within NaCas films was examined by a further increase of only the NH_4NO_3 content instead of a salt mixture with KNO_3 as indicated in Fig. 6-10. In contrast to KNO_3, the inner-film crystallizing of the NH_4NO_3 is generally suppressed. This is caused by the high water solubility of 2146 g_{anh}/kg_{H2O} (25 °C) and the material's residual moisture that was

measured to be approximately 10 % w/w in an environment of 25 °C and 50 % RH [Mer04].

In tensile strength and elongation at break, an optimum film composition was found at a NaCas / NH_4NO_3 mass ratio of 6:1. Especially, the enzymatically cross-linked material with that salt content reached a tensile strength of 2.6 MPa and an elongation of 297 % as shown in Fig. 6-10. Indeed, similar trends in the mechanical performance have been observed as for the literature data that refer to NaCas films with incorporated KNO_3 [Fro10]. For the non-cross-linked films, a loss in tensile strength was determined that proportionally follows the increase of the NH_4NO_3 content. Furthermore, the non-cross-linked films tend to break at lower strain, when the NaCas / NH_4NO_3 mass ratio is higher than 6:1. The rise of the mechanical instability is a sign for the disintegration of the protein molecules and the material's protein network. Thus, the highly concentrated NH_4NO_3 interferes the film formation within the NaCas material.

The application of the Activa MTG in the manufacturing of the NaCas films has been proven to counteract the protein destabilization until the optimum ratio of 6:1. Subsequently, a considerable loss in the mechanical performance of the cross-linked films has been recognized that is attributed to the partial inhibition of the MTG activity. The high concentration of ammonium in the material is additionally assumed to have resulted in the aggregation of the NaCas molecules. In a protein with altered conformation, the enzyme's sterical access to the protein's reactive amino acid residues is possibly blocked. The Fig. 6-16 relates to the inhibition kinetics of the Activa MTG that has revealed a negative effect of NH_4NO_3 in a concentration of higher than 25 mM. The SDS-PAGE analysis of film forming solutions confirms the result of the MTG's inhibition kinetics and is discussed in chapter 7.6. The corresponding data can be obtained from Fig. 6-17.

The usage of soluble ammonium salts as additives in protein-based films is a relatively new approach in this field of research. Up to date, only the incorporation of ammonium sulfate has been described in the literature [Fro10b]. The influence of NH_4NO_3 and $(NH_4)_2SO_4$ on the mechanical properties of the NaCas films can be directly compared, because the film manufacturing and the tensile measurements have been carried out in the same manner. Regarding the non-cross-linked films as well as for the films treated with Activa MTG, it was found that the protein network was destabilized to a higher extent by $(NH_4)_2SO_4$. The beneficial effect of ammonium salt and enzymatic cross-linking was confirmed only for the NaCas / salt mass ratio of 6:1. The further increase of the $(NH_4)_2SO_4$ content was shown to lead to a very weak protein network independently of MTG addition.

However, the trends in the modification of the mechanical film stability by the nitrate salts KNO_3 and NH_4NO_3 are quite comparable [Fro10, Sto12b]. The influence of the

inorganic additive salts therefore can be summarized in a first hypothesis: the stability of in particular an enzymatically cross-linked NaCas film is determined by:

- ionic interaction with the protein molecules in the material structure
  - choice of the anion as the important factor

- modification of the MTG reaction kinetics
  - inhibition / activation

- solubility of the additive salt in water
  - supersaturation level determines mean crystal size and crystal number

- additive mixture: occurrence of a solid solution
  - altered solubility and phase transitions

The choice of the MTG source for the enzymatic cross-linking appears not to be crucial for the controlled modification of the films mechanical properties. Also in case of the NH_4NO_3 addition, the maltodextrin content of the Activa MTG is beneficial. The enzyme is stabilized the maltodextrin and a further enhancement of the mechanical performance of the NaCas film can be reached. Thus, the Activa MTG is still recommended instead of the pure MTG S2P not only because of advantages in the film manufacturing. In scale up of the production process of protein-based materials, the continuous availability of the MTG would be crucial. Hence, the Activa MTG would be preferred as it is produced in an established industrial scale, which is not yet the case for the recombinant, pure MTG.

7.3.3 Effect of the KNO_3 mix with urea

The product design of NaCas films and sheets with incorporated urea and KNO_3 aims in general for the application as nitrogen fertilizer mixture with an additional potassium source. The crystal morphology of KNO_3 cannot be modified by the addition of urea, but urea was analyzed to counteract the growth of the KNO_3 needles outside the material. The alignment of the KNO_3 crystals inside the film structure was explained in chapter 6.2.1.

Regarding the material composition, the plasticizing effect of urea on the protein-based films has to be considered [Sto11]. The mechanical stability of NaCas films with varied urea content is shown by the tensile strength and elongation trends in Fig. 6-11. In the study of this additive mix, the mass ratio NaCas / KNO_3 was kept constant at 6:1 and the urea content was increased continuously. The decrease of the tensile strength and the simultaneous increase of the elongation clearly indicate that urea acts as a plasticizer. Prior to the manufacturing of urea containing films, also the glycerol amount in the material composition has been reduced. The NaCas / glycerol mass ratio of 6:1 was suitable to ensure the film formation, especially, in those films with an urea content higher than the ratio NaCas / urea of 6:1.

The plasticizing property of urea in NaCas materials is attributed to a combined effect of increased volume in the material structure, hygroscopicity of the additive and partial denaturation of the NaCas proteins by the interaction with urea. It is common knowledge that additives like urea are able to increase the flexibility of polymer chains according to the free volume theory. Urea additionally attracts water due to its hygroscopic nature. The moisture increase acts plasticizing by making the polymer chains more flexible. The water itself works as a plasticizer, not only in NaCas films, but in every hydrophilic material [Mar04, Gal09, Rai11, Vie11].

Furthermore, urea is actually a frequently used protein denaturant and is able to widen and to change the protein's folding. The mechanism of urea's action in the protein folding is still controversially discussed. Here, the urea-induced decrease in the water-water interactions and hydrogen bond strength is a widely accepted explanation [Ben03, Das09, Can10].

The enhancement of the films mechanical parameters by the addition of Activa MTG indicates that the enzyme remained active in the presence of urea. The assumption is confirmed by the test of urea in the inhibition kinetics of MTG that is shown in Fig. 6-16 and discussed in chapter 7.6. Indeed, urea was determined to activate the Activa MTG by 30 % irrespectively of the urea concentration. In a film forming solution, already 1.5 µM urea may be suitable to reach a considerable enhancement in the mechanical performance of cross-linked protein films. The integration of urea in the material composition therefore is a new and promising optimization parameter to increase the tensile strength of highly flexible and cross-linked protein films.

7.4 Barrier properties

The vapor barrier properties and water resistance of polymer films are of high importance for every field of application and product design. The demands for the polymers barrier performance are of course based on the specific product and use. In the following, some examples are intended to briefly explain the diverse optimization goals:

In agriculture, e.g. the mulching films are typically applied on the agricultural fields and are subjected to changeable environmental conditions. Thus, the mulching films are desired to exhibit a very high stability in a humid environment at least over the plant cultivation period. The water vapor transfer of these films should be as low as possible in dry regions, since the mulching is needed to reduce the water evaporation from the soil. In humid landscapes, the transmission of moisture of less than 120 g/m²d is usually accepted in order to avoid the growth of mildew and moulds [Shr97, Sco02, Sin09, Wya12, Bas13c].

The design of food packaging material involves a similar discussion to create a protective environment for the specific food product. Regarding the water vapor transport, a compromise between the product's water loss as well as sweating and

decay of the food has to be found [Gen97, Par99, Gui05, Lin07, Roj07, Roj09, Rob10, Dem12].

On the contrary, high water vapor transmission is usually required for synthetic tissues. This application is further discussed in chapter 7.4.2.

Protein-based materials are hydrocolloids that typically contribute to a high water vapor transmission rate. Furthermore, the most effective plasticizers are known to enhance the polymer's sensitivity to water and moisture due to their hydrophilic nature. On the contrary, protein-based films have been extensively characterized to provide high barrier properties against oxygen, lipids and aroma [Khw04a, Khw04b, Buo05, Ugr07, Bru08, Kow11, Per11, Bai13, Wih13].

7.4.1 Moisture uptake

The isothermal moisture sorption of cross-linked NaCas films with varied KNO_3-NH_4NO_3 solid solution was detected dynamically in a closed environment with 25 °C and the humidity ranging from 5 to 95 % RH. In Fig. 6-13 (I), the water activity a_w represents the relative air humidity in order to match the parameter to existing water sorption models. The data were precisely fitted with the Guggenheim-Anderson-De Boer (GAB) equation that is commonly used for the modeling of sorption isotherms of foods. The GAB model delivers a sigmoidal curve progression by means of the Langmuir and BET theories of physical adsorption as the theoretical background. Various authors have recently described that the GAB model is well suitable for biopolymers deriving from proteins of plant and animal origin. The fitting to the own data from the NaCas films confirmed this knowledge [Van84, Gen94, Kim01, Sah06, Kri07, Fab10, Soa11, Son11].

The ratio of KNO_3 and NH_4NO_3 within the salt mixture appeared not be relevant for the overall moisture uptake of the tested NaCas films (Fig. 6-13 (I)). Additionally, the average material moisture of NaCas and gelatin films at 25 °C and 50 % RH was analyzed and the data are presented in Fig. 6-13 (II). The effect of the protein basis on the material moisture was negligible and also the trend of the slightly increased material moisture in presence of the KNO_3-NH_4NO_3 mix was not significant. Thus, it can be assumed that the content of the hydrophilic plasticizer governs the moisture sorption behavior of the protein-based materials to the greatest extent [Cou00, Kim01, Pom05, Fab10, Ver10].

7.4.2 Water vapor transfer of NaCas films

Also the water vapor transmission of the protein-based materials is ruled by the protein's hydrophilic property and the applied plasticizer. The water vapor barrier of the protein-based films is generally very poor [Lim99, Per99, Khw04b, Buo05, Cha06, Bru08, Per11, Bai13]. This was proven for the own NaCas films as well, but can be modified by the enzymatic cross-linking. This is possibly due to the linking of

polar amino acid residues and due to a smaller pore size in the cross-linked protein matrix. However, a reliable measurement of the materials porosity is not available by the state-of-the-art techniques because of the compressibility of the protein-based material structure. The apparent mesh size of a protein hydrogel still can be estimated by the Flory-Rehner method that gives rise to the previous assumption [Red06, Bet12].
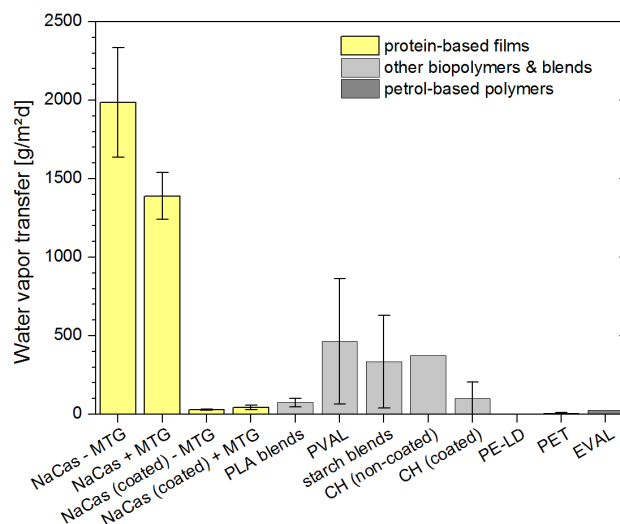
Fig. 7-5: Water vapor transfer of polymer films. Comparison of protein-based films with 200 µm film thickness, other biopolymers and blends as well as petrol-based polymers (thickness 50 µm). Analysis was carried out at 25 °C and 50 % RH. Additional material data from the literature [End09].

The water vapor transmission rate (WVTR) of the NaCas films was diminished in particular by the coating of the film surface with a hydrophobic substance like bees wax. The wax coating is already well known in the literature and the design of multi-layer systems is suggested to combine the high gas barrier of protein films with the low water vapor transmission of other polymers [Wel98, Chi02, Soh06, Riv09, Zha10].

A biomedical application of protein-based films is the synthetic wound dressing, where the WVTR needs to fulfill the requirement of 2000-2500 g/m²d. The high WVTR is adapted from the corresponding values of burned skin wounds [Que87, Pel12]. The own NaCas films already fit into this WVTR range, although the cross-linked films have to be further customized. The measured data are listed in Tab. 6-3.

7.5 Protein-based carrier for controlled release

7.5.1 Additive release

Protein-based materials have been proven to act as a polymeric carrier for active ingredients and are suitable for controlled-release systems. The incorporation of e.g. the nitrate salts KNO_3 and NH_4NO_3 as functional additives aimed for the continuous fertilizer supply in agricultural applications. The examination of the additive release behavior was thus conducted in a humid environment to simulate a heavy rain

situation. The results in chapter 6.3.2 make clear that the NaCas films have only a small effect on the retention of the nitrate salt diffusion into the surrounding solvent.

For the purpose of protein-based seed tapes and sheets, the fast release of the fertilizers can be beneficial. Here, a dilution of the additives into the soil would enhance the seed germination, because it avoids a local excess fertilizer concentration at the seeds.

In terms of cover films for agricultural fields, the fertilizer release is desired to be linear and continuous during the whole time of plant cultivation. The salad cultivation is an example of the horticultural use of the protein-based films. However, salad and other vegetables still need to grow for three months although this cultivation period is already short compared to other plants. Up till now, this aim cannot be reached with the protein-based carriers regarding both the controlled additive release and the environmental stability of the protein matrix.

The above given examples point out that mainly the field of application governs the design of the release characteristics of the polymeric carrier. Hence, the product goals usually define the material requirements. The product development with controlled-release systems is of huge interest not only for the agricultural sector. The results also from the presented product and process design can be transferred to a variety of applications. Protein hydrogels typically form from the protein-based materials by absorbing large amounts of water. They find interesting applications in encapsulation and delivery of active ingredients within the pharmaceutical, cosmetic and nutrition fields [Gan10, Bet12]. In general, the development and optimization further include the following key factors:

- choice of protein and processing parameters [Mil03, Agu10, Ver10, Che11]
  - control of material shelf life through heat-induced cross-linking, hydrophobicity and molecular weight of the protein

- usage of plasticizers [Pom05, Fab10, Ver10]
  - additional hygroscopicity and polymer chain relaxation
  - reduction of the water sensitivity by hydrophobic plasticizers

- cross-linking of the material's protein network
  - dissolution versus biodegradation and / or erosion
  - control of the mesh size in protein hydrogels [Bet12]

- choice of functional additives for the controlled release
  - solubility at the defined release conditions
  - protein – additive interactions

- protection
  - prolongation of the material's shelf life by hydrophobic coating

The three-dimensional polymer network of such a hydrogel is physically and / or chemically stabilized. A hydrophilic polymer matrix therefore resists the dissolution in the surrounding medium, but undergoes swelling during water absorption. The maximum amount of the material moisture is governed by the properties of the polymeric material which forms the hydrogel. In case of the proteins, the resulting hydrogels consist of polyampholytic polymer chains that contain ionisable polar amino acids. In this respect, the additive release from the protein hydrogels is ruled by the hydrophilicity of the ionisated proteins. The diffusion mechanism, water uptake and swelling of the protein-based materials are known to be sensitive to pH and ionic strength of the solvent [Tok91, Mis04, Gan10, Son10, Elz11, Bet12, Zhu12]. These hydration interactions of polymer and solvent as well as the ionic interference of polymer and additives are discussed in the following.

7.5.2 Water absorption and swelling kinetics

Biopolymers like the enzymatically cross-linked NaCas films typically show a swelling behavior during the water uptake that is due to the volume increase and polymer chain separation. The swelling and sorption kinetics are known to correlate strongly with the specific intermolecular chain interactions. The cross-linked polymers can absorb large amounts of the solvent as well, but the additional covalent bonds stabilize the swollen polymer network against dissolution [Mei99, Mil03, Bra05, Nan05, Dip06, Agu10].

The water sorption of hydrophilic polymers represents the solvent's diffusion into the polymer that can be classified according to kinetics of the mass transfer. The knowledge about the hydration of the material is used in development of polymeric carrier systems. In pharmaceutical applications and likewise in agriculture, the controlled release of active ingredients is ruled by the characteristics of the polymer matrix [Vla01, Gan10].

The protein films water uptake behavior at 25 °C is shown in Fig. 6-12 by using enzymatically cross-linked NaCas and gelatin films as examples. As defined in the DIN EN ISO 62 standard, the analysis was carried out by immersing film specimens into water and gravimetric determination of their mass change [DIN99]. The film compositions have been further altered with respect to the incorporation of the salt additives. Potassium nitrate or the mixture of KNO_3 and NH_4NO_3 in the molar ratio of 1:1 have been added in order to analyze the potential effect of salts on the water uptake of the protein-based films.

Indeed, it was found that the hydration of the analyzed material is mostly governed by the protein basis. The water uptake of the cross-linked NaCas films was determined to be eight times higher than the corresponding data of the gelatin film with the overall similar film composition. Therefore, the water uptake has to be related to the molecular structure of the specific protein. Here, the research is still at

the beginning, but qualitative considerations can be made to explain the proposed correlation:

Sodium caseinate consists of the four casein fractions that are all described to miss a distinct secondary structure and only the α_{S2}- and κ-caseins are stabilized by disulphide bonds. The intermolecular interactions of the caseins are mostly of weak, non-covalent nature [Bou06, Men10]. The flexible molecular structure and loose assembly of the protein network of the caseinate is therefore assumed to contribute to the high water absorption.

Gelatin instead is known to partly regenerate the triple-helix structure of the collagen from which the gelatin was produced from. This phenomenon was observed during the gelling of aqueous gelatin solutions below 40 °C. Recently, it was proven that disulphide bonds maintain the native structure of the chains even in the denatured state [Big04, Gor08]. The conditions of the gelatin's helix-coil transition have been fulfilled in the manufacturing of the films. Thus, it can be stated that the cross-linked gelatin network within the films was stabilized by strong, covalent interactions that resulted in low intermolecular volume and porosity. The gelatin structure is seen to have low flexibility and so influenced the absorption of water molecules negatively.

The hydration of the protein-based polymers can be further modified by inorganic salts. This effect was proven to be dependent on the protein origin as well. In Fig. 6-12 (I) and Fig. 6-12 (II), the water uptake of the NaCas-based films and of the gelatin-based films is shown, respectively. Whereas the water uptake of the gelatin films was not changed by the incorporated salt additives, the NaCas films exhibited a distinct synergy with the nitrate salts within the films. The water absorption capacity of the NaCas films was therefore considerably decreased and a change from the Fickian diffusion behavior to an anomalous transport mechanism was determined. The magnitude of water uptake decrease was furthermore influenced by the salt composition and namely by the choice of cations in the mixed salt. A similar trend was observed by Mikkelsen [Mik94], who described that particularly the cation of a soluble salt has an important effect on the polymer expansion of cross-linked polyacrylamide. The restriction of the polymer expansion was discussed in the literature by using two hypotheses that are applicable to protein polymers as well. On the one hand, it is proposed that the cations of a soluble salt may form ionic bridges between the polymer's carboxyl groups [Bow90]. On the other hand, Salem *et al.* [Sal91] assumed that the salts interfere with the amide groups of the polymer. Thus, the formation of hydrogen bonds with the water molecules was explained to be inhibited.

7.5.3 Protein dissolution

The dissolution of non-cross-linked polymers involves two transport processes. These are the solvent diffusion from the bulk liquid into the polymer and the chain

disentanglement of the polymer molecules from the material structure. The mechanism of polymer dissolution is commonly described with a surface layer formation that is schematically drawn in Fig. 2-2 [Mil03].

When a NaCas film is subjected to an aqueous solvent, the protein disintegration is highly expected in particular for films that had not been cross-linked with MTG. Therefore, the protein dissolution was measured during the additive release tests. The Fig. 6-15 summarizes the results for all tested NaCas film compositions and indicates the temperature dependency of the protein release. The dissolution characteristic of the protein matrix has been determined to follow a sigmoidal profile. The lag times represent the water uptake and swelling, before the protein disentanglement caused the disintegration of the protein network [Mil03, Zem07, Agu10, Sie12].

Interestingly, it was found that the dissolution of the non-cross-linked films was dependent both on the temperature and on the presence of nitrate salts within the films. The NaCas film structure with the NH_4NO_3 / KNO_3 mix has been found to be rather insoluble at 5 °C during 30 min of exposure to water. Also the protein release of the NaCas films with KNO_3 was diminished to 80 % at that temperature, whereas the NaCas film specimens have been dissolved completely at all the applied temperatures. This phenomenon of partial insolubility can be similarly due to the ionic interactions of salt and protein molecules that are assumed for the cross-linked films in chapter 7.5.2 [Bow90, Sal91, Mik94].

7.6 Transglutaminase in process design: Activity vs. additive

The usage of the microbial transglutaminase (MTG) and other functional additives has been shown to be highly beneficial to the mechanical properties of NaCas films. This was proven for the addition of e.g. KNO_3, NH_4NO_3 and mixed crystals of those nitrate salts as presented in Fig. 6-9 as well as in Fig. 6-10 and in the previous literature [Fro10a]. However, the synergistic effect of the salts and the enzymatic cross-linking was observed to be limited to a critical salt concentration within the protein films. The limitation can be partly explained by an excess crystal size inside the films that have led to a mechanical instability of the materials. Indeed, this assumption is not applicable to the application of NH_4NO_3 that would not crystallize within the NaCas films at the given environmental conditions.

In order to have a complete insight into the effect of additives on the film formation, additional considerations have been made. Here, a correlation of MTG application and potential side effects on the enzyme kinetics by the other functional additives is proposed. Regarding the protein film manufacturing, this approach is seen to be an entirely new strategy for the customization of the final material's performance.

The information on activating compounds and inhibitors of the MTG from the *Streptomyces mobaraensis* organism is actually limited. A summary of the literature

review can be found in Tab. 14-1 where the focus was put mainly on interactions with salt ions. Furthermore, a variety of enzyme origins has been considered. The literature data are quite divergent when it comes to the influence of one particular substance. Therefore, the chosen functional additives have been examined and the activation and inhibition kinetics are to be found in Fig. 6-16.

All the examined inorganic salts are neutral to the transglutaminase reaction as the enzyme molecule does not own a co-factor site for those dissociated ions [Kas02]. The activation effect of KNO_3 and in particular of KCl can be explained by conformational changes of the MTG enzyme. A similar trend was previously found by Nozawa *et al.* [Noz99] for a scallop tissue transglutaminase that had been positively affected by NaCl and $NaNO_3$.

The inhibition of the MTG activity by the ammonium salts is due to a competitive inhibition of the MTG. The reaction pathway in Fig. 4-3 points out that ammonia is a side product of the MTG reaction. The excess concentration of ammonium ions therefore prevents the reaction progress considerably. This effect was already described to be useful to control the activity of mammal transglutaminases. Regarding the addition of $(NH_4)_2SO_4$ in enzymatically cross-linked protein-based films, Frohberg [Fro10b] observed a sudden drop of the mechanical performance at a critical salt concentration. It is likely that the inhibitory effect of the ammonium governed the decrease of the films mechanical properties [Tak86, Uek96].

The enhancement of the MTG activity by urea is possibly due to a relaxation of the enzyme's molecular structure that may have resulted in a better access of the reaction site. It is assumed that the MTG would be inactivated at urea concentrations higher than 50 mM, since urea generally acts as denaturing agent for proteins [Rai11]. However, the trends in Fig. 6-11 show that the enzyme stayed active and thus, the critical amount of urea was not reached in the protein film manufacturing.

The contribution of citric acid as an activating compound may result from a pH dependency of the enzyme followed by the activity decrease in a more acidic medium. Being a surfactant, the sodium dodecyl sulfonate ($C_{12}H_{25}NaO_3S$) is assumed to interact with the outer surface of the MTG molecules and causes the enzyme inactivation already at low concentration like the almost similar SDS [Mug93, Moj13].

The SDS-PAGE analysis of the MTG induced NaCas film forming solution demonstrate that KNO_3 and NH_4NO_3 are suitable additives although particularly the NH_4NO_3 decelerates the MTG reaction. Here, the Fig. 6-17 showed an incomplete cross-linking due to combined effect of competitive inhibition by NH_4NO_3 and heat inactivation. It has to be noted that the heat effect is avoided in the real process, because the film forming solution is homogenized for only 10 min after MTG addition and is subsequently poured into the casting molds. The MTG indeed remained active at a higher level than expected from the SDS-PAGE. This is proven by the protein

solubility as well as by the beneficial effect of the Activa MTG on the mechanical properties of NH_4NO_3 containing NaCas films. The NaCas release as a measure of the cross-linking degree is presented in Fig. 6-15 and the mechanical analysis of NaCas films with incorporated NH_4NO_3 is summarized in Fig. 6-10.

7.7 Plant cultivation with protein-based carriers

The NaCas films with incorporated fertilizer have been successfully applied in the product design of functional seed carrier systems. An evaluation on both the seed tapes with radish seed and the seed sheets as carrier for lettuce seed is given in chapter 6.5. Based on the product tests with the first prototypes, the following key factors have been determined for an optimization of the protein-based carrier material in plant seeding:

- plant nutrition balance and local fertilizer concentration
    - matching of fertilizer content by plant specification with respect to a critical fertilizer amount

- material moisture and water vapor barrier
    - avoidance of seed germination during storage by low material moisture
    - appropriate water vapor transfer to minimize rotting

- gas barrier [Che95a, Car04, Jim12]
    - oxygen supply for the seed and germ viability

The biodegradability of the carrier material is another important parameter for further development and marketing of the final products. In this regard, the usage of protein-based materials is beneficial, since the protein itself serves as a nitrogen source for the plant growth. This has been shown with both model plants, radish and lettuce, and the corresponding results are compared in Fig. 6-18 and Fig. 6-19. Additionally, the plant growth and the final yield of particularly radish have been considerably enhanced by the supply of other fertilizing agents that had been incorporated into the carrier material. Therefore, the protein-based seed tapes and sheets combine the advantages of the traditional paper-based seed carrier and the simultaneous application of fertilizer that is known from pilled seed.

Once the tested prototypes will reach the commercial launch, their material parameters and environmental impact have to be approved according to the national regulations. In Germany as well as in Europe, the certification and application of bio-based polymers is regulated the standard DIN 13432 on which the national regulations on packaging material and bio-waste relate on [BioAbfV13, DIN00, VerpackV09]. For this particular application of a new seeding technique, another point of view instead of the biopolymer material is possible: the protein basis of the material as well as the incorporated functional additives acts as food source for the

plants. The protein-based carrier therefore is substantial for the plant fertilization. Other substances like the plasticizer are neutral to the environment and can be considered as minor components. Hence, the author recommends to seek the licensing of the protein-based seed carrier as a method of fertilization. The composition of fertilizers is determined in the German regulation on the fertilizing agents in agriculture [DüMV12].

8. Conclusions and new approaches

Crystallization as feature for protein-based materials

The NaCas films are amorphous by the structure of their protein network. Functional additives can be rather easily incorporated into the protein matrix of the material and the crystallization of the additive within the film may occur. However, the nucleation and the beneficial effect are strongly dependent on the solubility of the additive in water, the material moisture as well as the thermodynamically favored crystal habit. Based on the work with crystallizing and non-crystallizing additives, the following general considerations on the integration of additive crystallinity within protein films can be made:

- Choice of additives // additive vs. enzymatic cross-linking

  The functionality and additional benefit of an additive is clearly in the focus. A sufficiently low solubility of the additive contributes to the inner-film crystallization, but is no primary goal in the product design. The combination of additive and enzymatic cross-linking offers a synergistic effect, if the additive acts as activating compound for the enzyme.

- Crystal size and shape of inner-film crystallized additives

  In particular the mechanical performance requires a rather isotropic crystal habit and a mean crystal size of less than the film thickness. The formation of acicularity has to be avoided by a suitable control mechanism.

- Retention of additive release

  Compact crystallized particles of suitable size decelerate the additive release kinetics from the protein-based carrier.

- Enhancement of the gas transfer

  The additive release is typically faster than the disintegration of the protein carrier. The dissolution of the additive is assumed to result in higher porosity of the protein-based material that results in an increased O_2 and CO_2 transmission.

Thus, the advantage of inner-film crystallization is first of all a matter of the desired product and material requirements. The control of the additive release is still restricted, but may be optimized in the future work by e.g. material shapes of higher thickness, the usage of hydrophobic proteins as raw material and the application of a hydrophobic coating.

Environmental conditions govern the material performance and quality

The distinct hydrophilicity of the protein-based films makes them prone to mechanical failures particularly at extreme values of air humidity. The usage of plasticizer aims for the elasticity control within a range of temperature and relative air humidity. Here,

the measurements of moisture uptake and water vapor transfer indicate that the commonly used hydrophilic plasticizers even enhance the material's sensitivity to water. Therefore, it is recommended to store the protein films at constant ambient conditions in order to keep their quality. When crystallized additives had been incorporated into the films, the crystalline phase has to be monitored because a solvent mediated phase transition of the crystal lattice may occur. This finding explains the time and humidity dependent formation of needle-like orthorhombic KNO_3 out of a trigonal morphology.

In the manufacturing of the protein-based material by the wet process, the drying step also involves a proper control of the environmental conditions. The KNO_3 containing NaCas films generally have to be dried at or below 50 % RH, but no particular trend on temperature variation was found. It behaved differently for pure NaCas films, where the mechanical properties can be controlled by the drying conditions and enzymatic cross-linking:
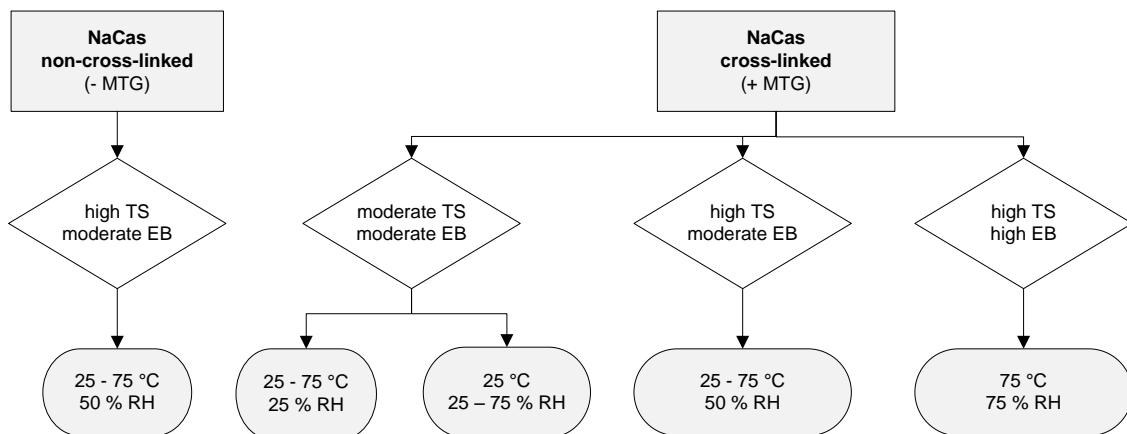
Fig. 8-1: Recommendations for the control of the mechanical properties of NaCas films by the drying conditions. TS… tensile strength; EB… elongation at break.

Enzyme activity control by functional additives

During this work, a variety of substances has been proven to change the enzyme kinetics of the microbial transglutaminase Activa MTG. The polymer additives had been chosen mostly because of their fertilizer functionality and to have included neutral inorganic salts and organic substances. The activating or inhibiting effect of the additives and the MTG activity results mainly in the increase or decrease of the reaction rate. The cross-linking level is usually not altered. Thus, enzyme activation or inhibition plays a minor role in the wet process, but is seen to have a huge impact in the scale up. The dry process, e.g. the extrusion technique is commonly used and the reactive extrusion is strongly dependent on the enzyme kinetics. Particularly the residence time can be diminished by MTG activation. Another way of process control may be the counteraction against high pressure issues by deceleration of the MTG reaction. Therefore, the synergy of enzymatic cross-linking and functional additives is seen to be a completely new approach in the control of the film extrusion process.

9. Summary

In the present work, the caseinate-based films and sheets have been successfully applied as carrier materials and release systems for functional additives. Therefore, the 100 % biodegradable films are highly suitable for the product design of ecologically valueable goods that fit to the aim of sustainability. The additional benefit of this product design has been explained and demonstrated by an example from the agricultural and horticultural purpose: mulch films and seed tapes.

For the first time, a deep insight is given on the crystallization of functional additives such as the fertilizer salt KNO_3 within caseinate films and the application of enzymatic cross-linking by microbial transglutaminase. The characterization and control of the additive's crystal habit is pointed to be essential for the preservation of the material appearance and mechanical performance. In the non-controlled case, KNO_3 crystallizes first as a metastable polymorph within the protein matrix. Following Ostwald's Rule of Stages, this crystal polymorph is described to undergo a phase transition to elongated orthorhombic crystals. These needle-like crystals may protrude the film surface and lead to mechanical instability due to a macroscopic defect structure. This thermodynamic process can be decelerated, but not stopped by the monitoring and adjustment of the drying process within the protein film manufacture or the control of the storage environment.

The hugh impact of the drying process on caseinate films has been analyzed for the first time also with respect to incorporated crystalline additives and an enzymatic cross-linking. It has been shown that the mechanical properties, e.g. the tensile strength and the elongation can be increased up to 3.4 MPa and up to 245 %, respectively. This is achieved by the choice of the environmental conditions, temperature and air humidity during the water evaporation after the film casting.

Known from industrial crystallization, the use of secondary additives is a highly suitable tool for the long-term control of the face-specific crystal growth. Among the screened substances, the combination of KNO_3 and NH_4NO_3 was found to benefit best to both mechanical properties and the desired, self-regulating compact crystal shape. The NH_4NO_3-$x$$KNO_3$ solid solution was observed to form several different co-crystal habits in the protein-based carrier that can be correlated to the composition of the solid solution and the varied water solubility. Compared to caseinate films with no crystallized additive, the elongation of the films was increased to 300 % meanwhile the tensile strength was maintained in a synergisitic effect with enzymatic cross-linking. The use of NH_4NO_3 as single fertilizer additive was determined to be limited because of the activity inhibition of the transglutaminase enzyme.

All the screened additives and known KNO_3 crystal growth inhibitors have also been tested on their influence on the reaction kinetics of the cross-linking enzyme. This is

clearly a matter of process design and the choice of the functional additive and crystal growth inhibitor might have a huge effect on the processing time and the overall material properties in a later process scale-up.

During the final application of mulch films and particularly plant seed carriers, the protein-based carrier is meant to absorb water or water vapor, dissolve and /or degrade dependent on the presence of cross-links in the material. Simultaneously, the incorporated additive is to be released. The diffusion and release of the nitrate salt additives have been determined to be only slightly restricted by a cross-linked protein matrix. However, the moisture sorption, water uptake and swelling characteristics of the caseinate polymer are reported to be influenced by the additive salts to a great extent. In case of caseinate, the interaction with the dissociated salt ions resulted in a hydrophobization of the protein and therefore in a by 70 % diminished water uptake.

The final product tests with protein-based plant seed carriers have clearly revealed the huge fertilization capacity of the protein itself as well as the seeding and plant growth tests showed the great potentials of tailor-made functionality. The amount of fertilizer in the seed carrier can be adjusted according to the specified plant nutrition balance. Using the protein-based carrier material, the biomass of the two model vegetable plants, radish and lettuce, was increased by up to 70 %.

Aiming for a closer look on the material optimization and product benefit, a completely new field of interdisciplinary research was opened that combines the knowledge from biopolymer engineering, industrial crystallization and product design as well as life cycle analysis approaches. Furthermore, the work points to the various interactions of protein-based carrier, functional additives, covalent modification and environmental aspects that summarize to the final physico-chemical material properties and additional value.

10. Zusammenfassung

Protein-basierende Materialien und insbesondere Caseinatfolien wurden in der vorliegenden Arbeit als Trägermaterial verwendet. Die zu 100 % biologisch abbaubaren Folien eignen sich deshalb für das Produktdesign ökologisch wertvoller Güter, die dem Nachhaltigkeitsgedanken Rechnung tragen. Der zusätzliche Mehrwert dieses Produktdesigns wurde beispielhaft an Hand von Mulchfolien und Saatbändern mit der Anwendung in Landwirtschaft und Gartenbau erklärt und erfolgreich demonstriert.

Erstmals wurde zudem ein tiefer Einblick in die Kristallisation funktionaler Additive wie z. B. das Düngemittel KNO_3 gegeben, das in Folien aus Caseinat eine kristalline Phase bildet. Auch die Möglichkeit der Anwendung der enzymatischen Quervernetzung der Proteinmatrix durch mikrobielle Transglutaminase und die Beeinflussung der Enzymaktivität durch die verwendeten Additivsalze wurden untersucht. Die Charakterisierung und die Kontrolle des Kristallhabitus wird als essentiell für den Erhalt sowohl des Erscheinungsbildes des Materials als auch der mechanischen Stabilität angesehen. Würde das Kristallwachstum von KNO_3 nicht kontrolliert werden, kristallisiert das Salz zunächst als ein metastabiles, trigonales Polymorph innerhalb der Proteinstruktur aus. Der Ostwald'schen Stufenregel folgend, wandelt sich dieses kristalline Polymorph dann in längliche, orthorhombische Nadeln um. Diese nadelförmigen Kristalle können die Folienoberfläche durchbohren und führen durch die makroskopische Defektstrukur zu mechanischer Instabilität. Der thermodynamische Prozess der Phasenumwandlung kann durch die Einflussnahme auf die Trocknungsbedingungen während der Folienherstellung und die Lagerbedingungen zwar verlangsamt, aber nicht verhindert werden.

Der große Einfluss des Trocknungsprozesses auf Caseinatfolien wurde erstmals bestimmt, auch in Bezug auf eingelagerte, kristalline Additive und auf eine enzymatische Quervernetzungsreaktion. Es wurde gezeigt, dass die mechanischen Eigenschaften, beispielsweise die Zugfestigkeit und die Bruchdehnung auf bis zu 3.4 MPa und auf bis zu 245 % gesteigert werden können. Dies geschieht durch die Wahl der Umweltbedingungen Temperatur und Luftfeuchtigkeit während der Verdunstung des Lösungsmittels Wasser nach dem Gießen der Folie.

Wie aus der industriellen Kristallisation bekannt ist, kann das phasenspezifische Kristallwachstum einer Substanz durch sekundäre Zuschlagstoffe beeinflusst und kontrolliert werden. Aus einem Screening heraus wurde die Kombination von KNO_3 und NH_4NO_3 als am besten geeignet bewertet, da einerseits die mechanischen Eigenschaften der Folie positiv beeinflusst und andererseits selbst-regulierend die gewünschte, kompakte Kristallform erhalten wurde. Die Mischkristalle NH_4NO_3-$x KNO_3$ bildeten verschiedene Morphologien aus, die in Zusammenhang mit der

Zusammensetzung des Mischkristalls und der Veränderung der Wasserlöslichkeit stehen. Verglichen mit Caseinatfolien ohne eingelagertes Additiv wurde die Dehnbarkeit der Folien auf 300 % erhöht, während die Zugfestigkeit durch einen Synergieeffekt mit der enzymatischen Quervernetzung auf gleichem Wert bebehalten werden konnte. Die Nutzung von NH_4NO_3 als alleinigem Düngemittel-Additiv ist hingegen nur eingeschränkt möglich, da das Ammoniumsalz in hoher Konzentration die Enzymaktivität der Transglutaminase inhibiert.

Alle untersuchten sekundären Additive und bekannte Kristallwachstumsinhibitoren von KNO_3 wurden auf ihre Wirkung auf die Reaktionskinetik des quervernetzenden Enzyms hin untersucht. Dies ist ein bedeutender Faktor hinsichtlich des Prozess-designs, da die Wahl des funktionalen Additivs und entsprechendem Kristallwachs-tumsinhibitor einen entscheidenden Einfluss auf die Verarbeitungs- und Verweilzeit sowie die resultierenden Materialeigenschaften bei einem späteren Scale-up des Produktionsprozesses haben kann.

In der Anwendung als Mulchfolien oder Saatgut-Träger nehmen Proteinfolien Feuchtigkeit auf, lösen sich auf und / oder werden entsprechend ihrem Quervernetzungsgrad abgebaut. Währenddessen ist die Freisetzung des eingelagerten Additivs beabsichtigt. Die Diffusion und Freisetzung von Nitratsalzen wird nur bedingt durch die Quervernetzung der Proteinmatrix verzögert. Dennoch konnte gezeigt werden, dass die Feuchtigkeits- und Wasseraufnahme sowie das Quellverhalten der Caseinatfolien in hohem Maße von den verwendeten Additivsalzen abhängen. Im Fall von Caseinat bewirkte die Wechselwirkung mit den dissoziierten Salzionen eine Hydrophobisierung des Proteins, die zu einer bis zu 70 % geringeren Wasseraufnahme führte.

Die Produkttests mit dem protein-basierenden Saatgut-Träger stellten klar die hohe Düngekapazität des Proteins selbst heraus. Außerdem zeigten die Aussäh- und Pflanzenwachstumsversuche die großen Potentiale der maßgeschneiderten Funkt-ionalität auf. Die Menge des Düngemittels im Saatgut-Träger kann der Nährstoffbilanz der jeweiligen Pflanze gezielt angepasst werden. So konnte die Biomasse der beiden Modellpflanzen, Radies und Kopfsalat, bis zu 70 % erhöht werden.

Aus der kombinierten Betrachtung von Materialoptimierung und Produktnutzen ist so ein völlig neues, interdisziplinäres Forschungsgebiet entstanden, das fundamentale Aspekte aus der Entwicklung von Biowerkstoffen, industrieller Kristallisation und so-wohl Produktdesign als auch Ansätze zur Lebenszyklusanalyse vereint. Des Weiteren weist diese Arbeit auf die verschiedenen Wechselwirkungen von protein-basierendem Trägermaterial, funktionalen Additiven, kovalenter Modifikation und Umwelteinflüssen hin, die zusammengefasst die physikalisch-chemischen Materialeigenschaften und den Mehrwert beeinflussen.

11. Abbreviations and symbols

11.1 Abbreviations

ACS	American Chemical Society
API	Active pharmaceutical ingredient
APS	Ammonium persulfate
ASTM	American Society for Testing and Materials
CSD	Crystal size distribution
DoE	Design of experiments
DWVSG	Dynamical water vapor sorption gravimetry
EB	Elongation at break
EN	European Organization for Standardization
eq.	Equation
Gly	Glycerol
GMO	Genetically modified organism
HDPE	High density polyethylene
ISO	International Organization for Standardization
LDPE	Low density polyethylene
M	Marker
MTG	Microbial transglutaminase
MW	Molecular weight
NaCas	Sodium caseinate
PE	Polyethylene
PEG	Polyethylene glycol
pK_a	Logarithmic acid dissociation constant
PP	Polypropylene
PTFE	Polytetrafluorethylene
PVC	Polyvinyl chloride
SD	Standard deviation
SDS	Sodium dodecylsulfate
SDS-PAGE	Sodium dodecylsulfate polyacrylamide gel electrophoresis
TEMED	Tetramethylethylene diamine
TG	Transglutaminase
TRIS	Tris(hydroxymethyl)aminomethane
TS	Tensile strength
UV, Vis	Ultraviolet, visible light
v, w	volume, weight
WVP, WVTR	Water vapor permeability, water vapor transmission rate

11.2 Symbols

A_0	[mm²]	Initial cross-sectional area
d	[m]	interplanar spacing
E_t	[MPa]	Youngs's module
F	[N]	Force
h	[mm]	Height
k	[s^{-n}]	Swelling front factor
L_0	[mm]	Initial length
m	[g]	Mass
MW	[g/mol; Da]	Molecular weight
M	[mol/L]	Molarity
M_t	[mol/L]	Additive concentration released at an incremental time t
M_∞	[mol/L]	Additive concentration at equilibrium state
n	[-]	Release exponent
n	[-]	Number of measurements per data point
n	[-]	Integer in Bragg's law
p	[-]	Probability
r	[mm]	Radius
R^2	[-]	Coefficient of determination
rpm	[min^{-1}]	Rotations per minute
s	[-]	absolute standard deviation
s_{rel}	[%]	relative standard deviation
t	[s]	Time
T	[%]	Total acrylamide concentration
T	[°C]	Temperature
T_g	[°C]	Glass transition temperature
U	[µmol/min]	Enzyme units
w	[mm]	Width
Y	[g_{anh}/kg_{H2O}]	Solubility (mass of solute per mass of solvent)
$\bar{x}$	[-]	Mean value
ε_B	[%]	Elongation at break
ε_M	[%]	Maximum elongation
θ	[°]	Diffraction angle
λ	[m]	Wavelength
σ_B	[MPa]	Tensile strength at break
σ_M	[MPa]	Maximum tensile strength

12. List of figures and tables

13. References

[AbfAblV09] Verordnung über die umweltverträgliche Ablagerung von Siedlungsabfällen (Abfallablagerungsverordnung - AbfAblV), issued by the government of the Federal Republic of Germany, date of first issue: 20th February 2001, last updated on 16th July 2009.

[Aeh07] Aehle, W.: Enzymes in industry: Production and applications, 3rd ed., Wiley-VCH, Weinheim, 2007.

[Agl10] Pagliaro, M., Rossi, M.: The future of glycerol, RSC Green Chemistry No. 8, 2nd ed., RSC Publishing, Cambridge, UK, 2010.

[Ahm07] Ahmad, A., Mohammed, F., Ahmad, M.: Polymers in medicine, in: Specialty polymers: Materials and applications, edited by Mohammed, F., I. K. International Publishing House, New Dehli, India, 2007, 357-396.

[Aji13] Ajinomoto Foods Deutschland GmbH, Hamburg, Activa® transglutaminase, Material safety data sheet and homepage, www.ajinomoto.de, 7th march 2013.

[Ami11] The agricultural films market in Europe, Applied Market Information (AMI), Ltd., Bristol, UK, 2011.

[Ala06] Alavudeen, A, Venkateshwaran, N., Winowlin Jappes, J. T.: Heat treatment, in: A textbook of engineering materials and metallurgy, Laxmi Publications, New Dehli, India, 2006, 87-100.

[Ala11] Alarida, K., Harown, J., Ahmaida, A., Marinelli, L., Venturini, C., Kodermaz, G., Tozzoli, R., Mandolesi, A., Bearzi, I., Catassi, C.: Coeliac disease in Libyan children: A screening study based on the rapid determination of anti-transglutaminase antibodies, Digestive and Liver Disease, 43 (2011) 9, 688-691.

[Ali97] Ali, Y., Ghorpade, V. M., Hanna, M. A.: Properties of thermally-treated wheat gluten films, Industrial Crops and Products, 6 (1997) 2, 177-184.

[All02]   Allahyarov, E., Lowen, H., Louis, A. A., Hansen, J. P.: Discrete charge patterns, Coulomb correlations and interactions in protein solutions, Europhysics Letters, 57 (2002) 5, 731-737.

[Als13]   Al-Saadi, J. M. S., Easa, A. M., Deeth, H. C.: Effect of lactose on cross-linking of milk proteins during heat treatments, International Journal of Dairy Technology, 66 (2013) 1, 1-6.

[And11]   Andersen, M. D., Faber, J. H.: Structural characterization of both the non-proteolytic and proteolytic activation pathways of coagulation Factor XIII studied by hydrogen–deuterium exchange mass spectrometry, International Journal of Mass Spectrometry, 302 (2011) 1–3, 139-148.

[Agu10]   Aguzzi, C., Cerezo, P., Salcedo, I., Sanchez, R., Viseras, C.: Mathematical models describing drug release from biopolymeric delivery systems, Materials Technology, 25 (2010) 3-4, 205-211.

[Ars07]   Arslan, A.: Milk protein fibers (part 1), Chemical Fibers International, 57 (2007) 3, 108-109.

[Aug02]   Augsburger, L. L.: Hard and soft shell capsules, in: Modern Pharmaceutics, 4th ed., edited by: Banker, G.S., Siepmann, J., Rhodes, C., Marcel Dekker, Inc., New York, USA, 2002, 512-575.

[Ave93]   Avena-Bustillos, R. J., Krochta, J. M.: Water vapor permeability of caseinate-based edible films as affected by pH, calcium cross-linking and lipid content, Journal of Food Science, 58 (1993) 4, 904-907.

[Bad05]   Badarani, A.: Gewinnung und Charakterisierung von Kaseinen aus nicht verkehrfähiger Milch für industrielle Anwendungen, PhD thesis, Faculty III – Process Sciences, Technical University, Berlin, 2005.

[Bai13]   Bai, H., Xu, J., Liao, P. and Liu, X.: Mechanical and water barrier properties of soy protein isolate film incorporated with gelatin, Journal of Plastic Film and Sheeting, 29 (2013) 2, 174-188.

[Bas13a]   ecovio F Blend C2224, production information and material data sheet, version 1.0, BASF SE Biodegradable Polymers, Ludwighafen, Germany, 17th January 2013.

[Bas13b]   ecovio F Film C2203, production information and material data sheet, version 1.0, BASF SE Biodegradable Polymers, Ludwighafen, Germany, 17th January 2013.

[Bas13c]   ecovio F Blend C2332, production information and material data sheet, version 1.0, BASF SE Biodegradable Polymers, Ludwighafen, Germany, 17th January 2013.

[Bau07]   Baur, E., Brinkmann, S., Osswald, T. A., Schmachtenberg, E.: Saechtling Kunststoff Taschenbuch, 30th ed., Carl Hanser Verlag, München, Germany, 2007.

[Bec11]   Beck, M., Jekle, M., Selmair, P. L., Koehler, P., Becker, T.: Rheological properties and baking performance of rye dough as affected by transglutaminase, Journal of Cereal Science, 54 (2011) 1, 29-36.

[Ben03]   Bennion, B. J., Daggett, V.: The molecular basis for the chemical denaturation of proteins by urea, Proceedings of the National Academy of Sciences, 100 (2003) 9, 5142-5147.

[Ber13]   Berger, S., Kim, Y., Kettering, J., Gebauer, G.: Plastic mulching in agriculture-Friend or foe of N_2O emissions?, Agriculture Ecosystems and Environment, 167 (2013) 43-51.

[Bet11]   Betoret, E., Betoret, N., Vidal, D., Fito, P.: Functional foods development: Trends and technologies, Trends in Food Science & Technology, 22 (2011) 9, 498-508.

[Bet12]   Betz, M., Hormansperger, J., Fuchs, T., Kulozik, U.: Swelling behaviour, charge and mesh size of thermal protein hydrogels as influenced by pH during gelation, Soft Matter, 8 (2012) 8, 2477-2485.

[Bie12]   Bier, J., Verbeek, C., Lay, M.: An eco-profile of thermoplastic protein derived from blood meal Part 1: allocation issues, The International Journal of Life Cycle Assessment, 17 (2012) 2, 208-219.

[Big04]   Bigi, A., Panzavolta, S., Rubini, K.: Relationship between triple-helix content and mechanical properties of gelatin films, Biomaterials, 25 (2004) 25, 5675-5680.

[BioAbfV13]   Bioabfallverordnung: Verordnung über die Verwertung von Bioabfällen auf landwirtschaftlich, forstwirtschaftlich und gärtnerisch genutzten Böden (Bioabfallverordnung – BioAbfV), issued by the government of the Federal Republic of Germany, date of first issue: 21th September 1998, last updated on 4th April 2013.

[Bor10]   Borzacchiello, A., Ambrosio, L.: Structure-property relationships in hydrogels, in: Hydrogels: Biological properties and applications, edited by: Barbucci, R., Springer-Verlag Italia, Milan, Italy, 2010, 9-20.

[Bow90]   Bowman, D. C., Evans, R. Y., Paul, J. L.: Fertilizer salts reduce hydration of polyacrylamide gels and affect physical properties of gel-amended container media, Journal of the American Society for Horticultural Science, 115 (1990) 382-386.

[Bou06]   Bouguyon, E., Beauvallet, C., Huet, J.-C., Chanat, E.: Disulphide bonds in casein micelle from milk, Biochemical and Biophysical Research Communications, 343 (2006) 2, 450-458.

[Bou08]   Bourtoom, T.: Edible films and coatings: characteristics and properties, International Food Research Journal, 15 (2008) 3, 237-248.

[Bra76]   Bradford, M. M.: Rapid and sensitive method for quantification of microgram quantities of protein utilizing principle of protein-dye binding, Analytical Biochemistry, 72 (1976) 1-2, 248-254.

[Bra97]   Bras, B.: Incorporating environmental issues in product design and realization, Industry and Environment, 20 (1997) 1-2, 1-19.

[Bra05]   Braun, D., Cherdron, H., Rehahn, M., Ritter, H., Voit, B.: States of order in polymers, in: Polymer synthesis: theory and practice, 4th edition, edited by Braun, D., Cherdron, H., Rehahn, M., Ritter, H., Voit, B., Springer Verlag, Berlin, Germany, 2005, 11-31.

[Bra07]   Braud, A., Jézéquel, K., Lebeau, T.: Impact of substrates and cell immobilization on siderophore activity by Pseudomonads in a Fe and/or Cr, Hg, Pb containing-medium, Journal of Hazardous Materials, 144 (2007) 1–2, 229-239.

[Bra12]   Brazel, Ch. S., Rosen, St. L.: Fundamental principles of polymeric materials, 3rd ed., John Wiley & Sons, Inc, Hoboken, New Jersey, USA, 2012.

[Bra13]   Bragg, W. L.: The diffraction of short electromagnetic waves by a crystal, Proceedings of the Cambridge Philosophical Society 17 (1913) 43-57.

[Bri16]   Bridgman, P. W.: Polymorphic changes under pressureof the univalent nitrates, Proceedings of the American Academy of Arts and Sciences, 51 (1916) 581-625.

[Bri04]   Briassoulis, D.: An Overview on the Mechanical Behaviour of Biodegradable Agricultural Films, Journal of Polymers and the Environment, 12 (2004) 2, 65-81.

[Bru08]   Bruno, M., Giancone, T., Torrieri, E., Masi, P., Moresi, M.: Engineering Properties of Edible Transglutaminase Cross-Linked Caseinate-Based Films, Food and Bioprocess Technology, 1 (2008) 4, 393-404.

[Buc11]   Buchfink, R.: Effects of impurities on an industrial crystallization process of ammonium sulfate, PhD thesis, Center of Engineering Sciences, Martin Luther University Halle-Wittenberg, Halle (Saale), Shaker Verlag, Aachen, Germany, 2011.

[Buo05]   Buonocore, G. G., Conte, A., Nobile, M. A. D.: Use of a Mathematical Model to Describe the Barrier Properties of Edible Films, Journal of Food Science, 70 (2005) 2, E142-E147.

[Büt11]   Büttner, K.: Optimierung einer mikrobiellen Transglutaminase mittels Sättigungsmutagenese und DNA-Shuffling, PhD thesis, Faculty of Natural Sciences I, Martin Luther University Halle-Wittenberg, Halle (Saale), 2011.

[Cad81]   Cady, H. H.: The Ammonium Nitrate-Potassium Nitrate System, Propellants, Explosives, Pyrotechnics, 6 (1981) 2, 49-54.

[Cad00]   Cadogan, D. F., Howick, C. J.: Plasticizers, in: Kirk-Othmer Encyclopedia of Chemical Technology, online version, 2000.

[Can93] Canselier, J. P.: The effects of surfactants on crystallization phenomena, Journal of Dispersion Science and Technology, 14 (1993) 6, 625-644.

[Can10] Canchi, D. R., Paschek, D., García, A. E.: Equilibrium Study of Protein Denaturation by Urea, Journal of the American Chemical Society, 132 (2010) 7, 2338-2344.

[Cao09] Cao, N., Yang, X., Fu, Y.: Effects of various plasticizers on mechanical and water vapor barrier properties of gelatin films, Food Hydrocolloids, 23 (2009) 3, 729-735.

[Car04] de Carvalho, R. A., Grosso, C. R. F.: Characterization of gelatin based films modified with transglutaminase, glyoxal and formaldehyde, Food Hydrocolloids, 18 (2004) 5, 717-726.

[Car10] Cardoso, C., Mendes, R., Pedro, S., Vaz-Pires, P., Nunes, M. L.: Quality Changes During Storage of Minced Fish Products Containing Dietary Fiber and Fortified with omega 3 Fatty Acids, Food Science and Technology International, 16 (2010) 1, 31-42.

[Car13] Carraher, Jr., Ch. E.: Introduction to polymer chemistry, 3rd ed., CRC Press, Boca Raton, FL, USA, 2013.

[Cat75] Cataldo, D. A., Haroon, M., Schrader, L. E., Youngs, V. L.: Rapid colorimetric determination of nitrate in plant-tissue by nitration of salicylic acid, Communications in Soil Science and Plant Analysis, 6 (1975) 1, 71-80.

[Cha03] Chattopadhyay, A. K.: Effect of polymeric surfactants on the behavior of polycrystalline materials with special reference to ammonium nitrate, in: Adsorption and aggregation of surfactants in solution, edited by: Shah, D. O., Mittal, K. L., Marcel Dekker, New York, USA, 2003, 655-674.

[Cha06] Chambi, H., Grosso, C.: Edible films produced with gelatin and casein cross-linked with transglutaminase, Food Research International, 39 (2006) 4, 458-466.

[Cha11]   Chaudhry, Q., Castle, L.: Food applications of nanotechnologies: An overview of opportunities and challenges for developing countries, Trends in Food Science & Technology, 22 (2011) 11, 595-603.

[Che95a]   Chen, H.: Functional Properties and Applications of Edible Films Made of Milk Proteins, J. Dairy Sci., 78 (1995) 11, 2563-2583.

[Che95b]   Cherian, G., Gennadios, A., Weller, C., Chinachoti, P.: Thermomechanical Behavior of Wheat Gluten Films: Effect of Sucrose, Glycerin, and Sorbitol, Cereal Chemistry, 72 (1995) 1, 1-6.

[Che08]   Chesworth, W.: Fertilizer raw materials, in: Encyclopedia of soil science, edited by: Chesworth, W., Springer, Dordrecht, The Netherlands, 2008, 245.

[Che11]   Chevillard, A., Angellier-Coussy, H., Cuq, B., Guillard, V., Cesar, G., Gontard, N., Gastaldi, E.: How the biodegradability of wheat gluten-based agromaterial can be modulated by adding nanoclays, Polymer Degradation and Stability, 96 (2011) 12, 2088-2097.

[Chi76]   Chien, Y. W., Lau, E. P. K.: Controlled drug release from polymeric delivery devices IV: in vitro-in vivo correlation of subcutaneous release of norgestomet from hydrophilic implants, Journal of Pharmaceutical Sciences, 65 (1976) 4, 488-492.

[Chi02]   Chick, J., Hernandez, R. J.: Physical, thermal, and barrier characterization of casein-wax-based edible films, Journal of Food Science, 67 (2002) 3, 1073-1079.

[Chi05a]   Chien, W. M., Chandra, D., Franklin, J., Rawn, C. J., Helmy, A. K.: X-ray diffractometry studies and lattice parameter calculation on KNO_3-NH_4NO_3 solid solutions, Powder Diffraction, 20 (2005) 2, 101-104.

[Chi05b]   Chien, W. M., Chandra, D., Helmy, A. K., Franklin, J., Rawn, C. J.: Experimental determination of NH_4NO_3-KNO_3 binary phase diagram, Journal of Phase Equilibria and Diffusion, 26 (2005) 2, 115-123.

[Chi07]   Chiellini, E., Corti, A., D'Antone, S.: Oxo-biodegradable full carbon backbone polymers – biodegradation behaviour of thermally oxidized

polyethylene in an aqueous medium, Polymer Degradation and Stability 92 (2007) 7, 1378-1383.

[Cho04]   Choong, K. L., Smith, R.: Optimization of batch cooling crystallization, Chemical Engineering Science, 59 (2004) 2, 313-327.

[Chr98]   Chronakis, I. S.: On the Molecular Characteristics, Compositional Properties, and Structural-Functional Mechanisms of Maltodextrins: A Review, Critical Reviews in Food Science and Nutrition, 38 (1998) 7, 599-637.

[Cie06]   Cieśla, K., Salmieri, S., Lacroix, M.: Modification of the properties of milk protein films by gamma radiation and polysaccharide addition, Journal of the Science of Food and Agriculture, 86 (2006) 6, 908-914.

[Coa61]   Coates, R. V., Crewe, J. M.: Solid Solutions in the System Ammonium Nitrate-Potassium Nitrate, Nature, 190 (1961) 4782, 1190-1191.

[Cog07]   Cognis: Safety data sheet (1907/2006/EG), Glycerol, Cognis GmbH, Düsseldorf, 2007.

[Col09]   Collighan, R. J., Griffin, M.: Transglutaminase 2 cross-linking of matrix proteins: biological significance and medical applications, Amino Acids, 36 (2009) 4, 659-670.

[Cou00]   Coupland, J. N., Shaw, N. B., Monahan, F. J., Dolores O'Riordan, E., O'Sullivan, M.: Modeling the effect of glycerol on the moisture sorption behavior of whey protein edible films, Journal of Food Engineering, 43 (2000) 1, 25-30.

[Cre01]   Crecchio, C., Stotzky, G.: Biodegradation and insecticidal activity of the toxin from Bacillus thuringiensis subsp. kurstaki bound on complexes of montmorillonite–humic acids–Al hydroxypolymers, Soil Biology and Biochemistry, 33 (2001) 4–5, 573-581.

[Dan00]   Dann, S. E.: Reactions and characterization of solids, The Royal Society of Chemistry, Cambridge, UK, 2000.

[Dan09]   Dangaran, K., Tomasula, P., Qi, P.: Structure and Function of Protein-Based Edible Films and Coatings, in: Edible Films and Coatings for

Food Applications, edited by: Huber, K. C., Embuscado, M. E., Springer, New York, USA, 2009, 25-56.

[Das09]   Das, A., Mukhopadhyay, C.: Urea-Mediated Protein Denaturation: A Consensus View, The Journal of Physical Chemistry B, 113 (2009) 38, 12816-12824.

[Dav63]   Davis, B. L., Adams, L. H. Transition rates of KNO3 high-pressure polymorphs, Journal of Physics and Chemistry of Solids, 24 (1963) 7, 787-794.

[Dav04]   Davis, J. R. Tensile Testing, 2nd edition ed. by Davis, J. R., ASM International, 2004.

[Dej00]   Dejewska, B.: The characteristics of the mixed crystals of the KNO3-NH4NO3-H2O System at 298 K, Cryst. Res Technol. 35 (2000) 9, 1059-1067.

[Del10]   Delgado-Pando, G., Cofrades, S., Ruiz-Capillas, C., Teresa Solas, M., Jiménez-Colmenero, F.: Healthier lipid combination oil-in-water emulsions prepared with various protein systems: an approach for development of functional meat products, European Journal of Lipid Science and Technology, 112 (2010) 7, 791-801.

[Dem12]   de Moura, M. R., Mattoso, L. H. C., Zucolotto, V.: Development of cellulose-based bactericidal nanocomposites containing silver nanoparticles and their use as active food packaging, Journal of Food Engineering, 109 (2012) 3, 520-524.

[Den09]   Denavi, G., Tapia-Blácido, D. R., Añón, M. C., Sobral, P. J. A., Mauri, A. N., Menegalli, F. C.: Effects of drying conditions on some physical properties of soy protein films, Journal of Food Engineering, 90 (2009) 3, 341-349.

[Dic06]   Dickinson, E.: Structure formation in casein-based gels, foams, and emulsions, Colloids and Surfaces A: Physicochemical and Engineering Aspects, 288 (2006) 1–3, 3-11.

[Die97]   Dieterich, W., Ehnis, T., Bauer, M., Donner, P., Volta, U., Riecken, E. O., Schuppan, D.: Identification of tissue transglutaminase as the autoantigen of celiac disease, Nature Medicine, 3 (1997) 7, 797-801.

[DIN96]   DIN EN ISO 527-1: Kunststoffe – Bestimmung der Zugeigenschaften – Teil 1: Allgemeine Grundsätze, Deutsches Institut für Normung e. V., April 1996.

[DIN99]   DIN EN ISO 62: Kunststoffe – Bestimmung der Wasseraufnahme, Deutsches Institut für Normung e. V., August 1999.

[DIN00]   DIN EN 13432: Verpackung – Anforderungen an die Verwertung von Verpackungen durch Kompostierung und biologischen Abbau – Prüfschema und Bewertungskriterien für die Einstufung von Verpackungen, Deutsches Institut für Normung e. V., Dezember 2000.

[DIN01]   DIN 53122-1: Prüfung von Kunststoff-Folien, Elastomerfolien, Papier, Pappe und anderen Flächengebilden – Bestimmung der Wasserdampfdurchlässigkeit – Teil 1: Gravimetrisches Verfahren, Deutsches Institut für Normung e. V., August 2001.

[DIN03a]   DIN EN ISO 527-3: Kunststoffe – Bestimmung der Zugeigenschaften – Teil 3: Prüfbedingungen für Folien und Tafeln, Deutsches Institut für Normung e. V., Juli 2003.

[DIN03b]   DIN EN 13655: Kunststoffe – Thermoplastische Mulchfolien für den Einsatz in der Landwirtschaft und im Gartenbau, Deutsches Institut für Normung e. V., Januar 2003.

[DiP06]   DiPierro, P., Chico, B., Villalonga, R., Mariniello, L., Damiao, A. E., Masi, P., Porta, R.: Chitosan-Whey Protein Edible Films Produced in the Absence or Presence of Transglutaminase: Analysis of Their Mechanical and Barrier Properties, Biomacromolecules, 7 (2006) 3, 744-749.

[DümV12]   Verordnung über das Inverkehrbringen von Düngemitteln, Bodenhilfsstoffen, Kultursubstraten und Pflanzenhilfsmitteln (Düngemittelverordnung - DüMV), issued by the government of the Federal Republic of Germany, first issued on 5th December 2012.

[Ebe00]   Ebewele, R. O.: Unit operations in polymer processing, in: Polymer science and technology, CRC Press, Boca Raton, FL, USA, 2000.

[Ebn13]   Microbial production of biopolymers and polymer precursors, edited by Rehm, B. H. A., Caister Academic Press, Norfolk, UK, 2009.

[Eis02]   Eisenthal, R., Danson, M. J.: Enzyme assays: A practical approach, vol. 257 in: The practical approach series, 2nd ed., Oxford University Press, Oxford, UK, 2002.

[Els12]   Elsner, J. J., Kraitzer, A., Grinberg, O., Zilberman, M.: Highly porous drug-eluting structures: from wound dressings to stents and scaffolds for tissue regeneration, Biomatter, 2 (2012) 4, 239-70.

[End09]   Endres, H.-J., Siebert-Raths, A.: Technische Biopolymere, Carl Hanser Verlag, München, 2009.

[Eng02]   Engelen, K., Lefebvre, M. H., Hubin, A.: Properties of a gas-generating composition related to the particle size of the oxidizer, Propellants Explosives Pyrotechnics, 27 (2002) 5, 290-299.

[Enn00]   Ennis, M. P., Mulvihil, D. M.: Milk proteins, in: Handbook of hydrocolloids, edited by: Phillips, G. O., Williams, P. A., Woodhead Publishing, Cambridge, UK, 2000, 189-218.

[EuB12]   What are bioplastics? - Material types, terminology and labels – an introduction, Fact sheet, European Bioplastics e.V., Berlin, Germany, online version last updated in August 2012, accessed on 30th June 2013.

[Fab10]   Fabra, M. J., Talens, P., Chiralt, A.: Water sorption isotherms and phase transitions of sodium caseinate–lipid films as affected by lipid interactions, Food Hydrocolloids, 24 (2010) 4, 384-391.

[Fai02]   Faithfull, N T.: The analysis of fertilizers, in: Methods in agricultural chemical analysis: a practical handbook, CABI Publishing, Oxon, UK, 2002, 111.

[Fak07]   Handbook of engineering biopolymers: Homopolymers, blends and composites, edited by Fakirov, S. and Bhattacharyya, D., Carl Hanser Verlag, München, Germany, 2007.

[Fat10]   Fathi-Azarbayjani, A., Qun, L., Chan, Y., Chan, S.: Novel Vitamin and Gold-Loaded Nanofiber Facial Mask for Topical Delivery, AAPS PharmSciTech, 11 (2010) 3, 1164-1170.

[Fat12]   Fatarella, E., Ciabatti, I., Cortez, J.: Activation of polymeric materials towards enzymatic postgrafting and cross-linking, Enzyme and Microbial Technology, 51 (2012) 5, 252-257.

[Fel06]   Feldman, Y., Puzenko, A., Ryabov, Y.: Dielectric relaxation phenomena in complex materials, in: Advances in chemical physics Volume 133: Fractals, diffusion and relaxation in disordered complex systems Part A, edited by: Coffey, W. T., Kalmykov, Y. P., series editor: Rice, S. A., John Wiley & Sons, Hoboken, New Jersey, USA, 2006, 84.

[Fel13]   Felton, L. E.: Remington: Essentials of Pharmaceutics, 1st ed., Pharmaceutical Press, London, UK, 2013.

[Fer04]   Fernández-Gutiérrez, J. A., San Martín-Martínez, E., Martínez-Bustos, F., Cruz-Orea, A.: Physicochemical Properties of Casein-Starch Interaction Obtained by Extrusion Process, Starch - Stärke, 56 (2004) 5, 190-198.

[Fis11]   Fischer, B., Scholz, H., Knutzen, G., Zarwel, H., Wähner, M.: Einflussfaktoren auf die Qualität der Kolostralmilch von Milchkühen der Rasse Deutsche Holsteins, Infothek des Landes Sachsen-Anhalt, Landesanstalt für Landwirtschaft, Forsten und Gartenbau, 2011.

[Fit12]   Fitzpatrick, J. J.: Crystallization process design, in: Handbook of food process design (Volume 1), edited by Ahmed, J., Rahman, M. S., Wiley-Blackwell, Chichester, UK, 2012, 648-681.

[Fku12a]   Bio-Flex F 1130, material data sheet, version 3.2, FKuR Kunststoff GmbH, Willich, Germany, 29th November 2012.

[Fku12b]   Terralene LL 1101, material data sheet, version 1.0, FKuR Kunststoff GmbH, Willich, Germany, 21st November 2012.

[Fla06]   Flanagan, J., Singh, H.: Conjugation of Sodium Caseinate and Gum Arabic Catalyzed by Transglutaminase, J. Agric. Food Chem., 54 (2006) 19, 7305-7310.

[Fol66]   Folk, J. E., Cole, P. W.: Transglutaminase: Mechanistic features of the active site as determined by kinetic and inhibitor studies, Biochim. Biophys. Acta, 122 (1966) 2, 244-264.

[For67]   Forest Products Laboratory: Casein glues: their manufacture, preparation and application, U.S. Department of Agriculture, in cooperation with the University of Wisconsin, Band 158 of Research Note FPL, Madison, Wisconsin, USA, 1967.

[Fos10]   Foster, A., Piepenbrock, M.-O. M., Lloyd, G. O., Clarke, N., Howard, J. A. K., Steed, J. W.: Anion-switchable supramolecular gels for controlling pharmaceutical crystal growth, Nat Chem, 2 (2010) 12, 1037-1043.

[Fox50]   Fox, T. G., Flory, P. J.: Second-order transition temperatures and related properties of polystyrene. I. Influence of molecular weight, Journal of Applied Physics, 21 (1950) 581-591.

[Fre09]   Freney, E. J., Garvie, L. A. J., Groy, T. L., Buseck, P. R.: Growth and single-crystal refinement of phase-III potassium nitrate, KNO_3, Acta Crystallographica Section B, 65 (2009) 6, 659-663.

[Fri97]   Frinault, A., Gallant, D. J., Bouchet, B., Dumont, J. P.: Preparation of Casein Films by a Modified Wet Spinning Process, Journal of Food Science, 62 (1997) 4, 744-747.

[Fro10a] Frohberg, P., Pietzsch, M., Ulrich, J. Effect of crystalline substances in biodegradable films, Chemical Engineering Research and Design, 88 (2010) 9, 1148-1152.

[Fro10b] Frohberg, P.: Untersuchungen zur Herstellung und Optimierung proteinogener Biowerkstoffe, PhD thesis, Martin-Luther-Universität Halle-Wittenberg, Halle (Saale), 2011.

[Ful09]   Fulladosa, E., Serra, X., Gou, P., Arnau, J.: Effects of potassium lactate
            and high pressure on transglutaminase restructured dry-cured hams
            with reduced salt content, Meat Science, 82 (2009) 2, 213-218.

[Gal09]   Galdeano, M. C., Mali, S., Grossmann, M. V. E., Yamashita, F., Garcia,
            M. A.: Effects of plasticizers on the properties of oat starch films,
            Materials Science & Engineering C-Biomimetic and Supramolecular
            Systems, 29 (2009) 2, 532-538.

[Gäl11]   Gällstedt, M., Hedenqvist, M. S., Ture, H.: Production, Chemistry and
            Properties of Proteins, in: Biopolymers - New Materials for
            Sustainable Films and Coatings, edited by Plackett, D., Wiley, Padstow,
            UK, 2011, 107-132.

[Gan10]   Ganji, F., Vasheghani-Farahani, S., Vasheghani-Farahani, E.:
            Theoretical description of hydrogel swelling: A review, Iranian Polymer
            Journal, 19 (2010) 5, 375-398.

[Gar13]   Garrett, R. H., Grisham, C. M.: Protein dynamics, in: Biochemistry, 5th
            ed., Brooks/Cole, Belmont, CA, USA, 2013, 407 – 550.

[Gen94]   Gennadios, A., Weller, C. L.: Moisture adsorption by grain protein films,
            Transactions of the Asae, 37 (1994) 2, 535-539.

[Gen96]   Gennadios, A., Ghorpade, V. M., Weller, C. L., Hanna, M. A.: Heat
            curing of soy protein films, Transactions of the Asae, 39 (1996) 2, 575-
            579.

[Gen97]   Gennadios, A., Hanna, M. A., Kurth, L. B.: Application of Edible
            Coatings on Meats, Poultry and Seafoods: A Review, Lebensmittel-
            Wissenschaft und-Technologie, 30 (1997) 4, 337-350.

[Gen02]   Protein-based films and coatings, edited by Gennadios, A., CRC Press,
            Boca Raton, Florida, USA, 2002.

[Ger12]   Gerrard, J. A., Cottam, J. R.: Protein cross-linking in food – structure,
            applications, implications for health and food safety, in: Food
            biochemistry and food processing, 2nd ed., edited by Simpson, B. K.,
            Nollet, L. M. L., Toldrà, F., Benjakul, S., Paliyath, G., Hui, Y. H., Wiley-
            Blackwell, Oxford, UK, 2012, 207-222.

[Gho09]   Ghosh, A., Ali, M. A., Dias, G. J.: Effect of Cross-Linking on Microstructure and Physical Performance of Casein Protein, Biomacromolecules, 10 (2009) 7, 1681-1688.

[Gra12]   Grabowska, K. J., van der Goot, A. J., Boom, R. M.: Salt-modulated structure formation in a dense calcium caseinate system, Food Hydrocolloids, 29 (2012) 1, 42-47.

[Gre91]   Greenberg, C. S., Birckbichler, P. J., Rice, R. H.: Transglutaminases: multifunctional cross-linking enzymes that stabilize tissues, The FASEB Journal, 5 (1991) 15, 3071-7.

[Gri10]   Grinberg, O., Binderman, I., Bahar, H., Zilberman, M.: Highly porous bioresorbable scaffolds with controlled release of bioactive agents for tissue-regeneration applications, Acta Biomaterialia, 6 (2010) 4, 1278-1287.

[Gu11]   Gu, Y., Chen, L., Yang, H.-L., Luo, Z.-P., Tang, T.-S.: Evaluation of an injectable silk fibroin enhanced calcium phosphate cement loaded with human recombinant bone morphogenetic protein-2 in ovine lumbar interbody fusion, Journal of Biomedical Materials Research Part A, 97A (2011) 2, 177-185.

[Gue10]   Guerrero, P., Retegi, A., Gabilondo, N., de la Caba, K.: Mechanical and thermal properties of soy protein films processed by casting and compression, Journal of Food Engineering, 100 (2010) 1, 145-151.

[Gui05]   Guilbert, S., Cuq, B.: Material formed from proteins, in: Handbook of biodegradable polymers, edited by Bastioli, C., Rapra Technology, Shawbury, UK, 2005, 339-384.

[Gui05b]   Guilbert, S., Gontard, N.: Agro-polymers for edible and biodegradable films: review of agricultural polymeric materials, physical and mechanical characteristics, in: Innovations in food packaging, Elsevier, London, UK, 2005, 263-276.

[Guo03]   Guo, C., Campbell, B. E., Chen, K., Lenhoff, A. M., Velev, O. D.: Casein precipitation equilibria in the presence of calcium ions and phosphates, Colloids and Surfaces B-Biointerfaces, 29 (2003) 4, 297-307.

[Gup02]   Gupta, S. P. S.: Powder Diffraction, Proceedings of II International School on Powder Diffraction, Allied Publishers, New Dehli, 2002.

[Hat07]   Hatti-Kaul, R., Törnvall, U., Gustafsson, L., Börjesson, P.: Industrial biotechnology for the production of bio-based chemicals – a cradle-to-grave perspective, Trends in Biotechnology, 25 (2007) 3, 119-124.

[Hat11]   Hati, K., Bandyoopadhay, K.: Fertilizers (mineral, organic), effect on soil physical properties, in: Encyclopedia of agrophysics, edited by: Glinski, J., Horabik, J., Lipiec, J., Springer Science + Business Media, Dordrecht, The Netherlands, 2011, 296 – 299.

[Hec12]   Heck, T., Faccio, G., Richter, M., Thoeny-Meyer, L.: Enzyme-catalyzed protein crosslinking, Applied Microbiology and Biotechnology, 97 (2013) 2, 461-475.

[Hen96]   Henisch, Heinz K.: Crystal growth in gels, Dover Publications, New York, USA, 1996.

[Her97]   Herden, A., Lacmann, R.: The crystallization of potassium nitrate. II. Growth rate dispersion, Journal of Crystal Growth, 179 (1997) 3–4, 592-604.

[Her08]   Hernandez-Izquierdo, V. M., Krochta, J. M.: Thermoplastic Processing of Proteins for Film Formation—A Review, Journal of Food Science, 73 (2008) 2, R30-R39.

[Hes05]   Hesse, M., Meier, H., Zeeh, B.: Spektroskopische Methoden in der organischen Chemie, 7th ed., Georg Thieme Verlag, Stuttgart, 2005.

[Hil99]   Hilhorst, R., Dunnewind, B., Orsel, R., Stegeman, P., van Vliet, T., Gruppen, H., Schols, H. A.: Baking Performance, Rheology, and Chemical Composition of Wheat Dough and Gluten Affected by Xylanase and Oxidative Enzymes, Journal of Food Science, 64 (1999) 5, 808-813.

[Hof04]   Kristallisation in der industriellen Praxis; edited by: Hofmann, G., Wiley-VCH Verlag GmbH & Co. KGaA, Weinheim, 2004.

[Hol75]   Holden, J. R., Dickinson, C. W.: Crystal structures of three solid solution phases of ammonium nitrate and potassium nitrate, The Journal of Physical Chemistry, 79 (1975) 3, 249-256.

[Hu12]   Hu, X., Cebe, P., Weiss, A. S., Omenetto, F., Kaplan, D. L.: Protein-based composite materials, Materials Today, 15 (2012) 5, 208-215.

[Hun92]   Hung, S. C., Zayas, J. F.: Protein Solubility, Water Retention, and Fat Binding of Corn Germ Protein Flour Compared with Milk Proteins, Journal of Food Science, 57 (1992) 2, 372-376.

[Ike08]   IKEA: Specification Formaldehyde requirements of wood-based materials and products: Spec. no: IoS-MAT-0003, Version no.: AA-10899-6, 2008.

[ISO95]   ISO 2528: Sheet materials – Determination of water vapour transmission rate – Gravimetric (dish) method, International organization for standardization, 1995.

[ISO03]   ISO 15106-2: Plastics – Film and sheeting – Determination of water vapor transmission rate – Part 2: Infrared detection method, International organization for standardization, 2003.

[Jac01]   Jackson, M. R.: Fibrin sealants in surgical practice: An overview, The American Journal of Surgery, 182 (2001) 2, Supplement 1, S1-S7.

[Jan99]   Jangchud, A., Chinnan, M. S.: Peanut Protein Film as Affected by Drying Temperature and pH of Film Forming Solution, Journal of Food Science, 64 (1999) 1, 153-157.

[Jim12]   Jiménez, A., Fabra, M. J., Talens, P., Chiralt, A.: Effect of sodium caseinate on properties and ageing behaviour of corn starch based films, Food Hydrocolloids, 29 (2012) 2, 265-271.

[Joh11]   Johnson, K. A., Goody, R. S.: The Original Michaelis Constant: Translation of the 1913 Michaelis–Menten Paper, Biochemistry, 50 (2011) 39, 8264-8269.

[Juv11]   Juvonen, H., Smolander, M., Boer, H., Pere, J., Buchert, J., Peltonen, J.: Film formation and surface properties of enzymatically crosslinked

casein films, Journal of Applied Polymer Science, 119 (2011) 4, 2205-2213.

[Kam07]   Kamiński, S., Cieślińska, A., Kostyra, E.: Polymorphism of bovine beta-casein and its potential effect on human health, Journal of Applied Genetics, 48 (2007) 3, 189-198.

[Kan68]   Kane, C. V.: Article for agricultural use, US 3384993, United States Patent Office, patented May 28, 1968.

[Kap08]   Kapanen, A., Schettini, E., Vox, G., Itavaara, M.: Performance and Environmental Impact of Biodegradable Films in Agriculture: A Field Study on Protected Cultivation, Journal of Polymers and the Environment, 16 (2008) 2, 109-122.

[Kas02]   Kashiwagi, T., Yokoyama, K., Ishikawa, K., Ono, K., Ejima, D., Matsui, H., Suzuki, E.: Crystal Structure of Microbial Transglutaminase from *Streptoverticillium mobaraense*, J. Biol. Chem., 277 (2002) 46, 44252-60.

[Kas12]   Kasirajan, S., Ngouajio, M.: Polyethylene and biodegradable mulches for agricultural applications: a review, Agronomy for Sustainable Development, 32 (2012) 2, 501-529.

[Ker08]   Kerns, E. H., Di, L.: Solubility of salts, in: Drug-like properties: Concepts, structure design and methods, Elsevier Science, Burlington, MA, USA, 2008, 78-80.

[Khan10]   Khan, F., Mahmud, T., Islam, M. S., Jalil, R.-U.: Effect of Hydrophobic Excipients on the Release Behavior of Dexamethasone and Betamethasone from Biodegradable Poly (DL-lactide) Polymeric Implants, Bangladesh J. Sci. Ind. Res., 45 (2010) 3, 189-196.

[Kho12]   Khondee, N., Tathong, S., Pinyakong, O., Powtongsook, S., Chatchupong, T., Ruangchainikom, C., Luepromchai, E.: Airlift bioreactor containing chitosan-immobilized Sphingobium sp. P2 for treatment of lubricants in wastewater, Journal of Hazardous Materials, 213–214 (2012) 0, 466-473.

[Khw04a]   Khwaldia, K., Banon, S., Perez, C., Desobry, S.: Properties of Sodium Caseinate Film-Forming Dispersions and Films, J. Dairy Sci., 87 (2004) 7, 2011-2016.

[Khw04b]   Khwaldia, K., Banon, S., Desobry, S., Hardy, J.: Mechanical and barrier properties of sodium caseinate-anhydrous milk fat edible films, International Journal of Food Science and Technology, 39 (2004) 4, 403-411.

[Kim92]   Kim, S. W., Bae, Y. H., Okano, T.: Hydrogels: Swelling, Drug Loading, and Release, Pharmaceutical Research, 9 (1992) 3, 283-290.

[Kim01]   Kim, S. J., Ustunol, Z.: Solubility and Moisture Sorption Isotherms of Whey-Protein-Based Edible Films as Influenced by Lipid and Plasticizer Incorporation, Journal of Agricultural and Food Chemistry, 49 (2001) 9, 4388-4391.

[Kip97]   Kipp, S., Lacmann, R., Rolfs, J.: Crystallization of potassium nitrate (KNO3) in aqueous solution Part II. Kinetical studies under the influence of additives, Journal of Crystal Growth, 171 (1997) 1-2, 183-189.

[Kle80]   Kleyn, D. H., Klostermeyer, H.: Dehydroalanin als Reaktionsprodukt bei der Erhitzung von β-Casein, Z. Lebensm. Unters. Forsch., 170 (1980) 1, 11-13.

[Klo77]   Klostermeyer, H., Reimerdes, E. H.: Heat induced crosslinks in milk proteins and consequences for the milk system, Advances in experimental medicine and biology, 86B (1977) 263-275.

[Kow11]   Kowalczyk, D., Baraniak, B.: Effects of plasticizers, pH and heating of film-forming solution on the properties of pea protein isolate films, Journal of Food Engineering, 105 (2011) 2, 295-305.

[Kra29]   Kracek, F. C.: The Polymorphism of Potassium Nitrate, The Journal of Physical Chemistry, 34 (1929) 2, 225-247.

[Kra05]   Krauskopf, L. G., Godwin, A.: Plasticizers, in: PVC Handbook, 1st ed., edited by Wilkes, C.E., Summers, J.W., Daniels, C.A., Hanser Verlag, Munich, Germany, 2005, 173 - 200.

[Kri07]   Kristo, E., Biliaderis, C. G., Zampraka, A.: Water vapour barrier and tensile properties of composite caseinate-pullulan films: Biopolymer composition effects and impact of beeswax lamination, Food Chemistry, 101 (2007) 2, 753-764.

[Kua13]   Kuan, Y.-H., Bhat, R., Patras, A., Karim, A. A.: Radiation processing of food proteins – A review on the recent developments, Trends in Food Science & Technology, 30 (2013) 2, 105-120.

[Kum03]   Kumar, N., Nath, R.: Ferroelectric polarization switching in KNO3: PVDF films, Journal of Physics D-Applied Physics, 36 (2003) 11, 1308-1313.

[Küt05]   Kütemeyer, C., Froeck, M., Werlein, H. D., Watkinson, B. M.: The influence of salts and temperature on enzymatic activity of microbial transglutaminase, Food Control, 16 (2005) 8, 735-737.

[Lab08]   Laberge, M.: Enzymes, in: Biochemistry, Chelsea House - Infobase Publishing, New York, USA, 2008, 30 – 39.

[Lae70]   Laemmli, U. K.: Cleavage of structural proteins during assembly of head of bacteriophage-T4, Nature, 227 (1970) 5259, 680-685.

[Laf09]   Lafisco, M., Marchetti, M., Gómez Morales, J., Hernández-Hernández, M. a. A., García Ruiz, J. M., Roveri, N.: Silica Gel Template for Calcium Phosphates Crystallization, Crystal Growth & Design, 9 (2009) 11, 4912-4921.

[Lam03]   Lambuth, A. L.: Protein adhesives for wood, in: Handbook of adhesive technology, 2nd ed., edited by Pizzi, A., Mittal, K. L., Marcel Dekker, Inc., New York, USA, 2003, 457.

[Lan12]   Landratsamt Fürstenfeldbruck: Düngung im Haus- und Kleingarten (2012) www.garten-ffb.de/PDF/duengung.pdf, 5th Feb. 2013.

[Lee89]   van der Leeden, M., van Rosmalen, G., de Vreugd, K., Witkamp, G.: Einfluss von Additiven und Verunreinigungen auf Kristallisationsprozesse, Chemie Ingenieur Technik 61 (1989) 5, 385-395.

[Les03]   Leskovac, V.: Steady state kinetics of bisubstrate reactions, in: Comprehensive enzyme kinetics, edited by Leskovac, V., Kluwer Academic / Plenum Publishers, New York, USA, 2003, 139-169.

[Lic04]   Li-Chan, E. C. Y.: Properties of proteins in food systems: an introduction, in: Proteins in food processing, editied by: Yada, R. Y., CRC Press, Boca Raton, FL, USA, 2004, 2-26.

[Lim99]   Lim, L.-T., Mine, Y., Tung, M. A.: Barrier and Tensile Properties of Transglutaminase Cross-linked Gelatin Films as Affected by Relative Humidity, Temperature, and Glycerol Content, Journal of Food Science, 64 (1999) 4, 616-622.

[Lin06]   Lin, C.-C., Metters, A. T.: Hydrogels in controlled release formulations: Network design and mathematical modeling, Advanced Drug Delivery Reviews, 58 (2006) 12–13, 1379-1408.

[Lin07]   Lin, D., Zhao, Y.: Innovations in the Development and Application of Edible Coatings for Fresh and Minimally Processed Fruits and Vegetables, Comprehensive Reviews in Food Science and Food Safety, 6 (2007) 3, 60-75.

[Llo12]   Llorens, A., Lloret, E., Picouet, P. A., Trbojevich, R., Fernandez, A.: Metallic-based micro and nanocomposites in food contact materials and active food packaging, Trends in Food Science & Technology, 24 (2012) 1, 19-29.

[Lo08]   Lo, S. F., Hayter, M., Chang, C. J., Hu, W. Y., Lee, L. L.: A systematic review of silver-releasing dressings in the management of infected chronic wounds, Journal of Clinical Nursing, 17 (2008) 15, 1973-85.

[Lor09]   Lorber, B., Sauter, C., Theobald-Dietrich, A., Moreno, A., Schellenberger, P., Robert, M. C., Capelle, B., Sanglier, S., Potier, N., Giege, R.: Crystal growth of proteins, nucleic acids, and viruses in gels, Progress in Biophysics & Molecular Biology, 101 (2009) 1-3, 13-25.

[Lu03]   Lu, S. Y., Zhou, N. D., Tian, Y. P., Li, H. Z., Chen, J.: Purification and properties of transglutaminase from Streptoverticillium mobaraense, Journal of Food Biochemistry, 27 (2003) 2, 109-125.

[Lus10]   Lustosa, B. H. B., Leonel, M.: Development of instant blends of cassava flour and casein: effect of protein contents and extrusion parameters on viscosity, Ciencia E Tecnologia De Alimentos, 30 (2010) 3, 693-699.

[Lyo12]   Hydrogel micro and nanoparticles, edited by: Lyon, L. A., Serpe, M. J., Wiley-VCH, Weinheim, Germany, 2012.

[Maa13]   Maathuis, F. J. M., Diatloff, E.: Roles and functions of plant nutrients, in: Plant mineral nutrients – Methods and protocols, edited by: Maathuis, F. J. M., Humana Press, New York, USA, 2013, 1 – 22.

[Mac11]   Macierzanka, A., Bordron, F., Rigby, N. M., Mills, E. N. C., Lille, M., Poutanen, K., Mackie, A. R.: Transglutaminase cross-linking kinetics of sodium caseinate is changed after emulsification, Food Hydrocolloids, 25 (2011) 5, 843-850.

[Mád98]   Mádi, A., Punyiczki, M., di Rao, M., Piacentini, M., Fésüs, L.: Biochemical characterization and localization of transglutaminase in wild-type and cell-death mutants of the nematode Caenorhabditis elegans, European Journal of Biochemistry, 253 (1998) 3, 583-590.

[Mag98]   Mager Stellmann, J., Osinsky, D., Markkanen, P.: Glycol ethers, in: Encyclopaedia of accupational health and safety, Vol. 4, edited by Mager Stellmann, J., International Labour Office, International Labour Organization, Genf, 1998, 194-201.

[Mar04]   Marcilla, A., Beltrán: Mechanisms of plastizicers action, in: Handbook of plastizicers, edited by: Wypych, G., William Andrew Publishing, Toronto, Canada, 2004, 107-120.

[Mar08]   Marx, C. K., Hertel, T. C., Pietzsch, M.: Random mutagenesis of a recombinant microbial transglutaminase for the generation of thermostable and heat-sensitive variants, Journal of Biotechnology, 136 (2008) 3-4, 156-162.

[Mar11]   Martin-Closas, L., Pelacho, A.: Agronomic potential of biopolymer films, in: Biopolymers: new materials for sustainable films and coatings, edited by: Plackett, D., John Wiley & Sons, Chichester, UK, 2011, 277-299.

[Mas12]   Massard, C., Bernard, L., Cueff, R., Raspal, V., Feschet-Chassot, E., Sibaud, Y., Sautou, V., Awitor, K. O.: Photopolymerizable hybrid sol gel coating as a barrier against plasticizer release, Progress in Organic Coatings, 75 (2012) 1–2, 116-123.

[Mat00]   Matveev, Y. I., Grinberg, V. Y., Tolstoguzov, V. B.: The plasticizing effect of water on proteins, polysaccharides and their mixtures. Glassy state of biopolymers, food and seeds, Food Hydrocolloids, 14 (2000) 5, 425-437.

[McC65]   McCrone, W. C.: Polymorphism, in: Physics and chemistry of the organic solid state, 2nd volume, edited by: Fox, D., Labes, M. M., Weissberger, A., Interscience, New York, USA, 1965, 726-767.

[McC74]   McCauley, J. W., Roy, R.: Controlled nucleation and crystal growth of various $CaCO_3$ phases by silica-gel technique, American Mineralogist, 59 (1974) 9-10, 947-963.

[McD01]   McDonald, A. J. S., Standing, D. B.: Nutrient Acquisition, Assimilation and Utilization, in: eLS, John Wiley & Sons, 2001.

[McD04]   McDermott, M. K., Chen, T. H., Williams, C. M., Markley, K. M., Payne, G. F.: Mechanical properties of biomimetic tissue adhesive based on the microbial transglutaminase-catalyzed crosslinking of gelatin, Biomacromolecules, 5 (2004) 4, 1270-1279.

[Mee02]   Meenan, P. A., Anderson, S. R., Klug D. L.: The influence of impurities and solvents on crystallization, in: Handbook of industrial crystallization, 2nd ed., edited by Myerson, A. S., Butterworth-Heinemann, Woburn (MA), USA, 2002, 67.

[Mei99]   Meier, F., Schiewe, B., Esker, A., Wegner, G.: Sorption and swelling in ultra-thin polymer films, Macromol. Symp., 145 (1999) 161-168.

[Men10]   Mendes de Souza, P., Fernández, A., López-Carballo, G., Gavara, R., Hernández-Muñoz, P.: Modified sodium caseinate films as releasing carriers of lysozyme, Food Hydrocolloids, 24 (2010) 4, 300-306.

[Mer04]   Mersmann, A.: Stoffdaten, in: GVT Hochschulkurs Kristallisation - Grundlagen, Anwendung und Forschung, edited by Kind, M., Ulrich, J., Karlsruhe, Germany, 2004.

[Mic13]   Michaelis, L., Menten, M. L.: Die Kinetik der Invertinwirkung, Biochem. Z. 49 (1913), 333−369.

[Mik94]   Mikkelsen, R. L.: Using hydrophilic polymers to control nutrient release, Fertilizer research, 38 (1994) 1, 53-59.

[Mil03]   Miller-Chou, B. A., Koenig, J. L.: A review of polymer dissolution, Progress in Polymer Science, 28 (2003) 8, 1223-1270.

[Mis04]   Mishra, S., Bajpai, J., Bajpai, A. K.: Evaluation of the water sorption and controlled-release potential of binary polymeric beads of starch and alginate loaded with potassium nitrate as an agrochemical, Journal of Applied Polymer Science, 94 (2004) 4, 1815-1826.

[Mit09]   Mitrus, M., Wojtowicz, A., and Moscicki, L.: Biodegradable polymers and their practical utility, in: Thermoplastic starch, edited by: Janssen, L., Moscicki, L., Wiley-VCH, Weinheim, Germany, 2009, 3-34.

[Moh05]   Mohanty, A. K., Tummala, P., Liu, W., Misra, M., Mulukutla, P. V., Drzal, L. T.: Injection Molded Biocomposites from Soy Protein Based Bioplastic and Short Industrial Hemp Fiber, Journal of Polymers and the Environment, 13 (2005) 3, 279-285.

[Moj13]   Mojallal-Tabatabei, Z., Asoodeh, A., Housaindokht, M. R. and Chamani, J.: Purification and biochemical characterization of angiotensin I-converting enzyme (ACE) from ostrich lung: The effect of 2,2,2-trifluoroethanol on ACE conformation and activity, Process Biochemistry, 48 (2013) 7, 1091-1098.

[Mor01]   Morot-Gaudry, J.-F.: Nitrogen assimilation by plants: physiological, biochemical and molecular aspects, Science Publishers, Enfield, NH, USA, 2001.

[Mor10]   Moreno, H. M., Carballo, J., Borderías, J.: Gelation of fish muscle using microbial transglutaminase and the effect of sodium chloride an pH levels, Journal of Muscle Foods, 21 (2010) 3, 433-450.

[Mug93]   Muga, A., Arrondo, J. L., Bellon, T., Sancho, J., Bernabeu, C.: Structural and functional studies on the interaction of sodium dodecyl sulfate with beta-galactosidase, Arch Biochem Biophys, 300 (1993) 1, 451-457.

[Mul01]   Mullin J. W.: Crystallization; 4th edition, Butterworth Heinemann, Oxford, UK, 2001.

[Mur90]   Murphy, J. M., Fox, P. F.: Functional properties of αs-κ- or β-rich casein fractions, Food Chemistry, 39 (1991) 2, 211-228.

[Mut10]   Mutch, N. J., Koikkalainen, J. S., Fraser, S. R., Duthie, K. M., Griffin, M., Mitchell, J., Watson, H. G., Booth, N. A.: Model thrombi formed under flow reveal the role of factor XIII-mediated cross-linking in resistance to fibrinolysis, Journal of Thrombosis and Haemostasis, 8 (2010) 9, 2017-2024.

[Mye02]   Myerson, A. S., Ginde, R.: Crystals, crystal growth and nucleation, in: Handbook of industrial crystallization, 2nd ed., edited by Myerson, A. S., Butterworth-Heinemann, Woburn (MA), USA, 2002, 61.

[Nan05]   Nandi, S., Winter, H. H.: Swelling behavior of partially cross-linked polymers: A ternary system, Macromolecules, 38 (2005) 10, 4447-4455.

[Nel05a]   Nelson, D. L., Cox, M. M.: Amino acids, peptides and proteins, in: Lehninger - Principles of biochemistry, 4th ed., W. H. Freeman and Company, New York, 2005, 75 – 115.

[Nel05b]   Nelson, D. L., Cox, M. M.: Enzymes, in: Lehninger - Principles of biochemistry, 4th ed., W. H. Freeman and Company, New York, 2005, 190 – 237.

[Nen06]   Nentwig, J.: Kunststoff-Folien: Herstellung – Eigenschaften – Anwendung, 3rd ed., Carl Hanser Verlag, Munich, Germany, 2006.

[New04]   Newton, J. M.: Drug release from capsules, in: Pharmaceutical capsules, 2nd ed., edited by: Podczeck, F., Jones, B.E., Pharmaceutical Press, London, UK, 2004, 213 – 238.

[Nim76]   Nimmo, J. K., Lucas, B. W.: The crystal structures of gamma-KNO_3 and beta-KNO_3 and alpha-gamma-beta phase transformations, Acta Crystallographica Section B-Structural Science, 32 (1976) JUL15, 1968-1971.

[Non89]   Nonaka, M., Tanaka, H., Okiyama, A., Motoki, M., Ando, H., Umeda, K., Matsuura, A.: Polymerization of several proteins by Ca^{2+}-independent transglutaminase derived from microorganisms, Agricultural and Biological Chemistry, 53 (1989) 10, 2619-2623.

[Noz99]   Nozawa, H., Mamegoshi, S., Seki, N.: Effect of neutral salts on activity and stability of transglutaminase from scallop adductor muscle, Comparative Biochemistry and Physiology B-Biochemistry & Molecular Biology, 124 (1999) 2, 181-186.

[Noz01]   Nozawa, H., Mori, T., Seki, N.: Different effects of NaCl on activities of transglutaminases from marine and freshwater shellfish muscles, Fisheries Science, 67 (2001) 2, 383-385.

[Noz05]   Nozawa, H., Mori, T., Kimura, M., Seki, N.: Characterization of a transglutaminase from scallop hemocyte and identification of its intracellular substrates, Comp Biochem Physiol B Biochem Mol Biol, 140 (2005) 3, 395-402.

[Nun11]   DiNunzio, J. C., McGinity, J. W.: Polymeric interactions with drugs and excipients, in: Polymeric materials: Medicinal and pharmaceutical applications (Volume 2), edited by Dumitriu, S., Popa, V., CRC Press, Boca Raton, FL, USA, 2011, 473-506.

[Nur13]   Nur Hanani, Z. A., McNamara, J., Roos, Y. H., Kerry, J. P.: Effect of plasticizer content on the functional properties of extruded gelatin-based composite films, Food Hydrocolloids, 31 (2013) 2, 264-269.

[Nyl96]   Nylén, P.: Fällungsanalyse (Gravimetrie) – Die Abhängigkeit der Löslichkeit vom pH-Wert, in: Einführung in die Stöchiometrie, 19th ed., edited by: Nylén, P., Wigren, N., Joppien, G., Steinkopff Verlag, Darmstadt, Germany, 1996, 178-185.

[Oga00]   Ogale, A. A., Cunningham, P., Dawson, P. L., Acton, J. C.: Viscoelastic, Thermal, and Microstructural Characterization of Soy Protein Isolate Films, Journal of Food Science, 65 (2000) 4, 672-679.

[Oh04]   Oh, J. H., Wang, B., Field, P. D., Aglan, H. A.: Characteristics of edible films made from dairy proteins and zein hydrolysate cross-linked with transglutaminase, International Journal of Food Science and Technology, 39 (2004) 3, 287-294.

[Ony10]   Onyango, C., Mutungi, C., Unbehend, G., Lindhauer, M. G.: Rheological and baking characteristics of batter and bread prepared from pregelatinised cassava starch and sorghum and modified using microbial transglutaminase, Journal of Food Engineering, 97 (2010) 4, 465-470.

[Orl02]   Orliac, O., Rouilly, A., Silvestre, F., Rigal, L.: Effects of additives on the mechanical properties, hydrophobicity and water uptake of thermo-moulded films produced from sunflower protein isolate, Polymer, 43 (2002) 20, 5417-5425.

[Pap12]   Papageorgiou, S. K., Katsaros, F. K., Favvas, E. P., Romanos, G. E., Athanasekou, C. P., Beltsios, K. G., Tzialla, O. I., Falaras, P.: Alginate fibers as photocatalyst immobilizing agents applied in hybrid photocatalytic/ultrafiltration water treatment processes, Water Research, 46 (2012) 6, 1858-1872.

[Par99]   Park, H. J.: Development of advanced edible coatings for fruits, Trends in Food Science & Technology, 10 (1999) 8, 254-260.

[Pat05]   Patel, M., Bastioli, C., Marini, L., Würdinger, E.: Life-cycle Assessment of Bio-based Polymers and Natural Fiber Composites, in: Biopolymers Online, Wiley-VCH, Weinheim, Germany, 2005.

[Pat10a]   Patzsch, K., Riedel, K., Pietzsch, M.: Parameter Optimization of Protein Film Production Using Microbial Transglutaminase, Biomacromolecules, 11 (2010) 4, 896-903.

[Pat10b]   Patzsch, K.: Untersuchungen zur Herstellung von Biokunststoffen durch enzymatische Vernetzung von Proteinen aus nachwachsenden

Rohstoffen, PhD thesis, Martin Luther University Halle-Wittenberg, Halle (Saale), Shaker Verlag, Aachen, Germany, 2010.

[Pel99]   Pellegrino, L., van Boekel, M. A. J. S., Gruppen, H., Resmini, P., Pagani, M. A.: Heat-induced aggregation and covalent linkages in β-casein model systems, International Dairy Journal, 9 (1999) 3–6, 255-260.

[Pel12]   Peles, Z., Zilberman, M.: Novel soy protein wound dressings with controlled antibiotic release: Mechanical and physical properties, Acta Biomaterialia, 8 (2012) 1, 209-217.

[Pep12]   Peppas, N. A., Slaughter, B. V., Kanzelberger, M. A.: Hydrogels, in: Polymer science: A comprehensive reference, edited by: M. Krzysztof and M. Martin, Elsevier, Amsterdam, The Netherlands, 2012, 385-395.

[Per99]   Perez-Gago, M. B., Nadaud, P., Krochta, J. M.: Water vapor permeability, solubility, and tensile properties of heat-denatured versus native whey protein films, Journal of Food Science, 64 (1999) 6, 1034-1037.

[Per11]   Pereda, M., Amica, G., Rácz, I., Marcovich, N. E.: Structure and properties of nanocomposite films based on sodium caseinate and nanocellulose fibers, Journal of Food Engineering, 103 (2011) 1, 76-83.

[Pla06]   Platt, D. F.: Agriculture and horticulture, in: Biodegradable polymers: market report, Smithers Rapra Limited, Shawbury, UK, 2006, 98.

[Pla08]   Plaster, E. J.: Soil fertility, in: Soil science and management, 5th ed., edited by: Plaster, E. J., Delmar Cengage Learning, 2009, 209.

[Pom05]   Pommet, M., Redl, A., Guilbert, S., Morel, M.-H.: Intrinsic influence of various plasticizers on functional properties and reactivity of wheat gluten thermoplastic materials, Journal of Cereal Science, 42 (2005) 1, 81-91.

[Pop11]   Popović, S., Peričin, D., Vaštag, Ž., Popović, L., Lazić, V.: Evaluation of edible film-forming ability of pumpkin oil cake; effect of pH and temperature, Food Hydrocolloids, 25 (2011) 3, 470-476.

[Por11]   Porta, R., Mariniello, L., Di Pierro, P., Sorrentino, A., Giosafatto, C. V. L.: Transglutaminase Crosslinked Pectin- and Chitosan-based Edible Films: A Review, Critical Reviews in Food Science and Nutrition, 51 (2011) 3, 223-238.

[Pos12]   Post, A. E., Arnold, B., Weiss, J., Hinrichs, J.: Effect of temperature and pH on the solubility of caseins: Environmental influences on the dissociation of αS- and β-casein, Journal of Dairy Science, 95 (2012) 4, 1603-1616.

[Pra09]   Prabhu, C., Wanjari, S., Gawande, S., Das, S., Labhsetwar, N., Kotwal, S., Puri, A. K., Satyanarayana, T., Rayalu, S.: Immobilization of carbonic anhydrase enriched microorganism on biopolymer based materials, Journal of Molecular Catalysis B: Enzymatic, 60 (2009) 1–2, 13-21.

[Pro09]   Fact sheet on bioplastics, Pro Europe – Packaging Recovery Organization s.p.r.l., online version last updated on March 2009, accessed on 30th June 2013.

[Pru06]   Prud´Homme, M., Krukowski, S. T.: Potash, in: Industrial minerals and rocks: commodities, markets and users, 7th ed., edited by: Kogel, J. E., Trivedi, N. C., Barker, J. M., Krukowski, S. T., Society for Mining, metallurgy and exploration (SME), Littleton, CO, USA, 2006, 736.

[Que87]   Queen, D., Gaylor, J. D., Evans, J. H., Courtney, J. M., Reid, W. H.: The preclinical evaluation of the water vapour transmission rate through burn wound dressings, Biomaterials, 8 (1987) 5, 367-71.

[Rai11]   Rai, R. N., Mudunuri, S. R., Reddi, R. S. B., Satuluri, V., Ganeshmoorthy, S., Gupta, P. K.: Crystal growth and nonlinear optical studies of m-dinitrobenzene doped urea, Journal of Crystal Growth, 321 (2011) 1, 72-77.

[Rap65]   Rapoport, E., Kennedy, G. C.: Phase diagram of KNO_3 to 40 kbars, Journal of Physics and Chemistry of Solids, 26 (1965) 12, 1995-1997.

[Red96]   Redl, A., Gontard, N., Guilbert, S.: Determination of Sorbic Acid Diffusivity in Edible Wheat Gluten and Lipid Based Films, Journal of Food Science, 61 (1996) 1, 116-120.

[Red06]   Reddy, T. T., Lavenant, L., Lefebvre, J., Renard, D.: Swelling behavior and controlled release of theophylline and sulfamethoxazole drugs in beta-lactoglobulin protein gels obtained by phase separation in water/ethanol mixture, Biomacromolecules, 7 (2006) 1, 323-330.

[Rhi00]   Rhim, J. W., Gennadios, A., Handa, A., Weller, C. L., Hanna, M. A.: Solubility, Tensile, and Color Properties of Modified Soy Protein Isolate Films, Journal of Agricultural and Food Chemistry, 48 (2000) 10, 4937-4941.

[Ric03]   Richter, G.: Praktische Biochemie – Grundlagen und Techniken, Georg Thieme Verlag, Stuttgart, 2003.

[Rie13]   Riedel, K.: Kovalente Modifikationen von Proteinen aus nachwachsenden Rohstoffen zur Optimierung von Filmeigenschaften, PhD thesis, Center of Engineering Sciences, Martin Luther University Halle-Wittenberg, Halle (Saale), 2013.

[Riv09]   Rivero, S., García, M. A., Pinotti, A.: Composite and bi-layer films based on gelatin and chitosan, Journal of Food Engineering, 90 (2009) 4, 531-539.

[Rob10]   Robertson, G. L.: Food packaging and shelf life: a practical guide, CRC Press, Boca Raton, FL, USA, 2010.

[Roj07]   Rojas-Graü, M. A., Raybaudi-Massilia, R. M., Soliva-Fortuny, R. C., Avena-Bustillos, R. J., McHugh, T. H., Martín-Belloso, O.: Apple puree-alginate edible coating as carrier of antimicrobial agents to prolong shelf-life of fresh-cut apples, Postharvest Biology and Technology, 45 (2007) 2, 254-264.

[Roj09]   Rojas-Graü, M. A., Oms-Oliu, G., Soliva-Fortuny, R., Martín-Belloso, O.: The use of packaging techniques to maintain freshness in fresh-cut fruits and vegetables: a review, International Journal of Food Science & Technology, 44 (2009) 5, 875-889.

[Rol97]   Rolfs, J., Lacmann, R., Kipp, S.: Crystallization of potassium nitrate (KNO3) in aqueous solution I. Growth kinetics of the pure system, Journal of Crystal Growth, 171 (1997) 1-2, 174-182.

[Rom12]   Rombouts, I., Lagrain, B., Delcour, J. A.: Heat-Induced Cross-Linking
            and Degradation of Wheat Gluten, Serum Albumin, and Mixtures
            Thereof, Journal of Agricultural and Food Chemistry, 60 (2012) 40,
            10133-10140.

[Rot12]   Material safety data sheet, Dodecan-1-Sulfonsäure Natriumsalz, article
            no. KK52, Carl Roth, Germany, 2012.

[Roy08]   Roylance, D.: Mechanical properties of materials, Massachusetts
            Institute of Technology, 2008.

[Sab01]   Sabato, S. F., Ouattara, B., Yu, H., D'Aprano, G., Le Tien, C.,
            Mateescu, M. A., Lacroix, M.: Mechanical and Barrier Properties of
            Cross-Linked Soy and Whey Protein Based Films, Journal of
            Agricultural and Food Chemistry, 49 (2001) 3, 1397-1403.

[Sah06]   Sahin, S., Sumnu, S. G.: Water activity and sorption properties of foods,
            in: Physical properties of foods, edited by: Sahin, S., Sumnu, S. G.,
            Springer Science + Business Media, New York, USA, 2006, 193-228.

[Sal91]   Salem, N., Vigna Guidi, G., Pini, R., Khater, A.: Quality of irrigation
            waters and water uptake of a polyacrylamide hydrogel, Agrochimica, 35
            (1991) 149-160.

[Sal11]   Salgado, P. R., Fernandez, G. B., Drago, S. R., Mauri, A. N.: Addition of
            bovine plasma hydrolysates improves the antioxidant properties of
            soybean and sunflower protein-based films, Food Hydrocolloids, 25
            (2011) 6, 1433-1440.

[San07]   Sangwal, K.: Effect of impurities on crystal growth kinetics, in: Additives
            and crystallization processes, edited by: Sangwal, K., Wiley, Chichester,
            West Sussex, England, 2007, 160.

[San10]   Sanchez-Garcia, M. D., Lopez-Rubio, A., Lagaron, J. M.: Natural micro
            and nanobiocomposites with enhanced barrier properties and novel
            functionalities for food biopackaging applications, Trends in Food
            Science & Technology, 21 (2010) 11, 528-536.

[Sch88]   Schaffer, W. J., Mikkola, D. E.: Phase stability of ferroelectric KNO$_3$ switching devices during polarization aging, Journal of Applied Physics, 64 (1988) 5, 2563-2570.

[Sch06]   Schubert, S.: Pflanzenernährung, Verlag Eugen Ulmer, Stuttgart, Germany, 2006.

[Sch11]   Schellenberger, P., Demangeat, G., Lemaire, O., Ritzenthaler, C., Bergdoll, M., Oliéric, V., Sauter, C., Lorber, B.: Strategies for the crystallization of viruses: Using phase diagrams and gels to produce 3D crystals of Grapevine fanleaf virus, Journal of Structural Biology, 174 (2011) 2, 344-351.

[Sco87]   Scott, J. F., Zhang, M., Godfrey, R. B., Araujo, C., McMillan, L.: Raman spectroscopy of submicron KNO3 films, Phys Rev B Condens Matter, 35 (1987) 8, 4044-4051.

[Sco02]   Scott, G., Wiles, D. M.: Degradable hydrocarbon polymers in waste and litter control, in: Degradable polymers: principles and applications, edited by: Scott, G., 2nd ed., Kluwer Academic Publishers, Dordrecht, The Netherlands, 2002, 449 - 480.

[Seg02]   Seguro, K.: Transglutaminase, in: Encyclopedia of bioprocess technology – Fermentation, biocatalysis and bioseparation, Wiley, New York, USA, 2002.

[Sei91]   Seitz, J., Keppler, C., Hüntemann, S., Rausch, U., Aumüller, G.: Purification and molecular characterization of a secretory transglutarninase from coagulating gland of the rat, Biochimica et Biophysica Acta (BBA) - Protein Structure and Molecular Enzymology, 1078 (1991) 2, 139-146.

[Sie99]   Siew, D. C. W., Heilmann, C., Easteal, A. J., Cooney, R. P.: Solution and film properties of sodium caseinate/glycerol and sodium caseinate/polyethylene glycol edible coating systems, Journal of Agricultural and Food Chemistry, 47 (1999) 8, 3432-3440.

[Sie12]   Siepmann, J., Siepmann, F.: Swelling controlled drug delivery systems, in: Fundamentals and applications of controlled release drug delivery,

edited by Siepmann, J., Siegel, R. A., Rathbone, M. J., Springer, New York, USA, 2012, 153-170.

[Sin08]   Singh, N., Blackburn, W. H., Lyon, A.: Bioconjugation of soft nanomaterials, in: Biomedical nanostructures, edited by: Gonsalves, K., Halberstadt, C., Laurencin, C. T., Nair, L. S., John Wiley & Sons, Hoboken, NJ, USA, 2008, 61 – 92.

[Sin09]   Sinkevičienė, A., Jodaugienė, D., Pupalienė, R., Urbonienė, M.: The influence of organic mulches on soil properties and crop yield, Agronomy Research, 7 (2009) special issue 1, 485-491.

[Sko07]   Skoog, D A., Holler, F. J., Crouch, S R.: Principles of Instrumental Analysis, 6th ed., Thomson Brooks, Cole, USA, 2007.

[Smi91]   Smith, J. D., Harrison, H. C.: Evaluation of polymers for controlled-release properties when incorporated with nitrogen fertilizer solutions, Communications in Soil Science and Plant Analysis, 22 (1991) 5-6, 559-573.

[Soa11]   Soazo, M., Rubiolo, A. C., Verdini, R. A.: Effect of drying temperature and beeswax content on moisture isotherms of whey protein emulsion film, Procedia Food Science, 1 (2011) 0, 210-215.

[Soh06]   Sohail, S. S., Wang, B., Biswas, M. A. S., Oh, J.-H.: Physical, Morphological, and Barrier Properties of Edible Casein Films with Wax Applications, Journal of Food Science, 71 (2006) 4, C255-C259.

[Son07]   Soni, S K., Soni, R.: Introduction and fundamentals of microbiology - Microorganisms as biogeochemical agents, in: Microbes: a source of energy for the 21st century, edited by Soni, S. K., New India Publishing, New Dehli, India, 2007, p. 140.

[Son10]   Song, F., Zhang, L.-M., Shi, J.-F., Li, N.-N.: Novel casein hydrogels: Formation, structure and controlled drug release, Colloids and Surfaces B: Biointerfaces, 79 (2010) 1, 142-148.

[Son11]   Song, F., Tang, D.-L., Wang, X.-L., Wang, Y.-Z.: Biodegradable Soy Protein Isolate-Based Materials: A Review, Biomacromolecules, 12 (2011) 10, 3369-3380.

[Sou85]   Southward, C. R.: Manufacture and applications of edible casein products. I. Manufacture and properties, New Zealand Journal of Dairy Science and Technology, 20 (1985) 79-101.

[Sta07]   StatSoft, Inc., STATISTICA (data analysis software system), version 8.0, Tulsa, OK, USA, www.statsoft.com, 2007.

[Sta11a]   Stanescu, V.-N., Olteanu, M., Florea-Spiroiu, M., Pincu, E., Meltzer, V.: Starch/chitosan film forming hydrogel, Rev. Roum. Chim., 56 (2011) 8, 827-832.

[Sta11b]   Stadtwerke Gelnhausen GmbH: Stickstoffdüngung im Nutzgarten (2011) www.wasserschutzgebiet-hailerer-aue.de/download/ garten_flyer_stickstoffduengung_2011.pdf, 5th Feb. 2013.

[Sta13]   Stangierski, J., Zabielski, J., Grześ, B.: Modification of functional quality of raw myofibril preparation obtained from water-washed mechanically recovered chicken meat, European Food Research and Technology, 236 (2013) 3, 449-458.

[Sto10]   Stolte, I., Frohberg, P., Pietzsch, M., Ulrich, J.: Biodegradable Polymers – From Protein to Sustainability, poster, Projekttag Stoffliche Biomassenutzung, Bundesministerium für Ernährung, Landwirtschaft und Verbraucherschutz, Berlin, 15.12.2010.

[Sto11]   Stolte, I., Frohberg, P., Pietzsch, M., Ulrich, J.: Crystals in protein films: What are they good for?, Abstract, ISIC 18 – 18th International Symposium on Industrial Crystallization, Zürich, Switzerland, 13 – 16th September 2011.

[Sto12a]   Stolte, I., Frohberg, P., Pietzsch, M., Ulrich, J.: Crystals in protein films: What are they good for?, Chemical Engineering Science, 77 (2012), 196-200.

[Sto12b]   Stolte, I., Frohberg, P., Pietzsch, M., Ulrich, J.: Protein and beyond: material development using inner-film crystallized additives, Extended abstract, 15th International Conference „Polymeric Materials", Halle (Saale), 12 – 14th September 2012.

[Sto12c]   Stolte, I., Frohberg, P., Pietzsch, M., Ulrich, J., Protein and beyond: material development using inner-film crystallized additives, Poster, 15th International Conference „Polymeric Materials", Halle (Saale), 12 – 14th September 2012.

[Str12]   Strobel, L. A., Rath, S. N., Maier, A. K., Beier, J. P., Arkudas, A., Greil, P., Horch, R. E., Kneser, U.: Induction of bone formation in biphasic calcium phosphate scaffolds by bone morphogenetic protein-2 and primary osteoblasts, Journal of Tissue Engineering and Regenerative Medicine, 97A (2012) 2, 177-185.

[Stu94]   Stuchell, Y. M., Krochta, J. M.: Enzymatic Treatments and Thermal Effects on Edible Soy Protein Films, Journal of Food Science, 59 (1994) 6, 1332-1337.

[Suz97]   Suzuki, Y., Tanihara, M., Nishimura, Y., Suzuki, K., Kakimaru, Y., Shimizu, Y.: A novel wound dressing with an antibiotic delivery system stimulated by microbial infection, ASAIO J, 43 (1997) 5, M854-7.

[Sze94]   Szpendowski, J., Śmietana, Z., Chojnowski, W., Świgoń, J.: Modification of the structure of casein preparations in the course of extrusion, Food / Nahrung, 38 (1994) 3, 253-258.

[Tab10]   Tabone, M. D., Cregg, J. J., Beckman, E. J., Landis, A. E.: Sustainability Metrics: Life Cycle Assessment and Green Design in Polymers, Environmental Science & Technology, 44 (2010) 21, 8264-8269.

[Tak86]   Takagi, J., Saito, Y., Kikuchi, T., Inada, Y.: Modification of transglutaminase assay: use of ammonium sulfate to stop the reaction, Anal Biochem, 153 (1986) 2, 295-298.

[Tan05]   Tang, C. H., Yang, X. Q., Chen, Z., Wu, H., Peng, Z. Y.: Physicochemical and structural characteristics of sodium caseinate biopolymers induced by microbial transglutaminase, Journal of Food Biochemistry, 29 (2005) 4, 402-421.

[Tap05]   Tapia-Blacido, D., Sobral, P. J., Menegalli, F. C.: Effects of drying temperature and relative humidity on the mechanical properties of

amaranth flour films plasticized with glycerol, Brazilian Journal of Chemical Engineering, 22 (2005) 2, 249-256.

[Teo73]   Teot, A. S.: Crystal habit modification of inorganic salts using polymeric sulfonates or sulfates, US 3770390, United States Patent Office, patented Nov. 6, 1973.

[Tha09]   Thatiparti, T. R., Kano, A., Maruyama, A., Takahara, A.: Novel silver-loaded semi-interpenetrating polymer network gel films with antibacterial activity, Journal of Polymer Science Part A: Polymer Chemistry, 47 (2009) 19, 4950-4962.

[Thr03]   Threlfall, T.: Structural and Thermodynamic Explanations of Ostwald's Rule, Organic Process Research & Development, 7 (2003) 6, 1017-1027.

[Thr08]   Throne, T. L.: Part design, in: Understanding thermoforming, 2nd ed., Carl Hanser Verlag, Munich, Germany, 2008.

[Tit03]   Titiz-Sargut, S., Ulrich, J. Application of a protected ultrasound sensor for the determination of the width of the metastable zone, Chemical Engineering and Processing: Process Intensification, 42 (2003) 11, 841-846.

[Tok91]   Tokita, M., Tanaka, T.: Friction coefficient of polymer networks of gels, Journal of Chemical Physics, 95 (1991) 6, 4613-4619.

[Ueb68]   Ueberreiter K.: The solution process, in: Diffusion in polymers, edited by: Crank, J., Park, G. S., Academic Press, New York, USA, 1968, 219 – 257.

[Uek96]   Ueki, S., Takagi, J., Saito, Y.: Dual functions of transglutaminase in novel cell adhesion, Journal of Cell Science, 109 (1996), 2727-2735.

[Ugr07]   Ugrozov, V. V., Filippov, A. N., Sidorenko, Y. I.: Theoretical description of the hygroscopicity of hydrophilic biopolymers and their mixtures, Colloid Journal, 69 (2007) 2, 232-236.

[Ulr04]   Ulrich, J.: Fremdstoffbeeinflussung in der Kristallisation, in: Kristallisation in der industriellen Praxis, edited by: Hofmann, G., Wiley-VCH Verlag, Weinheim, Germany, 2004, 131-148.

[Ulr11]   Ulrich, J., Stelzer, T.: Crystallization, in: Kirk-Othmer Encyclopedia of Chemical Technology, John Wiley & Sons, Inc., Hoboken, NJ, USA, 2011.

[Uni98]   United Nations Industrial Development Organization (UNIDO) and International Fertilizer Development Center (IFDC): Fertilizer raw materials and reserves, in: Fertilizer manual, Kluwer Academic Publishers, Dordrecht, The Netherlands, 1998, 147.

[uniprot]   Protein Knowlegdebase, Universal Protein Resource (UniProt), database, www.uniport.org, entry: casein from *Bos Taurus*, 3rd march 2013.

[Van84]   Van den Berg, C.: Description of water activity of foods for engineering purposes by means of the GAB model of sorption, in: Engineering and foods, edited by: McKenna, B. M., Elsevier, London, UK, 1984, 311-321.

[Ver10]   Verbeek, C. J. R., van den Berg, L. E.: Extrusion Processing and Properties of Protein-Based Thermoplastics, Macromolecular Materials and Engineering, 295 (2010) 1, 10-21.

[VerpackV09]   Verordnung über die Vermeidung und Verwertung von Verpackungsabfällen (Verpackungsverordnung - VerpackV), issued by the government of the Federal Republic of Germany, first issued: 21st August 1998, last updated: 24th February 2012.

[Vie09]   Vieira, R. P., Fernandes, A. R., Kaneko, T. M., Consiglieri, V. O., Pinto, C., Pereira, C. S. C., Baby, A. R., Velasco, M. V. R.: Physical and physicochemical stability evaluation of cosmetic formulations containing soybean extract fermented by Bifidobacterium animalis, Brazilian Journal of Pharmaceutical Sciences, 45 (2009) 3, 515-525.

[Vie11]   Vieira, M. G. A., da Silva, M. A., dos Santos, L. O., Beppu, M. M.: Natural-based plasticizers and biopolymer films: A review, European Polymer Journal, 47 (2011) 3, 254-263.

[Vil11]   Vila, M., Sánchez-Salcedo, S., Cicuéndez, M., Izquierdo-Barba, I., Vallet-Regí, M.: Novel biopolymer-coated hydroxyapatite foams for removing heavy-metals from polluted water, Journal of Hazardous Materials, 192 (2011) 1, 71-77.

[Vin04]   Vingerhoeds, M., Harmsen, P. F. H.: Proteins: versatile materials for encapsulation, in: Fundamentals of Cell Immobilisation Biotechnology, Part I, 1st ed., edited by Nedovic, V., Willaert, R., Kluwer Academic Publishers, Dordrecht, The Netherlands, 2004, 73 – 102.

[Vir00]   Viroben, G., Barbot, J., Mouloungui, Z., Gueguen, J.: Preparation and characterization of films from pea protein, Journal of Agricultural and Food Chemistry, 48 (2000) 4, 1064-1069.

[Vla01]   Vlachou, M., Naseef, H., Efentakis, M., Tarantili, P. A., Andreopoulos, A. G.: Swelling Properties of Various Polymers Used in Controlled Release Systems, Journal of Biomaterials Applications, 16 (2001) 2, 125-138.

[Voe11]   Voet, D., Voet, J. G.: Mechanisms of enzyme action, in: Biochemistry, 4th ed., edited by: Voet, D., Voet, J. G., John Wiley & Sons, Inc., Hoboken, NJ, USA, 2011, 467 – 556.

[Wal02]   Walsh, G.: Proteins - Biochemistry and biotechnology, Wiley, Chichester, UK, 2002.

[Wan08]   Wang, J. Q., Wu, W. H., Lin, Z. H.: Kinetics and thermodynamics of the water sorption of 2-hydroxyethyl methacrylate/styrene copolymer hydrogels, Journal of Applied Polymer Science, 109 (2008) 5, 3018-3023.

[Wan09]   Wang, N., Ruan, C., Yu, Y., Zheng, Y., Yu, J.: Composition and structure of acrylonitrile based casein fibers, Chemical Fibers International, 59 (2009) 2, 88-89.

[Wan10]   Wang, H., Song, H.-R., Chen, X.-S., Deng, Y.-J.: Release of ibuprofen from PEG-PLLA electrospun fibers containing poly(ethylene glycol)-β - poly(α-hydroxy octanoic acid) as an additive, Chinese Journal of Polymer Science, 28 (2010) 3, 417-425.

[Wel98]   Weller, C. L., Gennadios, A., Saraiva, R. A.: Edible bilayer films from zein and grain sorghum wax or carnauba wax, Food Science and Technology-Lebensmittel-Wissenschaft & Technologie, 31 (1998) 3, 279-285.

[Wet48]   Whetstone, J.: Solid solution formation between ammonium nitrate and potassium nitrate, Canadian Journal of Research Section B-Chemical Sciences, 26 (1948) 6, 499-502.

[Wey02]   Wey, J. S., Karpinski, P H.: Batch crystallization, in: Handbook of industrial crystallization, edited by Myerson, A. S., 2nd ed., Butterworth-Heinemann, Woburn, MA, USA, 2002.

[Whi05]   Whitford, D.: Proteins – Structure and function, Wiley, Chichester, UK, 2005.

[Wid60]   Widdowson, F. V., Shaw, K.: Comparisons of casein and formalized casein with ammonium sulphate, calcium nitrate and urea for Italian ryegrass, The Journal of Agricultural Science, 55 (1960) 01, 53-59.

[Wie13]   Wieckhausen, Dierk: Development of batch crystallizations, in: Crystallization: Basic concepts and industrial applications, edited by Beckmann, W., Wiley-VCH, Weinheim, 2013, 187-202.

[Wih13]   Wihodo, M., Moraru, C. I.: Physical and chemical methods used to enhance the structure and mechanical properties of protein films: A review, Journal of Food Engineering, 114 (2013) 3, 292-302.

[Wit12]   Wittaya, Th.: Protein-based edible films: Characteristics and improvement of properties, in: Structure and function of food engineering, edited by: Eissa, A. A., InTech, Rjieka, Croatia, 2012.

[Wol13]   Wolfram Alpha LLC, WolframAlpha computational knowledge engine (2013) www.wolframalpha.com, entry "casein", 5th Feb. 2013.

[Wor05]   Worratao, A., Yongsawatdigul, J.: Purification and characterization of transglutaminase from Tropical tilapia (*Oreochromis niloticus*), Food Chemistry, 93 (2005) 4, 651-658.

[Wu08]   Wu, H. B., Chan, C. K. Effects of potassium nitrate on the solid phase transitions of ammonium nitrate particles, Atmospheric Environment, 42 (2008) 2, 313-322.

[Wwe12]   aid infodienst Ernährung, Landwirtschaft, Verbraucherschutz e. V.: Düngung mit Kompost (2012) www.was-wir-essen.de/hobby gaertner/rund_um_den_garten_duengung_kompost.php, 5th Feb. 2013.

[Yil98]   Yildirim, M., Hettiarachchy, N. S. Properties of films produced by cross-linking whey proteins and 11S globulin using transglutaminase, Journal of Food Science, 63 (1998) 2, 248-252.

[Yok04]   Yokoyama, K., Nio, N., Kikuchi, Y.: Properties and applications of microbial transglutaminase, Applied Microbiology and Biotechnology, V64 (2004) 4, 447-454.

[Yua07]   Yuan, J.-S., Fan, J.: Influence of additives on the crystallization habit of potassium nitrate, Journal of Synthetic Crystals, 36 (2007) 4, 853-858.

[Yuc11]   Yucel, U., Coupland, J. N.: Ultrasonic Characterization of Lactose Crystallization in Gelatin Gels, Journal of Food Science, 76 (2011) 1, E48-E54.

[Zem07]   Zema, L., Maroni, A., Foppoli, A., Palugan, L., Sangalli, M. E., Gazzaniga, A.: Different HPMC viscosity grades as coating agents for an oral time and/or site-controlled delivery system: an investigation into the mechanisms governing drug release, J Pharm Sci, 96 (2007) 6, 1527-36.

[Zha10]   Zhang, H., Mittal, G.: Biodegradable protein-based films from plant resources: A review, Environmental Progress & Sustainable Energy, 29 (2010) 2, 203-220.

[Zha11]   Zhang, Y.-N., Liu, N., Zhao, X.-H.: A study on the preparation and some functional properties of a cross-linked casein–gelatin composite by a microbial transglutaminase, International Journal of Food Science & Technology, 46 (2011) 12, 2641-2647.

[Zha12]   Zhang, L., Yi, H., Du, M., Ma, C., Han, X., Feng, Z., Jiao, Y., Zhang, Y.: Enzymatic characterization of transglutaminase from *Streptomyces*

mobaraensis DSM 40587 in high salt and effect of enzymatic cross-linking of yak milk proteins on functional properties of stirred yogurt, Journal of Dairy Science*,* 95 (2012) 7, 3559-3568.

[Zhu08]   Zhu, Y., Tramper, J.: Novel applications for microbial transglutaminase beyond food processing, Trends in Biotechnology*,* 26 (2008) 10, 559-565.

[Zhu12]   Zhu, D., Jin, L., Wang, Y., Ren, H.: Swelling behavior of gelatin-based hydrogel cross-linked with microbial transglutaminase, Journal of AQEIC (Asociación Química Española de la Industria del Cuero)*,* 63 (2012) 2, 11-20.

14. Appendix

Tab. 14-1: Activation / inhibition of the transglutaminase activity by additional compounds. The general Ca^{2+} dependency of the eukaryotic transglutaminases is not further considered in the review.

Substance	Enzyme origin	Effect	Ref.
NH_4Cl	*Caenorhabditis elegans* (worm)	**Inhibition:** 5 mM NH_4Cl → 64 % res. activity	[Mád98]
NH_4Cl $(NH_4)_2SO_4$	*Rattus norvegicus* (laboratory rat)	**Inhibition:** > 1 mM NH_4Cl / > $(NH_4)_2SO_4$ → no enzyme activity	[Sei91]
KCl	*Oreochromis niloticus* (tilapia fish)	**Inhibition:** 1 M KCl → 38 % res. activity	[Wor05]
KCl	*Patinopecten yessoensis* (scallop)	**Activation:** 0.8 M KCl → 8 fold higher activity	[Noz05]
Zn^{2+} Ba^{2+}, Ca^{2+}, Co^{2+}, Cu^{2+}, Fe^{2+}, Mg^{2+}, Mn^{2+}, Na^+	*Streptoverticillium mobaraense*	**Inhibition:** 1 mM $ZnCl_2$ → 20 % res. activity **No effect** on enzyme activity	[Lu03]
NaCl NaBr NaI $NaNO_3$ NaSCN Na_2SO_4	*Patinopecten yessoensis (scallop)*	**Activation:** 0.8 M NaCl → 12 fold increase **Activation:** 0.8 M NaBr → 11 fold increase **Activation:** 0.5 M NaI → 7 fold increase **Activation:** 1 M $NaNO_3$ → 8 fold increase **Activation** up to 0.25 M NaSCN, followed by inhibition at higher concentration **Inhibition:** 0.5 M Na_2SO_4 → 3 fold activity loss	[Noz99]
NaCl	Various tissues of fish and aquatic invertebrates	**Activation:** 1 M NaCl → 5-10 fold higher activity	[Noz01]
NH_4Cl	Human factor XIIIa	**Inhibition:** 10 mM NH_4Cl → total inactivation	[Uek96]
$(NH_4)_2SO_4$	*Bos Taurus* (from bovine plasma)	**Inhibition:** 5 mM $(NH_4)_2SO_4$ → total inactivation	[Tak86]
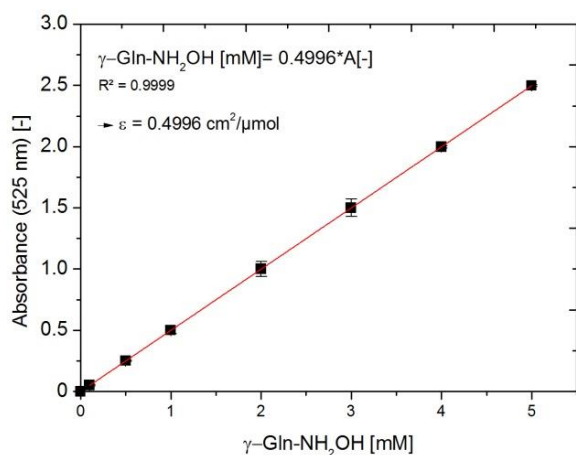
Fig. 14-1: Calibration of the hydroxamate assay for spectrophotometric determination of transglutaminase activity at 525 nm.
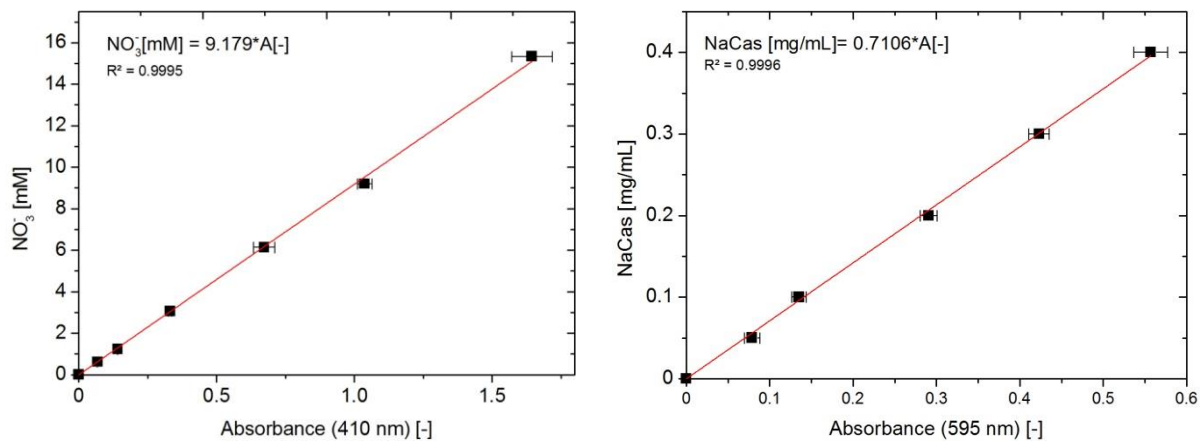
Fig. 14-2: Calibration of nitrate determination by spectrophotometric measurement at 410 nm (left) and calibration of the Bradford assay at 595 nm (right).

Tab. 14-2: Films A, B (NaCas non-cross-linked / cross-linked): Tensile strength and elongation at break of dependent on temperature (T) and relative humidity (RH) during drying process; n = 5.

Test	T [°C]	RH [% RH]	A		B	
			σ_M [MPa]	ε_B [%]	σ_M [MPa]	ε_B [%]
1	25	25	1.63±0.16	115±4	2.21±0.13	178±8
2	25	50	2.21±0.04	159±5	1.74±0.06	199±8
3	25	75	1.97±0.16	158±13	2.02±0.11	176±9
4	50	25	2.46±0.06	152±10	2.05±0.47	132±16
5	50	50	3.06±0.07	149±11	3.39±0.18	161±7
6	50	75	2.07±0.10	184±15	2.86±0.33	192±15
7	75	25	2.39±0.12	93±12	2.11±0.08	103±9
8	75	50	3.41±0.37	131±18	2.96±0.29	146±13
9	75	75	2.01±0.11	112±6	3.76±0.14	245±5

Tab. 14-3: Films C, D (NaCas + KNO$_3$ non-cross-linked / cross-linked): Tensile strength and elongation at break dependent on temperature (T) and rel. humidity (RH) during drying process; n = 5.

Test	T [°C]	RH [% RH]	C		D	
			σ_M [MPa]	ε_B [%]	σ_M [MPa]	ε_B [%]
1	25	25	1.43±0.04	140±7	2.16±0.19	201±11
2	25	50	1.71±0.03	187±12	2.83±0.22	200±25
3	25	75	0.92±0.14	121±11	1.61±0.04	181±12
4	50	25	1.27±0.07	132±8	1.68±0.21	120±25
5	50	50	1.39±0.04	165±7	2.68±0.10	178±9
6	50	75	1.24±0.02	193±13	1.96±0.14	184±3
7	75	25	1.25±0.04	100±9	1.08±0.03	66±13
8	75	50	1.22±0.06	141±12	2.44±0.28	209±21
9	75	75	0.83±0.06	114±8	1.38±0.11	146±16

Tab. 14-4: Water loss during drying and film formation of NaCas films at 25 °C and varied air humidity. Drying conditions were kept constant for 12 h, then shift to storage conditions as defined in DIN EN ISO527-3 (25 °C and 50 % RH); n = 1.

Material		t [h]	Residual water content [%]		
			Drying at 25 % RH	Drying at 50 % RH	Drying at 75 % RH
Film A	- KNO_3	0	100	100	100
	- MTG	6	36.1	49.2	75.2
		12	15.4	27.5	53.3
		24	7.8	8.0	16.5
		36	7.8	8.0	8.1
		60	7.9	8.0	8.0
Film B	- KNO_3	0	100	100	100
	+ MTG	6	47.9	56.0	78.8
		12	23.0	32.9	60.3
		24	9.0	9.2	29.8
		36	9.0	9.1	9.1
		60	9.0	9.1	9.3
Film C	+ KNO_3	0	100	100	100
	- MTG	6	51.4	62.1	81.4
		12	19.1	28.4	64.6
		24	8.7	9.0	33.8
		36	8.8	8.9	8.9
		60	8.8	8.9	8.9
Film D	+ KNO_3	0	100	100	100
	+ MTG	6	35.4	47.9	73.4
		12	14.5	24.8	47.9
		24	9.7	10.1	19.1
		36	9.6	9.9	9.9
		60	9.7	9.9	9.9

Tab. 14-5: Cumulative crystal size distribution based on length for KNO_3 crystals produced by batch cooling crystallization from pure aqueous solution (reference) and in presence of components from the film forming solution. Data refers to Fig. 6-6.

Size fraction [µm]	Reference KNO_3 in d-H_2O [%]		KNO_3 in Tris / HCl buffer pH 7 [%]	Glycerol / KNO_3 3:1 in d-H_2O [%]	Urea / KNO_3 2:1 in d-H_2O [%]
0	0.00	± 0.00	0.00	0.00	0.00
0-50	0.00	± 0.00	0.00	1.00	0.00
50-100	0.52	± 0.35	3.89	20.70	2.58
100-150	6.40	± 0.94	21.11	37.66	9.79
150-200	15.40	± 2.84	46.31	52.87	16.49
200-250	24.38	± 3.14	64.75	65.34	21.65
250-300	33.29	± 4.02	77.46	76.06	29.38
300-350	44.87	± 5.67	85.25	79.55	40.72
350-400	54.82	± 6.33	91.80	84.04	48.45
400-450	61.83	± 7.31	96.31	86.28	54.12
450-500	70.65	± 8.05	98.36	88.03	60.31

Tab. 14-5 continued

500-550	77.28	± 6.50	98.98	89.28	64.43
550-600	81.26	± 7.44	99.18	90.02	71.13
600-650	87.10	± 2.78	99.59	91.27	77.32
650-700	89.00	± 2.34	99.59	92.27	80.93
700-750	90.89	± 1.89	99.59	92.77	82.99
750-800	92.53	± 1.28	99.59	92.77	85.05
800-850	94.76	± 0 34	99.80	93.27	89.18
850-900	96.82	± 0.15	100.00	94.01	93.81
900-950	97.51	± 0.14	100.00	94.51	94.85
950-1000	97.94	± 0.16	100.00	94.76	95.36
>1000	100.00	± 0.00	100.00	100.00	100.00

Tab. 14-6: Mean aspect ratios from KNO_3 crystal growth experiments, referring to Fig. 6-7.

Additive	Additive / KNO_3	Conc. [mM]	D_{50} (length) [µm]	D_{50} (width) [µm]	Aspect ratio [-]
(Reference)	-	0	351.35	85.09	4.13
Tris	-	20	349.34	71.07	4.92
Tris	-	50	514.51	131.13	3.92
Tris	-	860	195.2	70.07	2.79
Glycerol	1:1000	3.8	367.36	114.11	3.22
Glycerol	1:100	38.4	324.32	134.13	2.42
Glycerol	1:10	384.1	329.32	138.13	2.38
Glycerol	3:1	12650.67	166.21	30.03	5.53
NH_4NO_3	1:1000	3.8	n.b.	n.b.	n.b.
NH_4NO_3	1:100	38.4	419.66	59.06	7.11
NH_4NO_3	1:10	384.1	221.54	150.15	1.48
KCl	1:1000	3.8	193.91	77.08	2.52
KCl	1:100	38.4	229.82	101.1	2.27
KCl	1:10	384.1	207.25	69.07	3.00
$Ca(H_2PO_4)_2$	1:1000	3.8	n.b.	n.b.	n.b.
$Ca(H_2PO_4)_2$	1:100	38.4	130.78	57.06	2.29
$Ca(H_2PO_4)_2$	1:10	384.1	340.61	52.05	6.54
$C_{12}H_{25}NaO_3S$	1:52612	0.07	497.50	98.10	5.07
Urea	2:1	12931.51	405.40	66.07	6.14
Citric acid in Tris buffer	1:1000	3.8 860	254.25	36.04	7.05
Citric acid in Tris buffer	1:100	38.4 860	100.10	46.05	2.17
Citric acid in Tris buffer	1:10	384.1 860	201.20	19.02	10.58

Tab. 14-7: Mechanical properties of NaCas films with varied additive mix of KNO_3 and NH_4NO_3 (given in molar ratios) also in dependence of enzymatic cross-linking by different MTG sources (σ_M … tensile strength; ε_B … elongation at break); n = 5; data referring to Fig. 6-9.

NH_4NO_3 / KNO_3	- MTG				+ Activa MTG				+ MTG (*E. coli*)			
	σ_M [MPa]		ε_B [%]		σ_M [MPa]		ε_B [%]		σ_M [MPa]		ε_B [%]	
0:0	1.21	±0.04	105	±2	2.11	±0.09	185	±9	n.d.	n.d.	n.d.	n.d.
0:1	0.93	±0.01	108	±4	1.83	±0.05	209	±6	1.84	±0.09	185	±6
1:10	1.34	±0.05	103	±5	2.00	±0.11	226	±10	2.03	±0.06	209	±5
1:7.5	1.30	±0.03	103	±5	2.00	±0.16	246	±8	n.d.	n.d.	n.d.	n.d.
1:5	1.38	±0.02	106	±3	2.04	±0.08	265	±8	1.97	±0.04	231	±4
1:2.5	1.36	±0.03	110	±3	1.85	±0.04	272	±7	n.d.	n.d.	n.d.	n.d.
1:1	1.36	±0.02	112	±3	1.99	±0.06	298	±6	1.85	±0.04	226	6

Tab. 14-8: Mechanical properties of NaCas films with varied ammonium nitrate content, non-cross-linked and treated with MTG (Activa or recombinant); n = 5; data referring to Fig. 6-10.

NaCas / NH_4NO_3	- MTG				+ Activa MTG				+ MTG (*E. coli*)			
	σ_M [MPa]		ε_B [%]		σ_M [MPa]		ε_B [%]		σ_M [MPa]		ε_B [%]	
1:0	2.58	±0.13	127	±6	2.11	±0.09	185	±9	2.97	±0.17	174	±11
12:1	2.01	±0.09	125	±6	2.68	±0.09	281	±6	n.d.	n.d.	n.d.	n.d.
6:1	1.48	±0.08	132	±6	2.59	±0.06	297	±3	1.83	±0.11	234	±10
4:1	0.85	±0.03	116	±5	2.12	±0.11	226	±9	n.d.	n.d.	n.d.	n.d.
2:1	0.64	±0.02	87	±5	0.9	±0.05	153	±13	0.6	±0.04	133	±9

Tab. 14-9: Cumulative crystal size distribution based on length from the KNO_3 crystallization in presence of secondary additives for screening face specific crystal growth inhibitors. Data refers to Fig. 6-8.

Size fraction [µm]	NH_4NO_3 / KNO_3 1:1000 [%]	NH_4NO_3 / KNO_3 1:100 [%]	NH_4NO_3 / KNO_3 1:10 [%]	$Ca(H_2PO_4)_2$ / KNO_3 1:1000 [%]	$Ca(H_2PO_4)_2$ / KNO_3 1:100 [%]	$Ca(H_2PO_4)_2$ / KNO_3 1:10 [%]
0	0.00	0.00	0.00	0.00	0.00	0.00
0-50	0.00	0.00	0.00	0.00	1.57	0.00
50-100	0.00	2.02	1.93	0.00	22.11	3.18
100-150	0.00	6.06	13.13	0.00	48.92	10.51
150-200	0.00	12.12	33.20	0.00	68.88	21.02
200-250	0.00	20.20	54.83	0.00	85.32	30.89
250-300	0.00	28.79	70.66	0.00	92.95	38.54
300-350	0.00	36.87	81.08	0.00	96.28	46.82
350-400	0.00	45.45	86.87	0.00	97.46	56.37
400-450	0.00	52.53	90.73	0.00	98.63	64.33
450-500	0.00	58.08	92.66	0.00	99.22	71.02
500-550	0.00	64.14	95.37	0.00	99.80	75.48
550-600	0.00	67.17	97.30	0.00	100.00	78.98
600-650	0.00	68.18	98.07	0.00	100.00	84.08
650-700	0.00	69.70	99.23	0.00	100.00	85.67
700-750	0.00	72.73	99.61	0.00	100.00	87.58
750-800	0.00	74.24	99.61	0.00	100.00	88.85
800-850	0.00	77.27	99.61	0.00	100.00	91.72
850-900	0.00	79.29	99.61	0.00	100.00	92.99
900-950	0.00	82.32	99.61	0.00	100.00	93.63
950-1000	0.00	84.34	99.61	0.00	100.00	93.63
>1000	100.00	100.00	100.00	100.00	100.00	100.00

Tab. 14-9 continued

Size fraction	KCl / KNO$_3$ 1:1000	KCl / KNO$_3$ 1:100	KCl / KNO$_3$ 1:10	Citric acid / KNO$_3$ 1:1000	Citric acid / KNO$_3$ 1:100	Citric acid / KNO$_3$ 1:10
[µm]	[%]	[%]	[%]	[%]	[%]	[%]
0	0.00	0.00	0.00	0.00	0.00	0.00
0-50	0.31	0.00	0.00	1.84	3.04	0.90
50-100	7.84	9.86	11.75	10.66	35.57	8.36
100-150	27.59	23.94	28.42	23.16	65.73	24.78
150-200	45.14	38.03	43.99	34.93	82.43	41.79
200-250	60.50	50.35	55.74	46.32	91.54	57.31
250-300	72.41	60.21	64.21	55.51	97.18	73.13
300-350	82.45	69.37	75.14	62.50	98.48	84.48
350-400	88.71	78.52	81.42	69.12	99.35	93.13
400-450	94.04	81.34	86.34	73.53	99.57	98.21
450-500	96.24	87.68	92.62	78.68	99.78	99.10
500-550	97.18	89.44	95.63	82.35	99.78	99.40
550-600	98.43	91.20	96.17	86.40	100.00	100.00
600-650	99.06	95.07	96.99	87.87	100.00	100.00
650-700	99.69	97.54	97.81	91.91	100.00	100.00
700-750	100.00	97.54	98.91	93.75	100.00	100.00
750-800	100.00	98.24	99.45	94.49	100.00	100.00
800-850	100.00	98.59	99.73	95.22	100.00	100.00
850-900	100.00	98.94	99.73	97.06	100.00	100.00
900-950	100.00	98.94	99.73	97.79	100.00	100.00
950-1000	100.00	99.65	99.73	98.53	100.00	100.00
>1000	100.00	100.00	100.00	100.00	100.00	100.00

Tab. 14-10: Mechanical properties of NaCas films with constant glycerol and KNO₃ content as well as varied urea amount with and without cross-linking; n = 5; data referring to Fig. 6-11.

NaCas / glycerol / KNO₃ / urea	- MTG				+ Activa MTG			
	σ_M [MPa]		ε_B [%]		σ_M [MPa]		ε_B [%]	
6:1:1:0	14.99	±0.24	70	±3	13.43	0.35	18	±5
6:1:1:0.5	5.11	±0.15	81	±6	6.83	0.51	119	±8
6:1:1:1	3.99	±0.47	81	±2	4.87	0.2	148	±5
6:1:1:1.5	1.31	±0.09	95	±10	3.98	0.06	196	±4
6:1:1:2	0.81	±0.05	107	±0.5	3.18	0.07	192	±5

Tab. 14-11: Water uptake of enzymatically cross-linked films according to DIN EN ISO 62. NaCas / salt ratio constant at 6:1; n = 3; data refers to Fig. 6-12.

Protein film:	Water uptake (Δm) [%]											
	NaCas + Activa MTG						Gelatin (280 Bloom) + Activa MTG					
t [min]	-		+ KNO₃		+ NH₄NO₃ / KNO₃ 1:1		-		+ KNO₃		+ NH₄NO₃ / KNO₃ 1:1	
0	0	±0	0	±0	0	±0	0	±0	0	±0	0	±0
2	195	±28	140	±6	105	±4	--	--	--	--	--	--
5	511	±41	319	±54	127	±8	155	±5	77	±34	95	±11
10	873	±54	420	±51	192	±7	--	--	--	--	--	--
15	1263	±81	515	±81	288	±62	202	±34	100	±26	160	±3
30	1459	±245	812	±55	569	±59	261	±9	180	±6	218	±30
45	1950	±128	822	±24	667	±103	267	±37	190	±14	247	±42
60	2003	±105	939	±10	706	±23	242	±11	194	±8	292	±14

Tab. 14-12: Data from dynamic water vapor sorption gravimetry. Cross-linked NaCas films + Activa MTG have been measured; sorption isotherm to be found in Fig. 6-13 (I).

Rel. air humidity [% RH]	Δm [%]	
	NH₄NO₃ / KNO₃ 1:10	NH₄NO₃ / KNO₃ 1:1
0.48	-11.67	-10.92
10.05	-11.33	-10.39
20.04	-9.94	-8.80
30.02	-7.75	-6.68
40.00	-5.17	-4.11
49.99	-1.79	-0.71
60.02	3.75	4.82
70.05	13.42	13.96
75.11	20.55	21.08
80.15	29.32	29.71
85.11	42.80	42.67
90.40	60.04	59.08
95.00	87.21	83.81
94.89	98.90	95.64

Tab. 14-13: Residual humidity of protein films stored at constant environmental conditions 25 °C and 50 % RH determined by weight loss after drying at 50 °C, 24 h. Data refer to Fig. 6-13 (II).

	Material	Residual humidity [%]	Mean deviation [%]
1	NaCas + MTG	13.9	4.4
2	NaCas + MTG + KNO_3	13.4	3.7
3	NaCas + MTG NH_4NO_3 / KNO_3 1:1	16.2	3.0
4	Gelatin + MTG	13.5	2.4
5	Gelatin + MTG + KNO_3	13.6	1.7
6	Gelatin + MTG NH_4NO_3 / KNO_3 1:1	18.0	7.6

Tab. 14-14: Nitrate release from NaCas films with inner-film crystallized nitrate salt in NaCas / salt ratio of 6:1, non-cross-linked and treated with Activa MTG; n =3 if not otherwise stated; Data as visualized in Fig. 6-14.

t	Nitrate release (nitrate in the solvent) [%]					
	NaCas - MTG			NaCas - MTG + KNO_3		
[min]	5 °C		15 °C		25 °C	
0	0	n.d.	0	n.d.	0	n.d.
2	0	n.d.	0	n.d.	0	n.d.
5	0	n.d.	0	n.d.	0	n.d.
10	0	n.d.	0.1	n.d.	0	n.d.
15	0	n.d.	0	n.d.	0	n.d.
30	0	n.d.	0.1	n.d.	0	n.d.

t	NaCas - MTG + KNO_3					
[min]	5 °C		15 °C		25 °C	
0	0	±0	0	±0	0	±0
2	65.7	±15.5	78.2	±1.2	93.4	±5.0
5	102	±8.7	94	±0.6	100	±5.1
10	114.8	±2.5	104	±11.9	104.2	±106
15	111.5	±1.1	101.5	±10.1	104.2	±0.6
30	96.9	±5.0	99.5	±0.8	104	±8.0

t	NaCas – MTG + NH_4NO_3 / KNO_3 1:1			NaCas + MTG		
[min]	5 °C		15 °C		25 °C	
0	0	±0	0	±0	0	±0
2	87.6	±13.8	95.7	±12.3	104	±8.3
5	118.7	±12.7	120.8	±8.5	111.4	±15.6
10	114.3	±29.6	120.7	±12.9	117.8	±8.6
15	133.5	±13.3	122.8	±14.0	116.6	±4.4
30	121.8	±18.0	112.8	±3.8	111	±1.8

t	NaCas + MTG					
[min]	5 °C		15 °C		25 °C	
0	0	n.d.	0	n.d.	0	n.d.
2	0	n.d.	0	n.d.	0	n.d.
5	0	n.d.	0.2	n.d.	0	n.d.
10	0	n.d.	0.2	n.d.	0	n.d.
15	0	n.d.	0.4	n.d.	0	n.d.
30	0	n.d.	0.7	n.d.	0	n.d.

t	NaCas + MTG + KNO_3			NaCas + MTG + NH_4NO_3 / KNO_3 1:1		
[min]	5 °C		15 °C		25 °C	
0	0	±0	0	±0	0	±0
2	55.4	±6.2	61.4	±5.3	83	±1.5
5	92	±13.0	76.2	±6.1	90.3	±1.8
10	100.2	±4.2	101.5	±6.3	91	±1.4
15	114.2	±6.5	110.5	±4.3	93.5	±1.8
30	112.8	±7.7	111.5	±3.9	90.4	±2.8

t	NaCas + MTG + NH_4NO_3 / KNO_3 1:1					
[min]	5 °C		15 °C		25 °C	
0	0	±0	0	±0	0	±0
2	79.4	±15.7	72.7	±1.1	85.7	±3.5
5	105.1	±15.4	96.3	±6.3	91.2	±1.7
10	107.9	±7.9	109.2	±3.5	97.9	±1.3
15	118.7	±4.8	124.1	±3.4	98.1	±1.1
30	116.3	±13.6	121.7	±13.6	99.8	±2.6

Tab. 14-15: Protein release from the NaCas film structure determined by Bradford analysis of the protein concentration in the solvent medium; n = 3 if not otherwise stated. Measurement within the active ingredient release tests, data corresponding to Fig. 6-15.

t	Protein release (protein in the solvent) [%]											
	NaCas - MTG						NaCas - MTG + KNO$_3$					
[h]	5 °C		15 °C		25 °C		5 °C		15 °C		25 °C	
0	0	±0	0	±0	0	±0	0	±0	0	±0	0	±0
2	0	±1.4	13.3	±5.1	23.7	±0.9	0.4	±0.1	6.8	±1.0	9.3	±3.0
5	7.5	±1.8	21.3	±5.6	47.3	±0.2	2.6	±0.1	21.6	±4.0	12.8	±3.1
10	86.4	±2.2	47	±8.7	48.3	±7.2	14.2	±3.7	47.5	±6.8	40.1	±14.2
15	107.5	±12.1	71.5	±3.6	58.7	±7.4	29.1	±4.3	76.8	±7.9	84.1	±5.6
30	110.6	±12.8	87.7	±6.6	79.3	±6.9	72.7	±16.9	100.2	±6.4	121.8	±1.8
t	NaCas – MTG + NH$_4$NO$_3$ / KNO$_3$ 1:1						NaCas + MTG					
[h]	5 °C		15 °C		25 °C		5 °C		15 °C		25 °C	
0	0	±0	0	±0	0	±0	0	n.d.	0	n.d.	0	n.d.
2	0	±0.6	1.9	±0.9	11.6	±4.5	0	n.d.	0	n.d.	0	n.d.
5	0	±0.8	4.2	±1.5	24	±7.8	0	n.d.	0.1	n.d.	0	n.d.
10	0	±1.5	6.3	±1.9	63.7	±5.5	0	n.d.	0.2	n.d.	0	n.d.
15	0.7	±0.1	17.3	±1.8	95.8	±12.1	0	n.d.	0.4	n.d.	0.1	n.d.
30	2	±0.2	39.9	±4.4	104.2	±9.6	0	n.d.	0.5	n.d.	0.4	n.d.
t	NaCas + MTG + KNO$_3$						NaCas + MTG + NH$_4$NO$_3$ / KNO$_3$ 1:1					
[h]	5 °C		15 °C		25 °C		5 °C		15 °C		25 °C	
0	0	n.d.	0	n.d.	0	n.d.	0	n.d.	0	n.d.	0	n.d.
2	0	n.d.	2.6	n.d.	0	n.d.	0	n.d.	0.1	n.d.	0	n.d.
5	0	n.d.	9.8	n.d.	0	n.d.	0	n.d.	0.5	n.d.	0.5	n.d.
10	0	n.d.	8.9	n.d.	0	n.d.	0	n.d.	2.1	n.d.	2.1	n.d.
15	0	n.d.	5.4	n.d.	2.5	n.d.	0	n.d.	5.1	n.d.	9.6	n.d.
30	0	n.d.	9.4	n.d.	9.3	n.d.	6.5	n.d.	10.8	n.d.	19.1	n.d.

Tab. 14-16: Enzyme activity of microbial transglutaminase from Activa TG WM, Ajinomoto, tested with the hydroxamate assay. The activity is expressed in relative units, showing the dependency on the presence of other substances (enzyme activator / inhibitor) in the solution. Data corresponding to Fig. 6-16.

Additive [mM]	KNO$_3$		KCl		NH$_4$NO$_3$		(NH$_4$)$_2$SO$_4$	
0	100	±2.2						
0.0015	98.4	±0.8	99.6	±2.6	111.5	±5.2	101	±1.0
1.5	109.2	±4.4	99.4	±5.1	106	±10.4	97.3	±0.3
5	105.3	±2.7	124.5	±13.2	100.4	±0.8	96.3	±3.9
10	101.1	±1.2	127.5	±6.3	104.9	±9.3	98.5	±2.7
25	103.7	±5.1	142.3	±17.9	96.6	±2.2	94.2	±7.6
50	106.5	±3.5	154.6	±6.4	88.6	±4.3	90.2	±0.9

Tab. 14-16 continued

Additive [mM]	Ca(H$_2$PO$_4$)$_2$		Urea		Citric acid		C$_{12}$H$_{25}$NaO$_3$S	
0.0015	97.4	±3.5	137.1	±18.3	145.5	±3.8	123.9	±14.9
1.5	99.7	±2.1	138.4	±11.3	130.3	±13.3	70	±23.9
5	n.d.	n.d.	133.9	±11.3	125.7	±6.4	11.7	±1.1
10	n.d.	n.d.	132.5	±16.5	127.1	±6.2	11.4	±10.4
25	n.d.	n.d.	129.7	±5.0	110.7	±6.1	n.d.	n.d.
50	n.d.	n.d.	128.2	±3.9	100.6	±5.7	n.d.	n.d.

Tab. 14-17: Seed germination and plant growth tests for different seeding techniques including protein-based seed carriers. The biomass was determined gravimetrically right after harvest. Data refers to Fig. 6-18 and Fig. 6-19.

Radish (*Raphanus sativus var. sativus*)		
Method		**Biomass (whole plant) [g]**
A	Bulk seed	4.8 ± 0.6	0.7 ± 0.1
B	Paper based seed tape	6.2 ± 0.9	1.6 ± 0.2
C	Protein-based seed tape	10.8 ± 0.5	2.6 ± 0.1
D	Protein-based seed tape + KNO$_3$	15.6 ± 1.5	4.9 ± 0.5
Lettuce (*Lactuca sativa var. capitata*)		
Method		**Seed germination [%]**
i	Bulk seed	81.3	11.8 ± 4.1
ii	Pilled seed	75.0	23.2 ± 3.8
iii	Paper based seed tape	16.6	(seedlings died)
iv	Protein-based seed sheet	37.5	30.0 ± 2.3
v	Protein-based seed sheet + KNO$_3$	62.5	14.8 ± 9.3
vi	Protein-based seed sheet + urea	12.5	25.0 ± 10.5

Statement of authorship

I declare this document and the accompanying code have been composed by myself, and describe my own work, unless otherwise acknowlegded in the text. It has not been entered in any previous application for a degree. All verbatim extracts have been distinguished by quotation marks, and all sources of information have been specifically acknowledged.

Halle (Saale), 9th October 2013   Isabell Stolte

Curriculum vitae

Personal data

Name: Isabell Stolte
Date of birth: 12th June 1983
Place of birth: Aschersleben, Germany

Education and career

Since 06/2013   Research associate at Martin Luther University Halle-Wittenberg, Department of Polymer Engineering

Since 02/2011   Co-founder of PolyNature GmbH

10/2010 – 03/2012 ego.START Gründerstipendium

10/2009 – 09/2010 EXIST-Gründerstipendium

10/2009 – 05/2013 PhD study at Martin Luther University Halle-Wittenberg, Center of Engineering Sciences, Department of Thermal Processing

09/2007 – 03/2008 ERASMUS scholarship for a study period at 'La Sapienza' University in Rome, Italy

10/2003 – 09/2009 Study of bioengineering (Diploma) at Martin Luther University Halle-Wittenberg

List of publications

1. Stolte, I., Frohberg, P., Pietzsch, M., Ulrich, J., Kristalline Substanzen als neuer Weg zur Eigenschaftsverbesserung in proteinogenen Biopolymeren, Poster and abstract, ProcessNet Fachausschuss „Kristallisation", DECHEMA e.V., Magdeburg, Germany, 11th – 12th March 2010.

2. Stolte, I., Frohberg, P., Pietzsch, M., Ulrich, J., Innovative Biowerkstoffe aus Proteinen, Poster, Fachkongress Biobasierte Kunststoffe, Bundesministerium für Ernährung, Landwirtschaft und Verbraucherschutz, Berlin, Germany, 15th – 16th June 2010.

3. Stolte, I., Frohberg, P., Pietzsch, M., Ulrich, J., Biodegradable Polymers – From Protein to Sustainability, Poster, Projekttag Stoffliche Biomassenutzung, Bundesministerium für Ernährung, Landwirtschaft und Verbraucherschutz, Berlin, Germany, 15th December 2010.

4. Stolte, I., Frohberg, P., Pietzsch, M., Ulrich, J., Crystals in Protein Films: What Are They Good For?, Poster and abstract (extended abstract), 18th International Symposium on Industrial Crystallization (ISIC 18), Zürich, Switzerland, 13th – 16th September 2011.

5. Stolte, I., Frohberg, P., Pietzsch, M., Ulrich, J., Crystals in protein films: What are they good for?, Chemical Engineering Science **77** (2011) 196-200.

6. Stolte, I., Frohberg, P., Pietzsch, M., Ulrich, J., Crystals and proteins – an attractive symbiosis in biopolymer technology, Presentation and abstract, ACHEMA 2012, Frankfurt (Main), Germany, 18th – 22th June 2012.

7. Stolte, I., Frohberg, P., Pietzsch, M., Ulrich, J., Biopolymers from proteins – Functionality meets sustainability, Presentation and abstracts (short version and extended abstract), 18th International Symposium „Materials made of Renewable Resources" (naro.tech), Erfurt, Germany, 5th – 09th September 2012.

8. Stolte, I., Frohberg, P., Pietzsch, M., Ulrich, J., Protein and beyond: material development using inner-film crystallized additives, Poster and abstracts (short version and extended abstract), 15th International Conference „Polymeric Materials", Halle (Saale), Germany, 12th – 14th September 2012.